

**THE SEDIMENTOLOGY, SEA-LEVEL HISTORY AND POROSITY
EVOLUTION OF THE HOLKERIAN (LOWER CARBONIFEROUS) OF
GOWER**

by

Misfer Al Ghamdi

Thesis submitted for the degree of Master of Philosophy

School of Earth and Ocean Sciences

Cardiff University

March 2010

UMI Number: U585377

All rights reserved

INFORMATION TO ALL USERS

The quality of this reproduction is dependent upon the quality of the copy submitted.

In the unlikely event that the author did not send a complete manuscript and there are missing pages, these will be noted. Also, if material had to be removed, a note will indicate the deletion.



UMI U585377

Published by ProQuest LLC 2013. Copyright in the Dissertation held by the Author.
Microform Edition © ProQuest LLC.

All rights reserved. This work is protected against
unauthorized copying under Title 17, United States Code.



ProQuest LLC
789 East Eisenhower Parkway
P.O. Box 1346
Ann Arbor, MI 48106-1346


**NOTICE OF SUBMISSION OF THESIS FORM:
POSTGRADUATE RESEARCH**



**APPENDIX 1:
Specimen layout for Thesis Summary and Declaration/Statements page
to be included in a Thesis**


DECLARATION

This work has not previously been accepted in substance for any degree and is not concurrently submitted in candidature for any degree.

Signed  (candidate) Date 16-06-2010

STATEMENT 1


This thesis is being submitted in partial fulfillment of the requirements for the degree of MPhil (insert MCh, MD, MPhil, PhD etc, as appropriate)

Signed  (candidate) Date 16-06-2010

STATEMENT 2

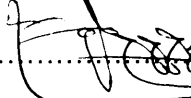
This thesis is the result of my own independent work/investigation, except where otherwise stated.

Other sources are acknowledged by explicit references.

Signed  (candidate) Date 16-06-2010

STATEMENT 3

I hereby give consent for my thesis, if accepted, to be available for photocopying and for inter-library loan, and for the title and summary to be made available to outside organisations.

Signed  (candidate) Date 16-06-2010

STATEMENT 4: PREVIOUSLY APPROVED BAR ON ACCESS

I hereby give consent for my thesis, if accepted, to be available for photocopying and for inter-library loans **after expiry of a bar on access previously approved by the Graduate Development Committee.**

Signed (candidate) Date

Acknowledgement

First of all, praise is due to almighty ALLAH with His compassion and mercifulness to allow me finalizing this MPhil project.

I would like to express the deepest appreciation to my employer Saudi Aramco for giving me the chance to do my master's degree studies. Special thanks go to Mr. Geraint W. Hughes, and Mr. Aus ALTawil for suggesting the advisor of my project Professor Paul Wright.

This thesis would not have been completed without the help, support, guidance, and efforts of many people. I owe my deepest gratitude to my advisor, Professor Paul Wright, for offering extremely perceptive comments, and for generously supporting the thesis with his expertise and for broadening my horizon. Thanks to Dr. Giovanna Della Porta for helping me with the literature and science. Thanks especially go to Earth and Ocean Sciences Department at Cardiff University and specially the Laboratory technicians.

It is a pleasure to thank those who made this thesis possible to whom I owe everything I am today. Thanks to my father for instilling in me the love of challenging and the pursuit of knowledge, and to him I dedicate this thesis. Special thanks go to my dear mother for her constant encouragement, helpful advice, care, and affection. If it were not for them, I would not be sitting here today.

This thesis would not have been possible without the emotional support of my other family members. I would like to show my gratitude to all my brothers and sisters for all support and advices.

I also appreciate the help and support from all persons who were directly or indirectly involved in my project. I would like to acknowledge the help of Mr. Najm AlQahtani for valuable help and advices through the entire project, and Ms. Ala Ghafur for the kind help, guidance, and assistance.

I owe my loving thanks to my wife and my son. They have lost a lot due to my research. Without their encouragement, patience and understanding it would have been impossible for me to finish this work.

TABLE OF CONTENTS

Acknowledgement	I
Table of Contents	II
Abstract	VII

CHAPTER 1. INTRODUCTION AND GEOLOGICAL BACKGROUND

1.1 Introduction	1
1.2 Aims of the Study	1
1.3 Objectives	4
1.4 Methodology	4
1.5 Data set	5
1.6 Geological settings	6
1.7 Tectonics	12
1.8 Sedimentology	14
1.8.1 Courceyan to Arundian interval	14
1.8.2 Holkerian Substage	16
1.8.3 Asbian to Brigantian Interval	16
1.9 Global Sea-Level	17
1.10 Palaeoclimate	17
1.11 Glacio-Eustasy	19

CHAPTER 2. LITERATURE REVIEW AND REVIEW OF PUBLISHED MODELS

2.1 Hunts Bay Oolite Literature Review	22
2.1.1 Regional Context	22
2.1.2 Previous Research on the Hunts Bay Oolite	23
2.1.3 Glacio-Eustasy in the Early Carboniferous	25
2.2 Review of Published Models of Modern and Mississippian Oolitic Carbonate Sandbodies	25
2.2.1 Tidal bar belts	26
2.2.2 Marine sand belts	26
2.2.3 Tidal Deltas	36
2.2.4 Tidal and Long Shore sandwaves	40
2.2.5 Barrier and Beach Sandbodies	42
2.2.6 Wave-dominated Sandbody: Structural Control	45

CHAPTER 3. HUNTS BAY OOLITE (HBO)

3.1 Introduction	47
3.2 Very Fine to Fine Crinoidal Association (A)	48
3.2.1 Field Appearance of Association (A)	48
3.2.2 Distribution and Frequency of Association (A)	51
3.2.3 Microfacies of Association (A)	51
3.2.4 Interpretation of Association (A)	54
3.3 Coarse Grade Oolitic Association (B)	57

3.3.1 Field Appearance of Association (B)	57
3.3.2 Distribution and Frequency of Association (B)	57
3.3.3 Microfacies of Association (B)	58
3.3.4 Interpretation of Association (B)	65
3.4 Coarse to Very Coarse Grade Oolitic Association (C)	67
3.4.1 Field Appearance of Association (C)	68
3.4.2 Distribution and Frequency of Association (C)	68
3.4.3 Microfacies of Lithofacies of Association (C)	69
3.4.4 Interpretation of Association (C)	74
3.5 Very Fine-to-Fine Grade Bioclastic and Peloidal Association (D)	76
3.5.1 Field Appearance of Association (D)	77
3.5.2 Distribution and Frequency of Association (D)	77
3.5.3 Microfacies of Lithofacies of Association (D)	77
3.5.4 Interpretation of Lithofacies of Association (D)	78
3.6 Summary	83
3.7 Depositional Model of the HBO	84

CHAPTER 4. REVIEW OF SEQUENCE STRATIGRAPHY AND TECTONICS, AND THE GLOBAL SEA-LEVEL CURVE

4.1 Sequence Stratigraphy and Tectonics	95
4.2 Global Sea-level Curve During the Holkerian	100

CHAPTER 5. DIAGENESIS OF HUNTS BAY OOLITE

5.1 Introduction	104
5.2 Grains Micritisation (Peloids) and Micrite Envelopes	104
5.3 Fenestral Porosity	108
5.4 Peloidal Cement	110
5.5 Fibrous (Fringe) Cement	113
5.6 Aragonite Dissolution	113
5.7 Non-ferroan Calcite Cements (blocky and drusy)	115
5.8 Early Dolomitisation	117
5.9 Syntaxial Cement	119
5.10 Neomorphism/Recrystallisation	121
5.11 Compaction / pressure solution	122
5.12 Late Stage Dolomitisation	124
5.13 Dedolomitisation	125
5.14 Fractures with Non-ferroan and Ferroan Calcite	125
5.15 Comparison HBO of the Logged Sections with Gully Oolite of Gower	127
5.16 Conclusion	128

CHAPTER 6. CONCLUSION AND FUTHER RESEARCH

6.1 Conclusions	130
6.2 Further Research	132

REFERENCES

134

APPENDICES

- A- Procedure for the preparation of stained acetate peels and thin-sections
- B- Geological maps of the three studied localities
- C- Detailed stratigraphic logs of the HBO in Langland Bay
- D- Detailed stratigraphic logs of the HBO in Three Cliffs Bay
- E- Detailed stratigraphic logs of the HBO in Port Eynon Bay

Abstract

The Holkerian (Lower Carboniferous, Mississippian) Hunts Bay Oolite (HBO) was studied in the south of Gower, along a section 15km long, up to 300m thick, at three locations: Langland Bay, Three Cliffs Bay and Port Eynon Bay. The HBO has been divided petrographically into four main associations (A, B, C and D), each with up to three lithofacies. Association A comprises crinoidal plates and bimodal grains of ooid, grapestone and aggregate grains; it represents open-marine offshore deposits. Association B consists of the main oolite factory in an active shoal setting. Association C, deposited in back-shoal settings, and represents mainly grapestones and aggregate. Associations B and C are the main sandbody constituents. D is the lagoonal part of the HBO and includes bioclasts and peloids which are associated with sponges. The High Tor Limestone to HBO transition is gradational, without sharp boundaries.

These associations accumulated in shoaling-upward sequences: offshore via active shoal to back shoal or lagoonal settings. Each sequence shows a thickening ESE to WNW trend. These cycles are not glacio-eustatic in origin but were likely tectonically-controlled and local, so that the sea-level curve of the HBO does not conform to the Holkerian global signal. Ramsay's (1987) and Scott's (1988) overall HBO-sandbody models are inapplicable to Ball's (1967) and Handford's (1988) marine sand-belt model as they lack differentiation between ramp and shield, and large bipolar cross-stratification. Considering all the HBO features exhibited, the deposystem lacks analogy to any modern or ancient examples, and represents a range of small sandbodies, and not major oolite shoals, as the source.

A paragenetic sequence has been derived and fifteen diagenetic events identified. Most HBO diagenetic features differ from those of the well documented Chadian Gully Oolite of Gower, especially in the early diagenesis phase; Gully Oolite contains ranges of emergence phases, and associated features such as vadose cementation and compaction, oomouldic fabrics, development of palaeosol and palaeokarsts.

CHAPTER 1. INTRODUCTION

1.1 Introduction

The Holkerian (Lower Carboniferous, Mississippian) Hunts Bay Oolite (HBO) (Fig. 1.1) of Gower in South Wales is well exposed along the coastline as a massive grey-coloured, commonly vertically-dipping unit. This study focuses on three main outcrops along the strike of the coastline forming part of the anticlinal structure related to Cefn Bryn and Port Eynon Thrust (Cossey et al., 2004). Respectively, from east to west, the sections crop out in Langland Bay, Three Cliffs Bay, and Port Eynon Bay; they extend for approximately 15 km., and are up to 300m in thickness (Ramsay, 1987).

HBO was deposited on a carbonate ramp in the sense of Ahr (1973), described as, a gradually dipping depositional surface of $<1^\circ$ toward the basin, where the shallow water sediments are updip and the basinal sediments downdip. The long-lasting early Carboniferous ramp in South Wales was formed due to a rise in sea level during the earliest Carboniferous (Wright, 1986). In addition, HBO represents the grainy part of the ramp where the major grainstones of oolitic shoal and related aggregate grains of the back shoal settings formed as a massive sandbody.

1.2 Aims of the Study

The aims of this study divide into three main parts: to elucidate the architecture of HBO along with the depositional systems; to interpret the sequence stratigraphy and sea-level history, including the fact that very shallow deposition prevailed for long periods, seemingly unaffected by sea-level changes (stasis); and to explore the porosity evolution in HBO.

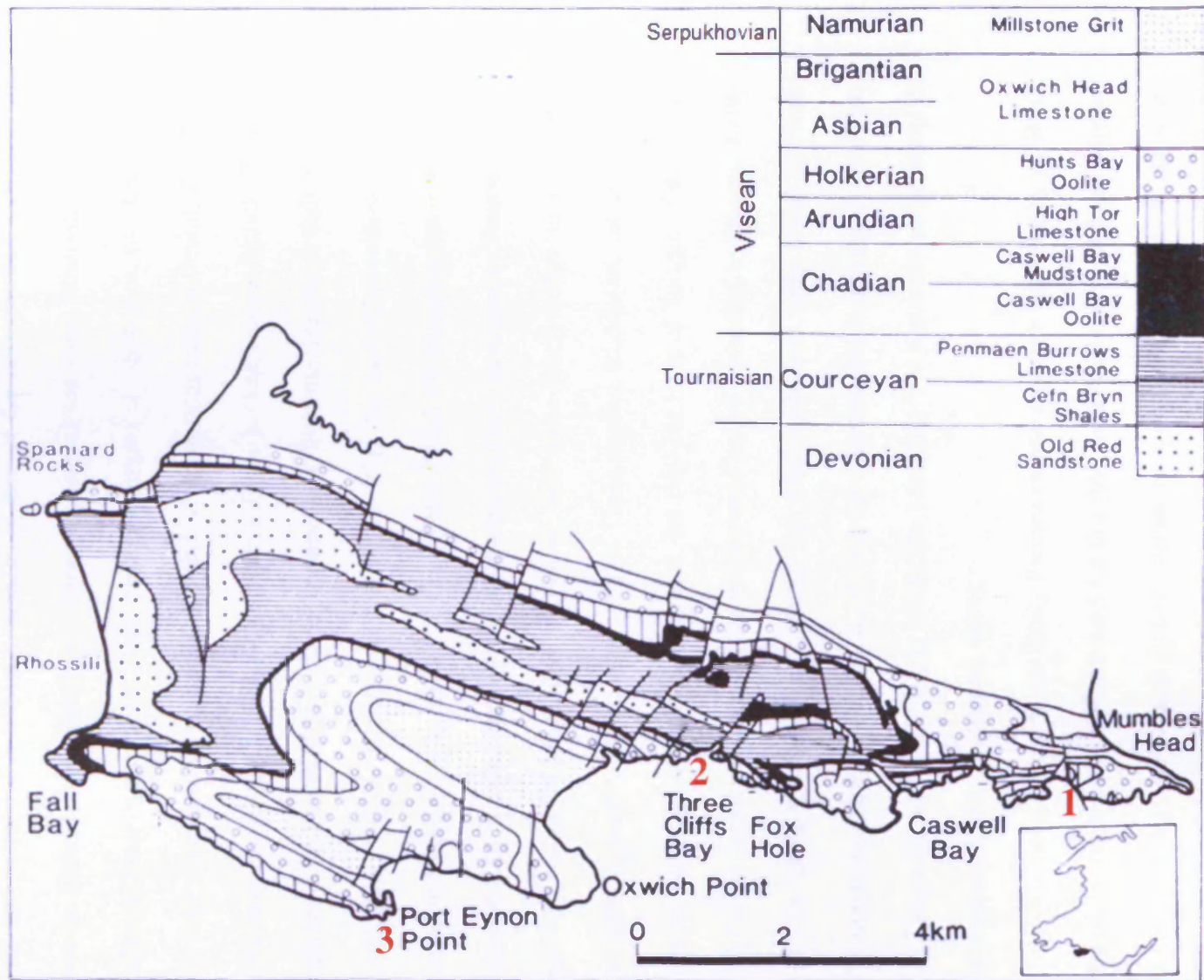


Figure 1.1: Map view of the Lower Carboniferous outcrops in the Gower Peninsula South Wales (numbers show the location of studied sections; 1. Langland Bay, 2. Three Cliffs Bay and 3. Port Eynon Bay). From Ramsay (1987).

HBO formed as a large carbonate sandbody which could have potential for a hydrocarbon reservoir. So, to explain the internal architecture along with the flow units and permeability barriers, we need to answer the next question: can its gross form be identified and predicted? There are several suggested Mississippian oolitic carbonate models, plus some other modern examples of sandbodies, which this study will later review and compare with HBO. If no analogue can be found, then HBO represents a setting that is non-actualistic. These ancient models include: tidal-bar belts from the Visean of the central Appalachians, from the Greenbrier Gulf in Illinois Basin USA study by Kelleher and Smosna (1993); the Early Carboniferous barrier-related settings review by Burchette et al. (1990); the USA Mississippian marine sand belt explained by Handford (1988); the marine sand belts described by Ramsay (1987) from the Holkerian succession of Gower; and some other models in the studies provided by Keith and Zuppann (1993). These ancient models are integrated with modern Bahamian examples, which are: the tidal-bar belts of Tongue of the Ocean and Exuma Sound (Ball, 1967); the marine sand belt of Joulter's Cay (Harris, 1979), and Lily Bank (Rankey et al., 2006); the tidal sandwaves body found in North Yucatan in the Strait (Harms et al., 1974); the shoreface/beach settings of the Turks and Caicos Islands (Lloyd et al., 1987); the Long Bay and carbonate ramp model of the Kuwait example (Lomando, 1999).

The second aim of this study focuses on the sequence stratigraphy of HBO. The issues that need to be addressed for this part are as follows: identifying whether or not there is evidence of 3rd-order sequences due to global changes in sea-level; proving whether or not lowstand surfaces exist within HBO, and whether Holkerian HBO shows ice-house cyclicality, as shown in the overlying Asbian carbonates (Wright and Vanstone, 2001).

The final part discusses the porosity evolution of HBO, for which this study investigates the cement origin and evidence of subaerial exposure. Meteoric cementation has been recorded within other Lower Carboniferous oolites, in the same succession, due to lowstand exposure surfaces (Searl, 1989).

1.3 Objectives

In order to achieve these aims, the following study objectives were followed; three large sections of Holkerian HBO in the Gower area, as identified by Ramsay (1987) (Fig. 1.1), were logged to determine depositional and sequential stratigraphic settings, and standard petrographic techniques were applied. Very poor weather during the Summer and Autumn of 2008 prevented completion of field work which was completed at the end of December 2008.

1.4 Methodology

Routine fieldwork was carried out to log the HBO as well as describe the peels and thin sections. Each specimen has an average thickness of 10cm. The number of samples collected depends on the size and site of the logged sections. The specimens were sampled in three different ways. The Three Cliffs Bay samples were collected every three meters, unless a change in lithology was observed. The Port Eynon Bay sampling method was to collect a small specimen every five meters, though with consideration for any change in lithology. In the last section, at Langland Bay, the strategy was to collect a sample every ten meters, or with every change in lithology, due to the closeness of the cliff to the sea and the difficulty of walking through that section. The fieldwork was arranged to take place during a month and a half in the summer of 2008 (mid-June to end of July), and another month in the autumn of the same year (late November to end of December). Several obstacles were experienced throughout the fieldwork, including bad weather and high tide intervals – the Bristol

Channel has the second highest tidal range in the world. The latter obstacle restricted access to some localities for significant parts of the day.

Hand specimens were examined in the field for physical characteristics, such as colour, grain size, degree of sorting, and sedimentary structures. All the hand specimens were sent to the lab to prepare them for staining. First, the samples were cut into two with an air saw. Then, one slab from each sample was polished, using a vibrating lap. After that, all polished samples were stained according to Dickson's method (1965, 1966). The staining techniques and processes are fully discussed in Appendix A.

Petrographic descriptions were applied to the acetate peels using standard light microscopy. After that, a selected number of samples, based on peel description, were sent back to the thin-sectioning lab. Then, further petrographic description was carried out on these sections. Baby oil was used before describing the thin-sections in order to clearly reveal textures and grains more clearly.

The overall descriptions (peels and thin sections) were used to construct stratigraphic logs. All three logged sections of the HBO were produced using Sedlog, this is software developed by the University of London, Royal Holloway, geologists.

1.5 Data Set

The data provided in the present study have been assembled from almost equal thicknesses in the three localities. All localities have well-exposed vertically-dipping units of the HBO, including all associations and subdivisions. Langland Bay is considered a difficult logged section for the reasons mentioned above, i.e. the presence of dangerous steep cliffs and the proximity of the sea, especially at high tide. The top part of the section is usually exposed when the tide is less than 2m high. At Three Cliffs Bay, the section shows the best exposed unit of the HBO, however, the

tide has its influence on the topmost part which is accessible only at very low tides. At Port Eynon Bay, the lower part of the section seems flat and very easy for logging, while near the top is steep cliff; the topmost part resembles the lower part, though it is usually submerged when the tide is higher than 2m. Some minor scaling errors may be encountered in the Llangland Bay and Port Eynon Bay sections. The geological maps of the three sections can be found in Appendix B.

All peels were prepared at Cardiff University (School of Earth and Ocean Sciences Labs), whereas the majority of the thin sections were made and stained at the Open University. 209 peels and 80 thin sections (12 thin sections were prepared and stained in the Cardiff University labs) have been used in this study. The numbers of peels and thin-sections for each locality are summarised in the table below (Table 1.1).

Location	Llangland Bay	Three Cliffs Bay	Port Eynon Bay
Total number of peels	38	70	101
Total number of thin-sections	18	23	39

Table 1.1 : The total number of peels and thin-sections of the HBO in the three different areas of study.

1.6 Geological settings

Early Carboniferous deposition began with the marine flooding of the Old Red Sandstone (ORS) 'continent' in earliest Tournaisian times. The ORS represents the deposition of a range of alluvial clastic sediments, shed from the Caledonian uplands (Cossey et al., 2004).

During the Carboniferous period, major events occurred. The tropical seas that bordered southern Britain, and which had persisted through the transgression northwards during the earliest Devonian Carboniferous, flooded the remnants of the

Caledonian mountains, resulting in the deposition of thick limestones. By the end of Carboniferous times, the last stage of assembling and bringing the continents together, in order to construct the supercontinent Pangaea, occurred (Fig. 1.2) when the northward-moving Gondwanan plate collided with the southern margin of the Old Red Sandstone (Laurussia) continent. The collision zone is represented by southwest England, constituting the Variscan Orogeny (Cossey et al., 2004).

The Holkerian HBO represents a significant part of the Lower Carboniferous carbonate system of South Wales, the product of an area of shallow-water carbonate deposition bordered to the north by the Wales-Barbant Massif, and to the south by the deep waters of the Culm Trough (Fig. 1.3). This has been named the 'South Wales-Mendip Shelf' (Cossey et al., 2004). Generally, the succession (Fig. 1.4) tends to increase in thickness from NNE to SSW, with the area with the thickest outcrop of the Lower Carboniferous (Dinantian) being to the south of the Pembroke Peninsula, where the exposed section reaches a thickness of 1500m.

The true age of HBO, based on the Carboniferous Time Scale (Fig. 1.5) of Davydov et al. (2004), is the Holkerian Stage (339.2-332.6 Ma), within the Visean Series (345.3-326.4 Ma), within the Dinantian Sub-system (359.2-326.4) within the Mississippian Sub-period (359.2-318.1 Ma), in the Carboniferous System (359.2-299.0 Ma). Tentatively, the boundary between the Devonian and Lower Carboniferous times is marked by a transitional zone, from the fluvial Old Red Sandstone facies to marine limestones and shale facies (Cossey et al., 2004).

According to Scott (1988), the sections of the Holkerian HBO in the current study of the Gower Peninsula exhibit three main formations (Table 1.2), from older to younger respectively. The first formation is the Overton Cliff Formation, which is

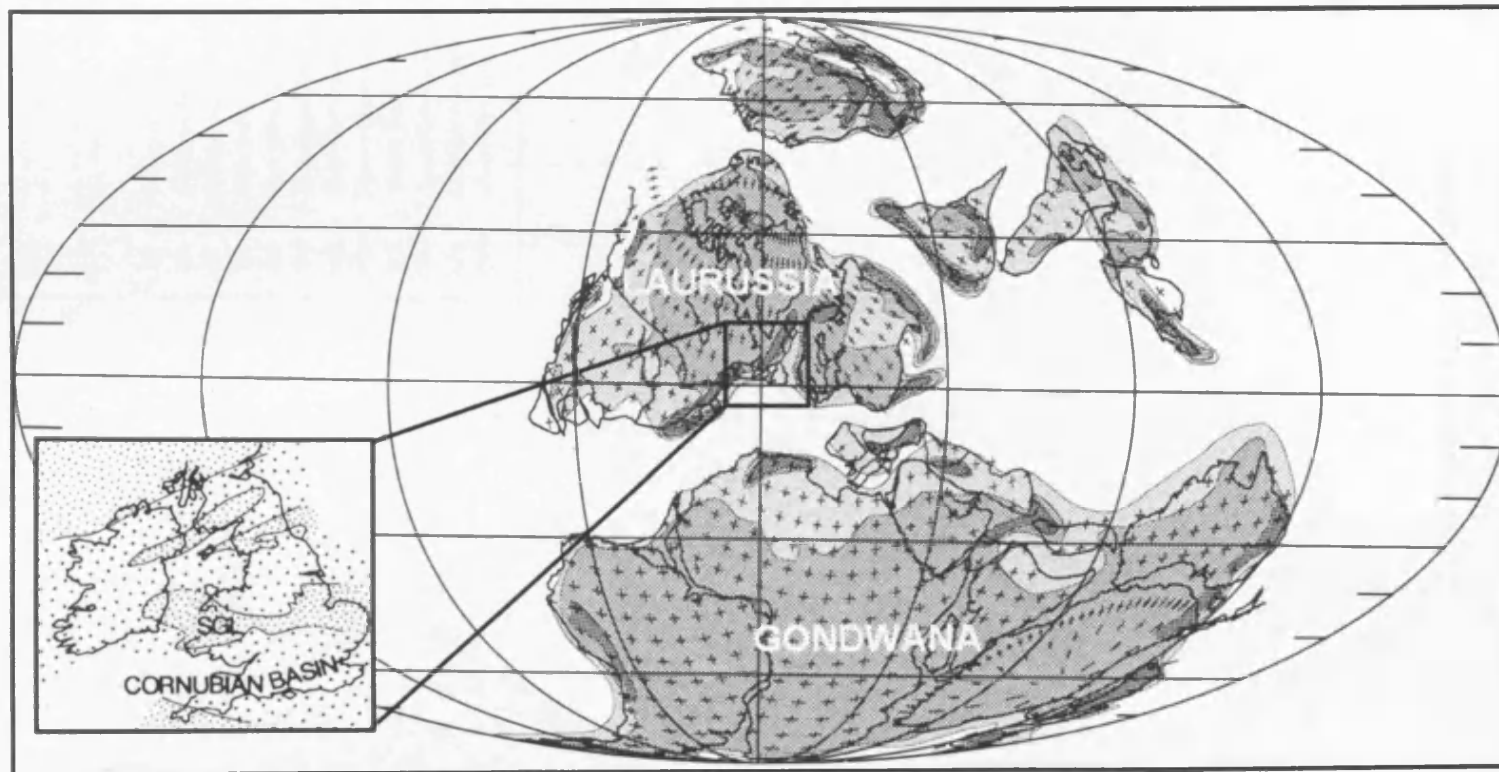


Figure 1.2: Palaeogeography of the Early Carboniferous. Oceans in white, shallow seas light grey, low land dark grey, and darker grey represents mountains. From Scotese et al. (1979). (Inset) Palaeogeography location of Southern Britain around the equator. The open stippled areas show the shallow seas and denser stippled areas are land areas. From Wright (1990).



Figure 1.3: A map view of Britain during the Lower Carboniferous showing the main structures and the position of the South Wales area. From Cossey et al., (2004).

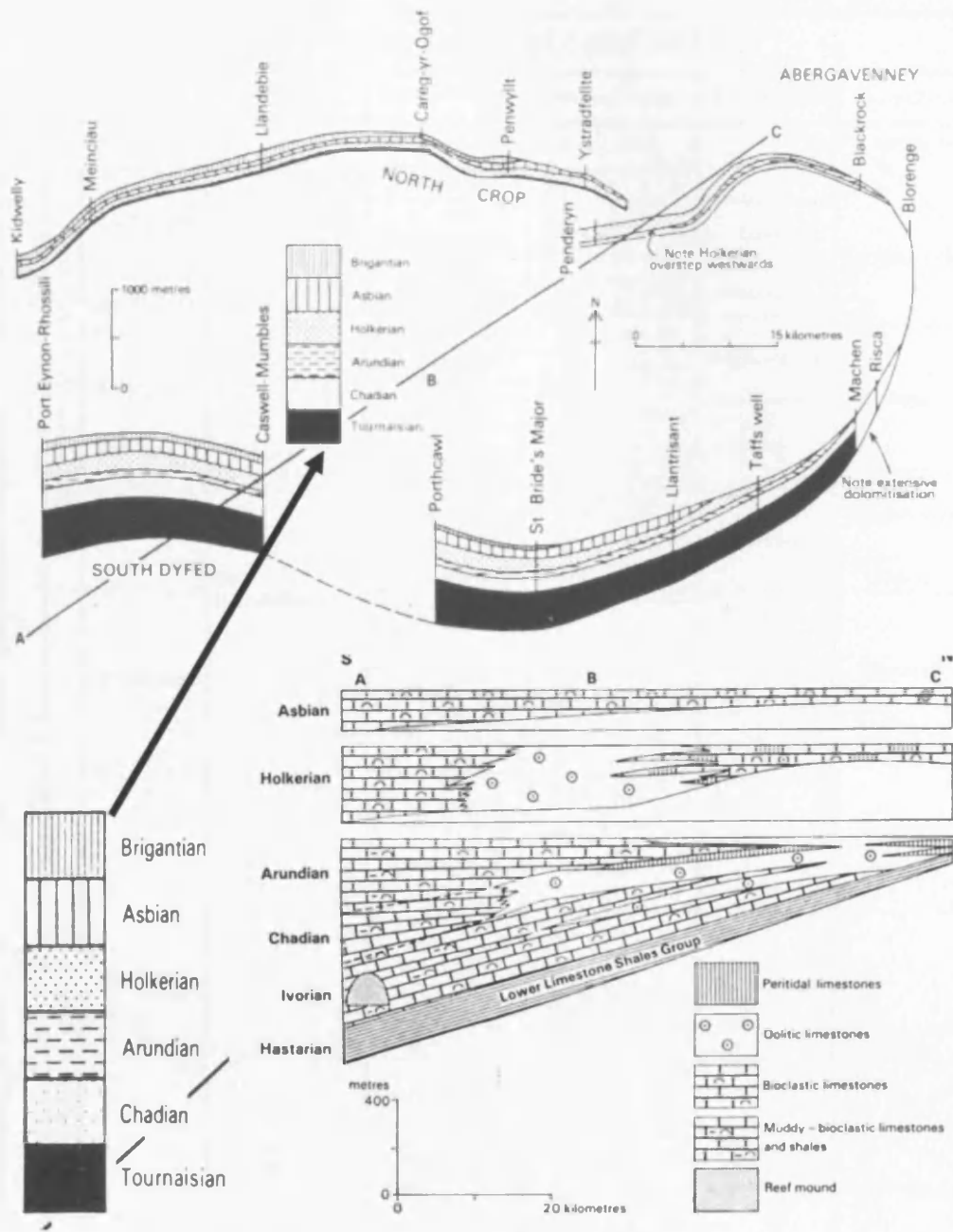


Figure 1.4: Section of part of the South Wales coalfield for the North crop and South crop successions. Note that the details of North Crop stratigraphy must be reconsidered in the light of later studies. From Leeder (1992). A-B-C represents a cross-section of the below succession.

The succession on the left side shows the cross-section (A) South Dyfed, (B) Gower and Vale of Glamorgan and (C) North east of Merthyr. From Wright (1987).

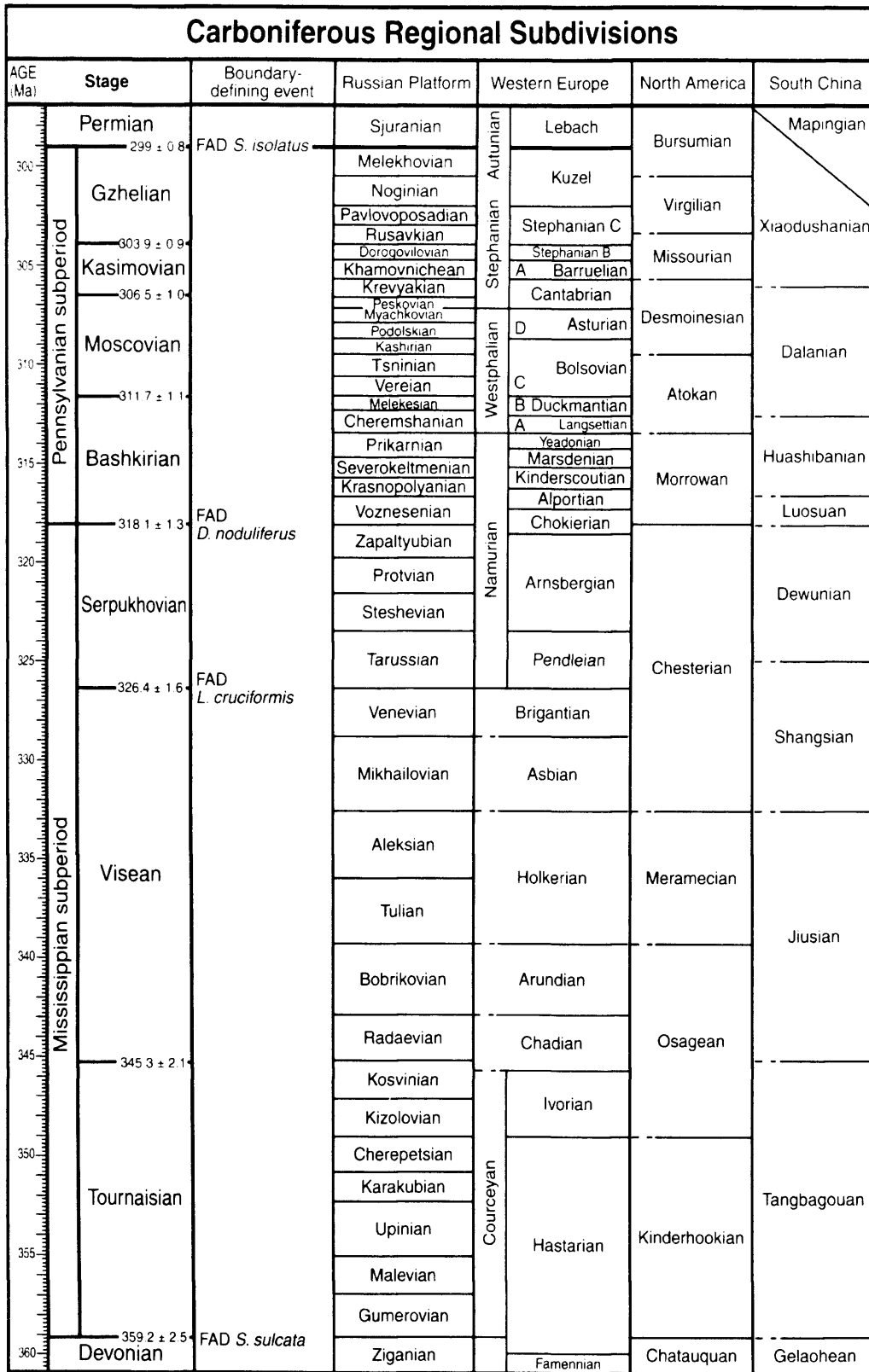


Figure 1.5: The Carboniferous System Time Scale. From Davydov et al. (2004).

Chronostratigraphic Time	Lithostratigraphic Formations	Descriptions
Asbian	Oxwich Head Limestone	Coarse oolitic and bioclastic limestones
Holkerian	Stormy Limestone	Micritic & Cryptmicrobial lithofacies
	Cornelly Oolite	Pwll Du Member: oolitic limestone common, and intraclasts
		Red Champer Member: Fine grained bioclastic limestones
		Deep Slade Member: Dominated by oolitic aggregate grains
Overton Cliff	Bioclastic limestones interbedded with shales	
Arundian	High Tor Limestone	Thickly bedded peloidal, bioclastic limestones

Table 1.2: The three main Formations of Holkerian of South Wales. Modified from Scott (1988).

mainly dominated by bioclastic limestones. The second formation is the Cornelly Oolite Formation, which represents the grainy part of the whole succession, and is dominated by oolitic sequences interbedded with bioclastic and peloidal limestones. This formation is divided into three members, as follows: Deep Slade Member, Red Chamber Member, and Pwll Du Member. The upper formation is the Stormy Limestone Formation which is dominated by more stabilised limestones with micritic and cryptmicrobial lithofacies. These formations are part of the Hunts Bay Oolite Group that was originally divided into two lithological units by Dixon and Vaughan (1911), and Kellaway and Welch (1955) within the Vale of Glamorgan area. Wilson et. al., (1990) referred in to these two divisions at the Cornelly Oolite Formation (CoO) and Stormy Limestone Formation (SrL).

1.7 Tectonics

South Wales experienced a severe Variscan deformation which formed WNW-ESE folds with a thrust-faults belt along the margin. This deformation

influenced the limestones, approximately (Leeder, 1992) during the early Carboniferous extension which took place in South Wales before the inversion of the Variscan shortening in post-Westphalian times. Though the effect of these extensional tectonics, especially to the lithosphere, was the reason behind the Dinantian basin formation (Leeder 1992), the Bristol Channel Basin formed at the junction of the South Wales foreland basin and the Culm Basin, due to Mesozoic extension (Gayer and Jones, 1989). The Devonian successions, thrust over north of Devon, and the Permo-Trias sediments over the Bristol Channel Basin, have obscured the contact between the South Wales Basin and the Culm Basin (Leeder, 1992). The fault structures within the Bristol Channel reactivated the Late Palaeozoic strike-slip fault which has been proved by seismic data to be a south-dipping Variscan thrust (Brooks et al., 1988).

The foreland basin formed within the Namurian-Westphalian D interval (319-305 Ma) by an increasing rate of subsidence with a magnitude of 130-250m/Ma (Burgess and Gayer, 2000). This happened, after Early Carboniferous rifting, in different stages, which started with thermal (Leeder and McMahon, 1988) and ended with flexural subsidence and the loading of thrust-sheets (Gayer et al., 1993). Flexural subsidence, as the mechanism behind the formation of the foreland coalfield basin of South Wales, was proposed first by Kelling (1988) who identified the increasing rate of subsidence, a shifting of the basin to the north direction, and the presence of a clastic-sediments influx from Orogeny to the south. In addition, the propagation of Variscan structures all over the basin, towards the foreland settings, was demonstrated by Gayer and Jones (1989), and Gayer et al. (1993), to confirm the basin model of flexural subsidence. The coalfield basin, a leftover of the eroded major coal basin within South Wales, plunges toward the centre as a synformal structure where the

northern limb dips smoothly south, and the southern limb almost vertically north (Burgess and Gayer, 2000). The overall structures of SW Britain, by the late Carboniferous, are represented by parallel blocks of different compartments that are bounded by NW-SE cross faults (Burgess and Gayer, 2000).

1.8 Sedimentology

The Dinantian successions in South Wales tend to increase in thickness southward and decrease northward, where stratigraphic breaks and different carbonate nearshore facies are found (George, 1958; Sullivan, 1966; George et al., 1976). The indications of these phases are: important cycles within the Dinantian because of tectonic and/or sea-level oscillation (Ramsbottom, 1973, 1977, 1979, 1981); shoaling sequences towards St George's Land; uplift and tilting along with erosion during the Dinantian; and main uplift and erosion by the end of the Dinantian (Leeder, 1992).

1.8.1 Courcayan to Arundian interval:

The sediments of this interval were deposited on a carbonate ramp which dipped southward (Wright, 1986). Ramp facies are distributed on inner, middle and outer-ramp settings, and were mainly controlled by the eustatic sea-level rise and the rate of subsidence. Inner ramp facies, especially those located on the North Crop of the South Wales Coalfield, constitute thin oolitic sandbodies, peritidal limestones, with repetitive cycles of subaerial exposure and fluvial incision due to rare uplifts. Mid-ramp facies outcrop extensively over the South Crop of the Coalfield, and around Bristol and the Mendips (Fig. 1.6). The main sediments associated with mid-ramp settings are bioclastic limestones with evidence of storm activity, and oolitic

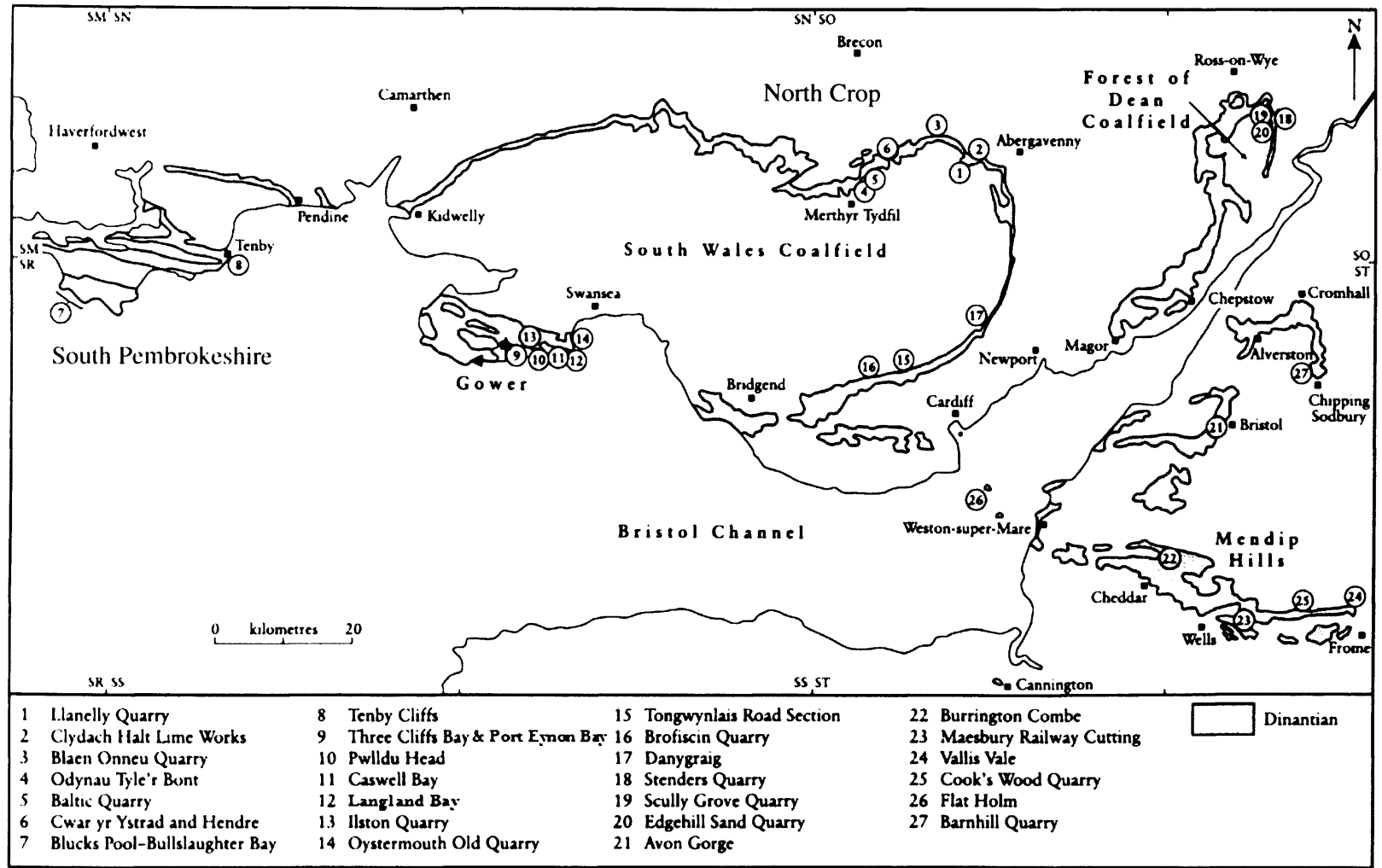


Figure 1.6: A map view of South Wales and Bristol-Mendip district showing the Dinantian outcrop distribution and key localities mentioned in text. Modified from Cossey et al., (2004).

sandbodies, such as the Gully Oolite (Caswell Bay Oolite), which prograded south and likely reflect highstand phases. Finally, outer-ramp facies are found to the south of the Pembroke Peninsula and Knap Farm Borehole, and characterised by muddy bioclastic limestones with rich faunas and mud mounds (Cossey et al., 2004).

1.8.2 Holkerian Period Stage

The Holkerian strata overstep older units in the North Crop due to regeneration of the subsidence or sea-level rise. By the end of this stage, a large sandbody had prograded toward south Pembrokeshire, and relative sea-level fell, which resulted in a non-sequence of general subaerial exposure (Cossey et al., 2004). Holkerian stage in South Wales is characterised by six formations. These formations are thickly bedded and cross-stratified oolitic barrier complex (Cornelly Oolite Formation), protected lagoonal, tabular-bedded dark grey bituminous bioclastic limestone (Dowlais Limestone Formation), back barrier lagoonal, heterolithic formation, interbedded porcellaneous calcite mudstones (Stormy Limestone Formation), offshore bioclastic limestone (Stackpole Limestone Formation), and interbedded limestone and shale (Overton Cliff Formation and Wash Member of the Pen-Y-Holt Limestone) (Scott, 1988; Barclay et. al., 1988; Barclay, 1989; Wilson et. al., 1990).

1.8.3 Asbian to Brigantian Stages

The strata of this interval consist of a thin succession in comparison with the earlier stages. Their facies resemble the shelf areas of northern England, with massive bioclastic, and some oolitic limestone separated by palaeokarstic surfaces and palaeosol clays. By the end of Brigantian stage, deeper-water deposits of Upper Limestone Shales influenced all areas (Cossey et al., 2004).

1.9 Global Sea-Level

Haq and Schutter (2008) reviewed sea-level curves throughout the whole Palaeozoic, by integrating the stratigraphic sections and biochronostratigraphic of pericratonic and cratonic basins. The characteristic cyclothem of the latest Visean record shows the effects of sea-level fluctuations in explaining glacio-eustasy (Wanless and Shepard, 1936; Veevers and Powell, 1987). Figure 1.7 shows only Carboniferous-Permian sea-level oscillations, however, Haq and Schutter (2008) identified 172 eustatic events for the Palaeozoic with a maximum magnitude of approximately 125m. They recorded long-term cycles of gradual sea-level rise during the Cambrian to Ordovician, and eustatic highs within the mid-Silurian to late Devonian, and in the late Carboniferous.

The Carboniferous time period lies within a long-term gradual decline in sea level that started in the late Devonian, until the boundary between the Mississippian and Pennsylvanian, with a short recovery in the early Mississippian (Fig. 1.7). Haq and Schutter (2008) again were able to record the duration (up to approximately 6.0 My) of the third-order cycles for the early-to-middle Mississippian, and described it as a long cycle because the general changes in duration throughout the Palaeozoic vary between approximately 0.5 to 3.0 My.

1.10 Palaeoclimate

The interval from mid-Tournaisian to later Visean was assumed to be a semi-arid climate with seasonal rainfall. Wright (1990) identified this type of climate over southern Britain, during the above period of 20 Ma, by three lines of evidence which are palaeosols, meteoric diagenesis and palaeokarsts. However, studies of palaeosols and palaeokarsts show that the climate during pre-Asbian was stable with rare alternations (Wright and Vanstone, 2001). Southern Britain was positioned around the

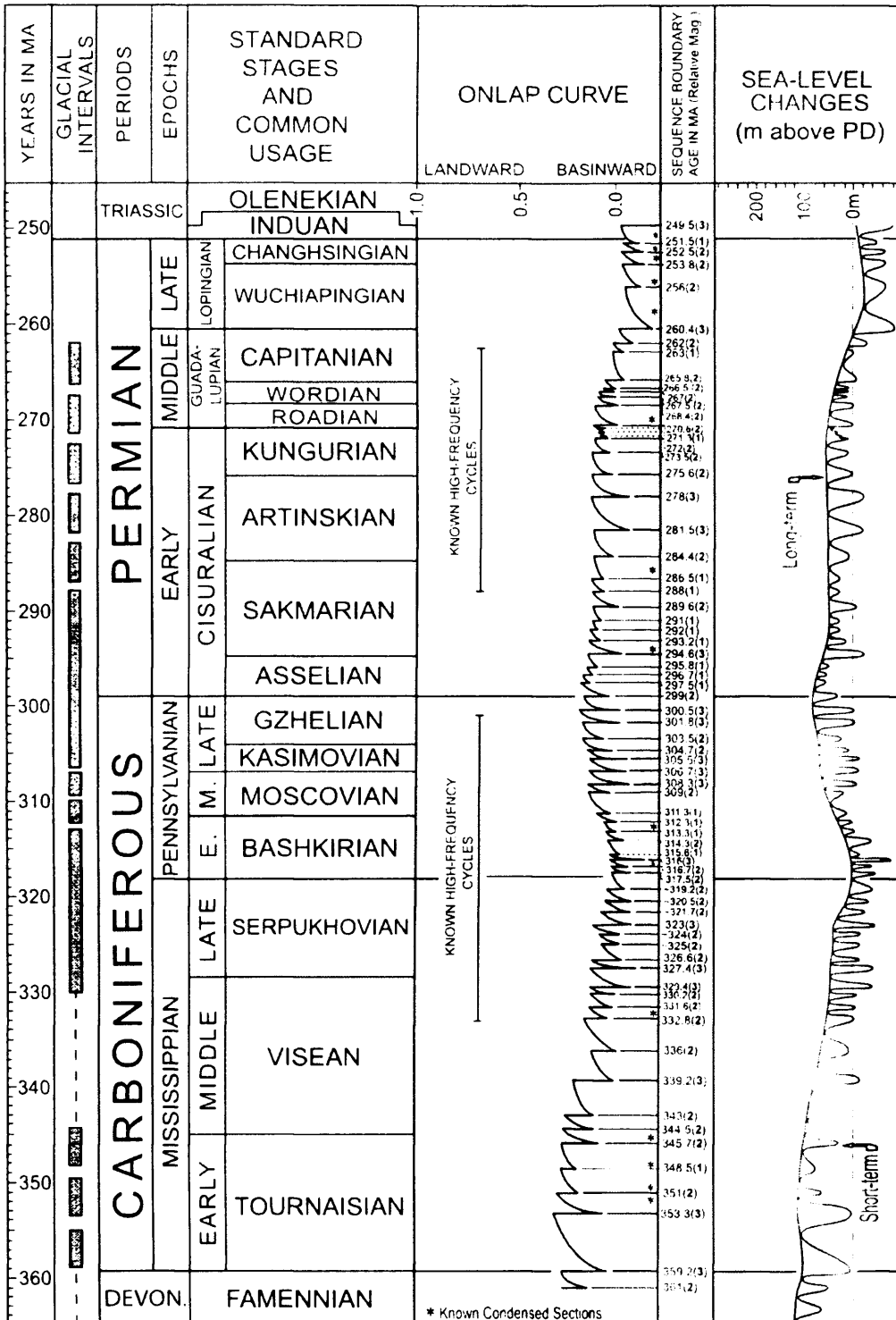


Figure 1.7: Carboniferous-Permian sea-level oscillations that show a long-term gradual decline that was started in late Devonian until the boundary between Mississippian and Pennsylvanian with a short recovery at the Early Mississippian. From Haq & Schutter (2008).

Equator (Fig. 1.2) (Rowley et al., 1985) with a broadly monsoonal system (Wright, 1990) of seasonal aridity. There is currently no detailed information on the Holkerian climates for the South Wales region.

1.11 Glacio-Eustasy

The Late Palaeozoic ice-house interval was the longest lived and most widely spread during the last five hundred million years. It may have alternated between ice-house climate modes, interrupted by greenhouse periods (Bishop et al., 2009). This glacio-eustasy resulted from the dynamics of Gondwana glaciation (Wanless and Shepard, 1936).

All the literature suggests that Carboniferous glacio-eustasy started around the early Asbian time (330 Ma) (Wright and Vanstone, 2001), though the Holkerian of South Wales does not yet show evidence of subaerial exposure surfaces or clear cyclothems. One aspect of this study is to assess the influence of glacio-eustatic sea-level changes on the deposition of HBO. In their recent review of late Palaeozoic glacial events (Glacioeustatic Fluctuation (GEF)), Rygel et al. (2008) recognize eight phases of GEF intervals throughout the Early Carboniferous to Early Permian (Fig. 1.8). Holkerian successions were the phase least influenced by GEF.

Bishop et al. (2009) have also suggested that glacio-eustasy started close to the boundary between the Meramecian and Chesterian of the late Viséan (equivalent to the Holkerian and Asbian boundary). This was based on integrated work on the Yellowpine and lower Battleship Wash Formations (Arrow Canyon, Nevada, USA). These formations were deposited in subtidal to intertidal settings, and their sediments show evidence of little to no subaerial exposure. The isotopic records collected from Tethyan and Euramerican stratigraphy also suggest glacio-eustasy began during late Viséan time (Smith and Read, 2000). The climate transition from greenhouse world to

ice-house world was based on the spreading of glaciogenic sediments, the parasequence patterns formed by glacio-eustatic forcing, and geochemical data (Mii et al., 1999, 2001; Smith and Read, 2000; Isbell et al., 2003; Batt et al., 2007). Hence, Lower Mississippian sediments show features of a greenhouse climate and the upper Mississippian sediments were influenced by an icehouse climate (Bishop et al., 2009).

Isbell et al. (2003) re-evaluated an early Visean glaciation, but Veevers and Powell (1987) proposed that glaciation took place during the Tournaisian time. However, differing views are held, for example by using the positive shifting of ^{13}C and ^{18}O and the radiogenic shifting of $^{87}\text{Sr}/^{86}\text{Sr}$, on the brachiopods of the late Visean. Mii et al. (1999, 2001) summarised events as follow: Tournaisian and/or early Visean glaciation, deglaciation within the Visean and early Serpukhovian, and then glaciation renewed during the Serpukhovian and Bashkirian.

In summary, there are conflicting views of when glacio-eustasy was active during the early Carboniferous, but by studying a very-shallow-water succession, such as HBO, some resolution to this conflict might be achieved.

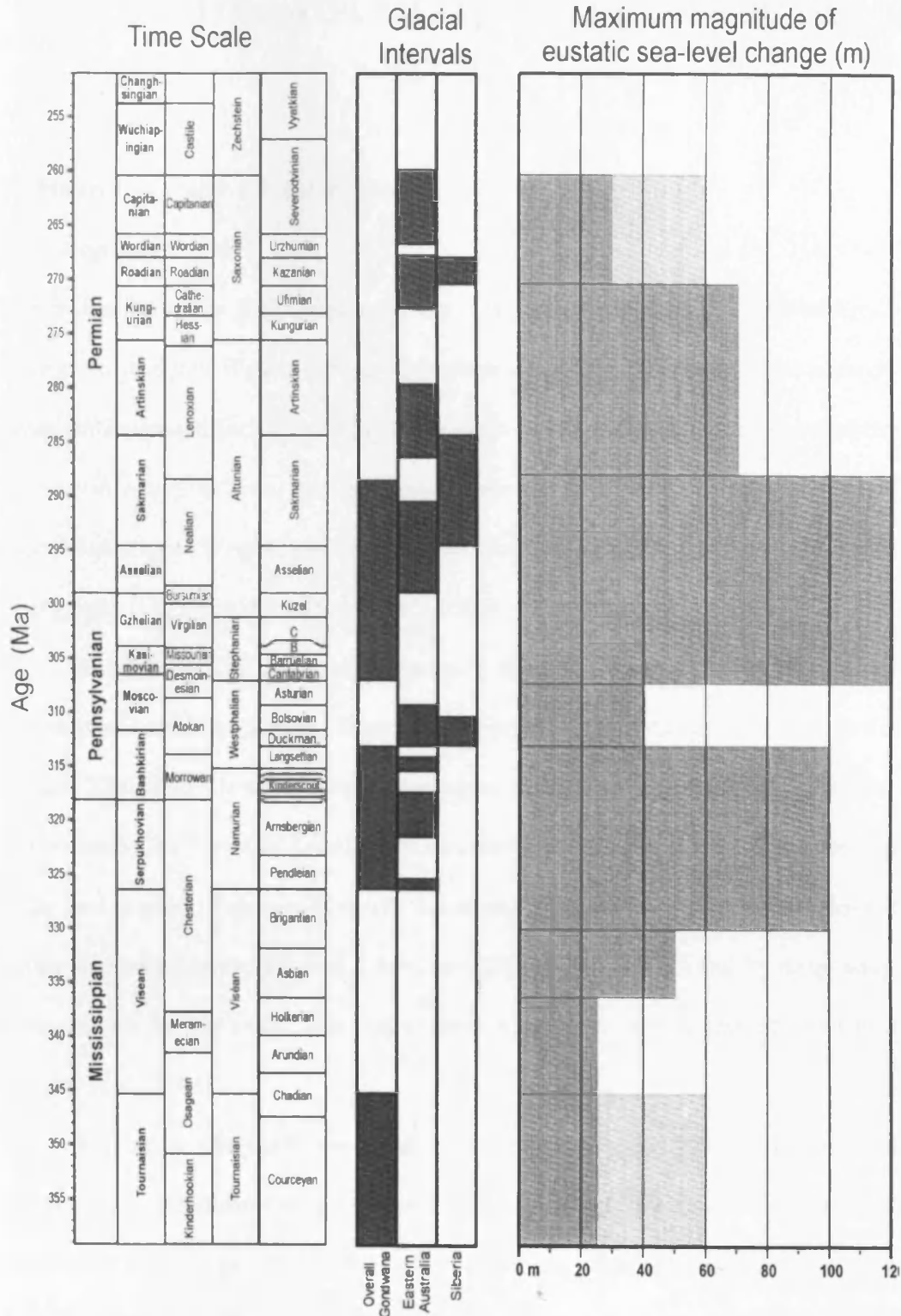


Figure 1.8: The eight phases of glacio-eustatic events that took place during the Carboniferous. In the Maximum magnitude column, the dark grey represents the common values and the light grey are rare events. From Rygel et al. (2008).

CHAPTER 2. LITERATURE REVIEW AND REVIEW OF PUBLISHED

MODELS

2.1 Hunts Bay Oolite Literature Review

2.1.1 Regional Context

The Holkerian Hunts Bay Oolite represents a major part of the early Carboniferous succession in South Wales (with average thickness 270m). It separates the strongly depth differentiated facies patterns of the storm-dominated ramp successions of the Courceyan-Arundian from the generally shallower and highly cyclic Asbian and Brigantian stages (Wright, 1987). The most recent review of the overall setting and stratigraphy is provided by (Cossey et al., 2004).

The Lower Carboniferous carbonates in South Wales are part of a wider province in south west Britain. Some authors refer to this carbonate province as the Mendip Shelf area whose outcrops are bounded to the south west by Milford Haven, to the east by the Forest of Dean, and across the River Severn to Bristol and Mendip in the east to south. This area is mostly dominated by carbonate successions, bounded during deposition to the north by a land area (St. George's Land) and by deep water environments in the south, now represented by clastics successions of the Culm (Cossey et al., 2004).

In earliest Carboniferous times a major transgression flooded the alluvial plains of the Devonian Old Red Sandstone, depositing limestones and shales of Courceyan stage age. During the Courceyan to Arundian interval, a thick progradational ramp succession was deposited over what is now the South Wales Coalfield with intervals of oolitic sandbodies, peritidal limestone, repeated subaerial exposure, and bioclastic limestones all the way to outer ramp facies. During the

Holkerian, there was a rise in sea level which was followed by a major progradation of carbonate sandbodies toward the south. Afterward, in the Asbian to Brigantian times shallow water conditions extended over much of the region with sedimentation controlled by glacio-eustatic sea level oscillations. At the end of the Dinantian, there was an increase in depth affecting all depositional environments which occurred in all areas, associated with the Upper Limestone Shales (Cossey et al., 2004).

2.1.2 Previous Research on the Hunts Bay Oolite

The only detailed study applied to this section was by Ramsay (1987). His aims were to investigate the sedimentary processes, and the depositional environments that had existed within Holkerian times. The Holkerian succession was interpreted as deposits of offshore and lower shoreface on a wave-dominated ramp, due to an increase in depth of deposition on ramp settings, including a tidally-influenced linear marine sand belt and back barrier sand flat.

Ramsay (1987) recognised five different facies through the Holkerian successions (Fig. 2.1); he used the naming method “Facies Association A, B,C, D and E.” this review will briefly discuss these facies and the depositional environments of each association. The facies associated with A are bioturbated packstones; some with lenses, and grainstones, this association was deposited on the offshore. Facies Association B, dominantly either structureless or with minor of sedimentary structures, is for the oolitic limestone alternating with bioclastic packstone or grainstone. This association has been interpreted as a shoreface environment adjacent to an oolitic shoal. Facies Association C, the most dominant facies throughout the Hunts Bay Oolite, consists of different oolite grainstone units such as ebb-tidal channel, laminated ebb-spits around tidal deltas, coarsening-upward sediments of flood channels, and well developed oolitic grainstones. Facies Association D varies

between packstones and mudstone which occur in fining-upward successions which were interpreted as having been deposited in wide lagoons. Facies Association E, the least common facies, is associated with coral bioherms in a lower shoreface setting.

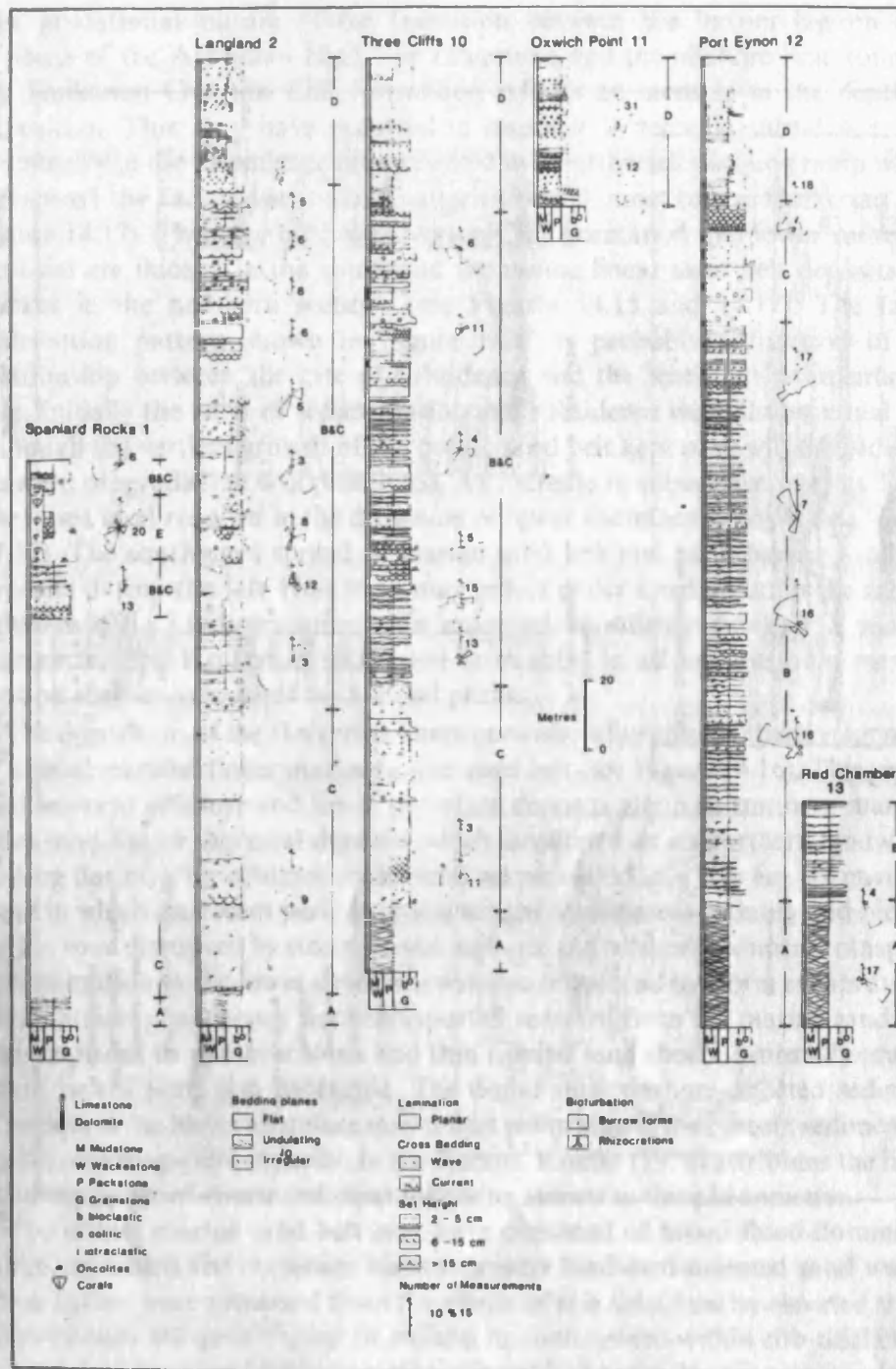


Figure 2.1: sedimentary logs of S. Wales Holkerian in Gower area include lithofacies, sedimentary structures, and palaeocurrent readings. From Ramsay (1987).

2.1.3 Glacio-Eustasy in the Early Carboniferous

One aspect of this study is to assess the influence of glacio-eustatic sea level changes on the deposition of the Hunts Bay Oolite. Rygel et al. (2008) documented eight phases of Glacioeustatic Fluctuation (GEF) in a recent review for the late Palaeozoic. GEF had the least influence on the Holverian. Wright and Vanstone (2001) have suggested that Carboniferous glacio-eustasy started abruptly in the early Asbian times. The very shallow water deposits represented by the Hunts Bay Oolite will likely record any early signs of glacio-eustatic activity before the Asbian.

2.2 Review of Published Models of Modern and Mississippian Oolitic Carbonate Sandbodies

In this section, a number of examples of modern and ancient sandbodies will be discussed as a framework, and then used later to assess possible analogues for the HBO. Categorising different types of sandbodies, based on the modern examples, indicate that the deposystems are associated with tidal, wave and storm activities, and are distributed in platform margins or on ramp settings. As a result, these sandbodies have been classified into four major types according to their dominant processes: tide-dominated, wave- and tide-dominated, wave-dominated, and aeolian sandbodies.

The first two categories relate to rimmed steep-margined platforms and are divided into four major types: tidal bar belts, marine sand belts, tidal deltas and tidal sand waves. All the above types have modern examples that will be discussed briefly, followed by ancient examples. Sandbodies deposited by tide-dominated processes vary in their architectures based on the energy levels exerted on the transport paths (Johnson and Baldwin, 1996), producing ribbons, sand waves and sheets with complex internal structures. These structures are less well known in the modern

carbonate system, even with the variation in energy levels. Table 2.1 summarises the details of each example.

2.2.1 Tidal bar belts

Tidal bar belts are elongated shoals and are perpendicular to the platform margins due to high energy tidal flows with magnitudes exceeding 1m/s. Modern examples linked with this type of deposition are the southern margin of the Tongue of the Ocean, and Exuma Sound in the Great Bahama Bank (Fig. 2.2) (Ball, 1967). The structures and sediments associated with these bars reflect sand waves and show a coarsening-upwards sequence where storm layers at the base are overlain by trough and planar cross-stratification at the top; the sediments are oolitic as a main element of the bars. Between the bars, sea grasses and microbial mats are common with scattered sand waves.

An ancient example of the tidal-bar belt model is the Mississippian of the Illinois Basin and West Virginia (Fig. 2.3) (Kelleher and Smosna, 1993). Here, sediments are dominated by bioclastic grainstones and packstones sealed by muddier facies. Visean sandbodies developed as tidal bars in a northwest-to-southwest direction, with the thickness of the oolitic body varying from zero to a maximum of twelve metres, and located in a ramp-like setting between the basin setting deposits and a ramp-like shallow platform.

2.2.2 Marine sand belts

Characteristic of this sandbody type are extensive sandflats parallel to the platform margin; tidal processes are not strong compared with those forming the tidal-

Table 2.1a. Comparison between modern and Mississippian example of oolitic sandbodies. Mo: modern; Missi: Mississippian.

	Tidal bar belts	
	Missi.: Greenbrier Group Kelleher & Smosna (1993)	Mo.: Exuma Sound Ball (1967)
Length / area	0.5-5 km	12-20 km
Width	.5-1.5 km	0.5-1 km
Thickness	5-12 m	3-9 m
Spacing	0.7-4 km	
Grain type	Peloids & ooids	Ooid growth
Ave. Grain size	47-66% medium sand sized ooids	Medium sand size, well-sorted
Geometry	flat-bases and convex tops	
Internal architectures	Large to medium trough cross-beds and planar beds, bidirectional foresets, tidal bedding, desiccation, reverse grading, wavy and ripple bedding, reactivation surfaces, sand holes, mud drapes, tidal bundles, planar erosion surfaces.	Storm-layered bases to trough and planar cross-stratification. Burrowed oolitic Medium- and small- scale cross-beds sets Medium-scale ripples
Associated facies	bioclastic grainstones and packstones, draped by muddier facies	Megaskeltons (clam & gastropods shells) Muddy pelletoidal sediments.
Contacts	Overlain by red shales with subaerial-exposure	
Other features	Spillover lobes Pelletal-skeletal packstones.	Spillover lobes (L: 3000 ft, W: 1500 ft)
Palaeocurrent patterns		
Relation to bottom topography	Perpendicular to the platform margin and parallel to Greenbrier hinge line.	Upon the crest of slope break at the platform margin
Orientation	Foresets dipping 15-30 degrees. Bars trend NW-SE.	Variable, dipping at 5-10 degrees. Convex up toward the east

Table 2.1b. Comparison between modern and Mississippian example of oolitic sandbodies. Mo: modern; Missi: Mississippian.

	Marine sand belts			
	Missi.: Damme Field Handford (1988)	Missi.: Holkerian S. Wales Ramsay (1987)	Mo.: Joulter's Cays Harris (1979)	Mo.: Lily Bank Rankey et. al., (2006)
Length / area	16 km	15 km	40 km / 400 km ²	27km
Width	3.2 km	6 km	1-2 km	4km
Thickness	5.5 m	60-280 m		
Spacing				40m
Grain type	Porous, skeletal, ooid grainstones Sandy peloid-ooid skeletal grainstones	Oolitic grainstones	83% ooids, 4% skeletal grains, and 1% mud	
Ave. Grain size	Coarse-grained	Coarse to fine grained	very well sorted medium sand-size	
Geometry	Lenticular body of shallowing upward succession along seaward margin	A shore-parallel linear marine oolitic sand belt where it is thicker towards the north.		linear shoulder bars (asymmetrical) and parabolic bars (symmetrical)
Internal architectures	Bipolar cross-beds Ripples	Burrow-mottled Planar cross-sets Trough cross-sets Small-scale wave-knitted cross sets Fining-upward sequence Planar-lamination Coarsening-upward sequence	Thin laminae to thin beds.	sandwaves (up to 1m tall), sandwaves (about 0.75m high), large- or medium-scale cross stratifications in the dip direction
Associated	Skeletal	Packstone, wackestone and	skeletal grainstone, ooid grainstone, mixed ooid	well-sorted ooid grainstone on

Table 2.1b. Comparison between modern and Mississippian example of oolitic sandbodies. Mo: modern; Missi: Mississippian. (continuous of Table 2.1a above)

facies	wackestones Quartzarenites Lime mudstones	mudstone of bioclastic sediments	grainstone to packstone, mixed fine peloid packstone to grainstone, pellet wackestone to packstone, and lithoclasts packstone.	the crest and moderately sorted siltier mud-lean packstone away from the crest
Contacts	From the bottom a gradational change open-marine skeletal wackestones From top interbedded with quartzarenites	Gradational contact with Arundian High Tor Limestone (barrier-lagoon-inlet). Terminates at a marked erosion surfaces with soil profile.	Abrupt contact with the shelf in the east and gradual contact with the interior of the platform in the west.	
Other features	Scours and lenticular channel- fill on strike oriented		Scattered Tidal channel systems and islands	
Palaeocurre nt patterns		Offshore transport toward the south. Bimodal pattern with landward- and seaward-oriented modes.		sandwaves show two different orientations on the flanks (121° and 62°) but both are perpendicular to the flow
Relation to bottom topography	Parallel to slope break and depositional strike	Parallel to depositional strike		parallel to a shelf break
Orientation	NW-SE			

Table 2.1c. Comparison between modern and Mississippian example of oolitic sandbodies. Mo: modern; Missi: Mississippian.

	Tidal Delta	Tidal Sandwaves
	Mo.: Lee Stocking Island, Bahamas Gonzalez & Eberli (1997)	Mo.: The Strait North of Yucatan Harms et al., (1974)
Length / area		10 km ²
Width		
Thickness / Volume	5.5-6 x 10 ⁵ m ³	5-6 m
Spacing		10 m in the centre, 100-400m north
Grain type	oooids	Ooids and bioclastic debris.
Ave. Grain size	Well-sorted medium sand size on dunes. Coarse grained sand in the inlet.	Well-sorted, fine-grained ooids, mixed with coarser bioclasts.
Geometry	Crest of sand waves contains steep lee and a gentle stoss side, current ripples and small dunes. Ebb stoss covered with climbing cusped and linguoid ripples, and composite dunes.	Asymmetrical sandwaves
Internal architectures	2- and 3-D dune Ripples	Ripples, small dunes (several centimeters high) and small sandwaves (less than 0.5 m high).
Associated facies	Bioclasts and interacls	Lithoclastic particles of sand to small-pebble sizes.
Contacts		
Other features		Average velocity 50 cm/sec. sediments have bimodal distribution.
Palaeocurrent patterns		
Relation to bottom topography		Fairly flat gently sloped.
Orientation	Slope angle 24.2 ^o	Very gentle sloping northward.

Table 2.1d. Comparison between modern and Mississippian example of oolitic sandbodies. Mo: modern; Missi: Mississippian.

	Barrier Island and Strandplains		Wave-dominated Sandbody
	Missi.: Gully Oolite Southwest Wales Burchette et al. (1990)	Mo.: Turks and Caicos Island, Long Bay (Lloyd et al, 1987)	Mo.: Kuwait-Saudi Arabian Coast of the Arabian Gulf Lomando (1999)
Length / area	150 km	5 km	Several kilometers
Width	30 km		
Thickness / Volume	19-80 m	0.5-2.5 m	
Spacing			
Grain type	Bioclasts, ooids	Oolitically coated particles.	Ooid, skeletal, intraclast grains
Ave. Grain size		Well-sorted, well-rounded medium-grained coated ooids.	
Geometry	Progradational strandplain, drowned barrier, migrated barrier landward.	Linear beach with sand-sheets	Shoal complex, well-developed coast ridges, tidal delta-channel.
Internal architectures	Medium-scale cross-stratified oolitic grainstones and packstones. Bioturbation packstones. Trough and planar cross-stratified oolitic grainstones, and tabular sets of low-angle cross-lamination. Coarsening upward sequence.	Dunes and ripples.	
Associated facies	Bioclastic wackestones Oolitic grainstones	Few fractions of coarser, uncoated skeletal grains.	
Contacts	Capped by palaeokarst and/or a palaeosol. peritidal back- barrier limestones.	Migrated sandwaves barlike sand buildups intersect with Long Bay Beach in offshore.	
Other features	Hardgrounds, oolitic intraclasts, and calcrete palaeosol.	Intensive boring by endoliths. Nearshore sand are poorly sorted with high fractions of skeletal frag.	hardgrounds
Palaeocurrent patterns	Polymodal directions		
Relation to bottom topography		Deposited on epeiric platforms.	Parallel to the bathymetry.
Orientation	Along strike.	Northeast-trending	

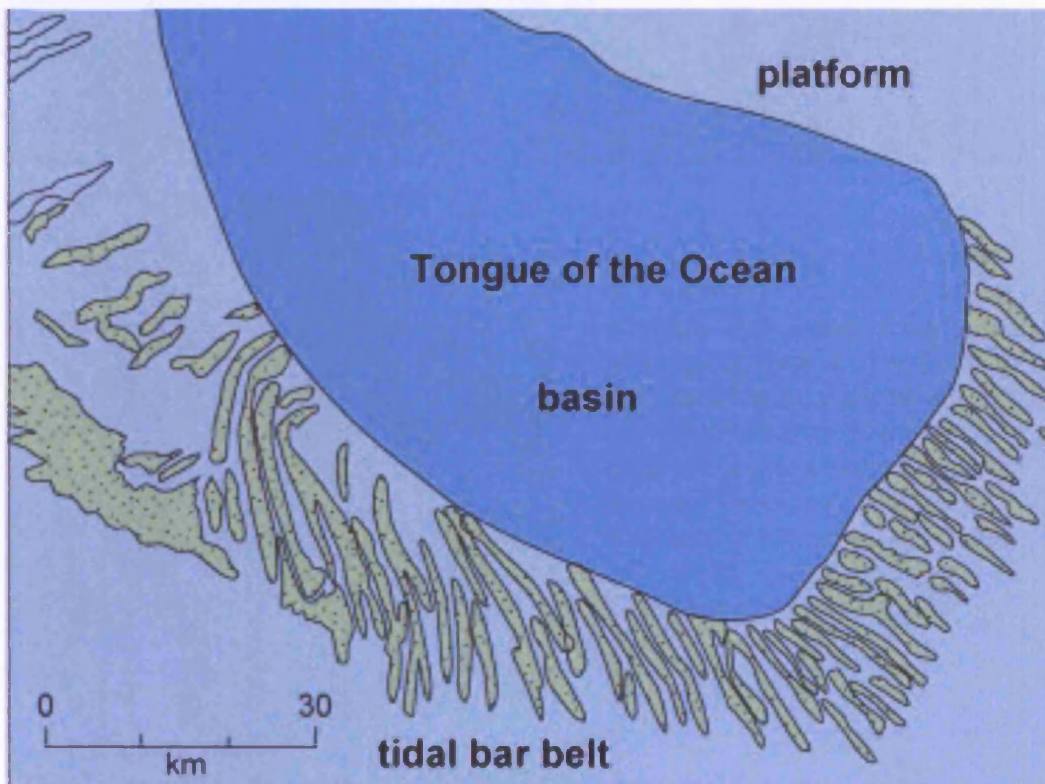
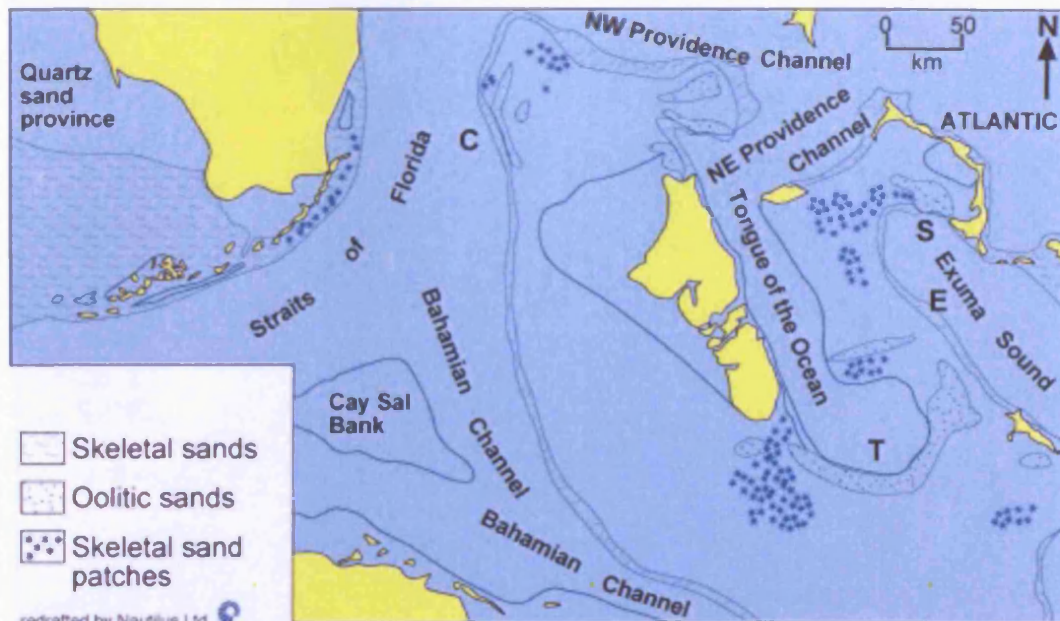


Figure 2.2. Upper: map of the general sand types on the Great Bahama Bank. The letters represent Holocene ooid shoals as follows: C: Cat Cay oolitic marine sand belt; E: Oolitic tidal deltas in island gaps on the margins of Exuma Sound; S: Schooner Cays oolitic tidal-bar belt; and T: oolitic tidal bar-belt at the south end of the Tongue of the Ocean. Below: map of the tidal bar belts, south of the Tongue of the Ocean. (Wanless and Tedesco, 1993).

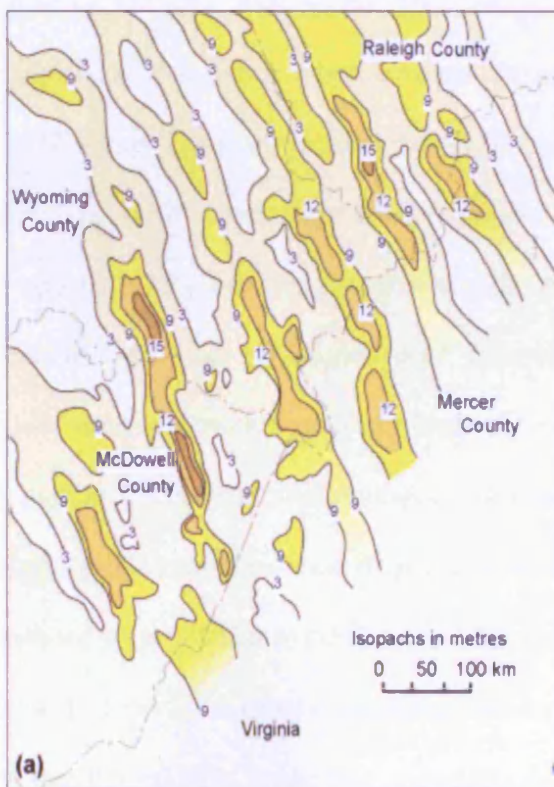
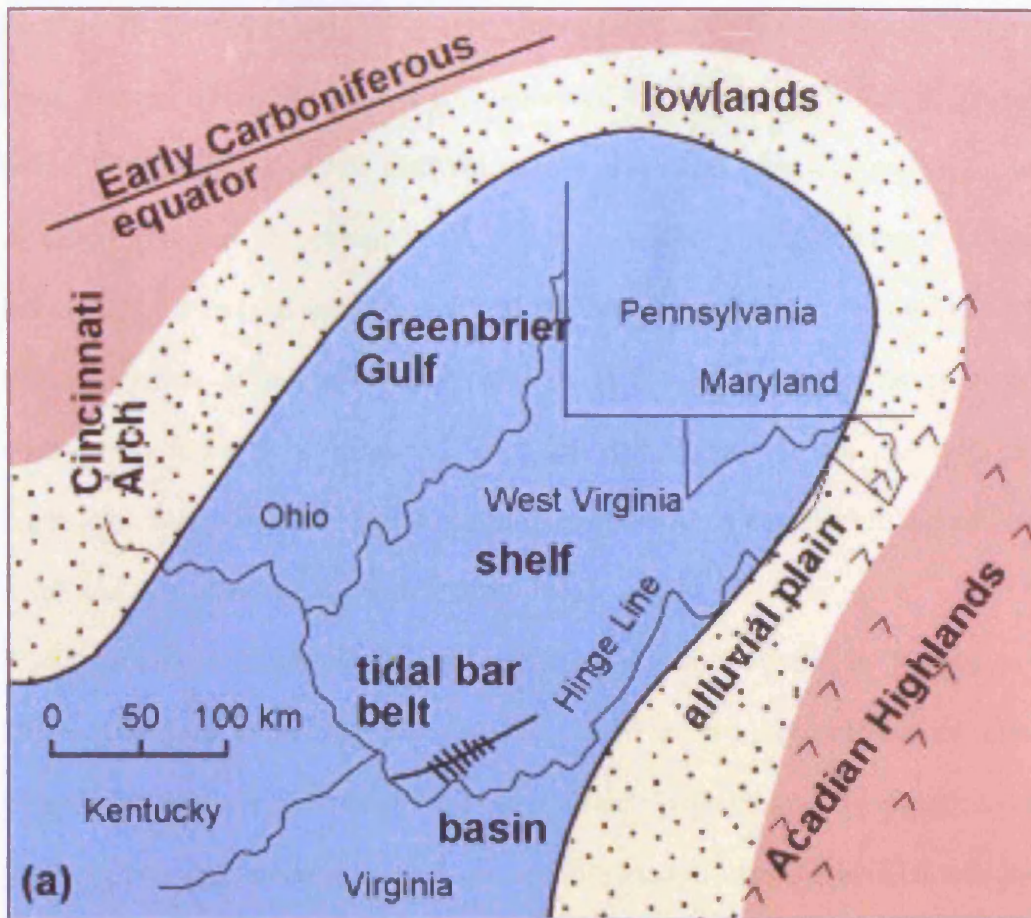


Figure 2.3. Ancient example of a tidal-bar belt model, the Visean of the Illinois Basin and West Virginia. Top: a map of the palaeogeography of Greenbrier Gulf showing tidal-bar belts along a tectonic hinge line. Left: these are oolitic sandbodies, running NW-SE, showing the thickness of the oolitic sand with the contour lines. Based on Kelleher and Smosna (1993).

bar belts (Ball, 1967; Hine, 1977). The oolitic facies are dominant in the windward areas, whereas the leeward areas are dominated by peloids and bioclasts, plus the ooids that migrated across the platform interior. The sandbodies may extend for tens of kilometres, and be approximately 1-4km in width. The sedimentary deposits, influenced by both tidal and wave activity, without a strong ebbing flow, have several features such as asymmetrical sandwaves up to 2m high, but they become more symmetrical toward the crest of the shoal. Tidal channels cut through these sandbodies. Storm activities have resulted in spillover lobes with dimensions of 500m width and an avalanche 1.5m high (Harris, 1979).

Recently a classic marine sand belt shoal has been revisited by Rankey et al. (2006), Lily Bank in the Bahamas (Fig. 2.4). There are two morphologies associated with the geometry of the studied ooid shoal: linear shoulder bars (asymmetrical) and parabolic bars (symmetrical), which are part of a marine sand belt parallel to a shelf break (27km long, 4km wide). The parabolic bars are similar to Ball's (1967) and Hine's (1977) spillover lobes, whereas the asymmetrical ones are similar to Hines's (1977) ramp. The asymmetrical bars characteristically have a gentle inclination, up to 2km long, with steeper slopes, where parallel sandwaves (up to 1m tall) ornament the crest of the bars oriented to the linear shoulder bar crest, approximately 40m from crest to crest, with well-sorted ooid grainstone on the crest and moderately sorted siltier mud-lean packstone away from the crest. The symmetrical bars features are complex: linked bars and sinuous-crested bars, including sandwaves (about 0.75m high); sandwaves show two different orientations on the flanks (121° and 62°) but both are perpendicular to the flow, and the average spacing between the bars is around 22m. However, the general stratigraphical model for these bars is comparable to that of Handford (1988). These bars, especially the linear shoulder bars, are flood- and/or

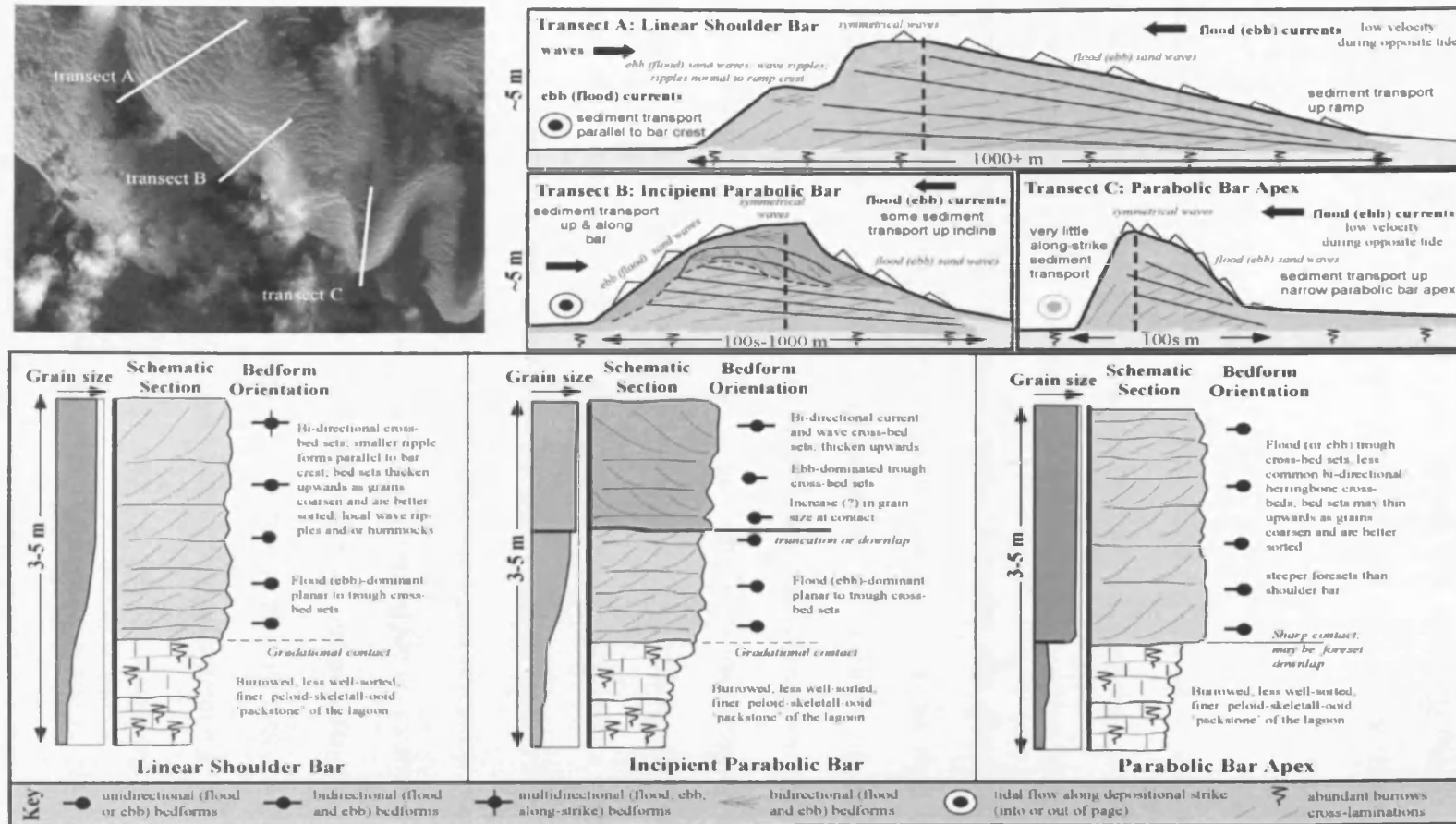


Figure 2.4. shows the stratigraphic model of ooid shoals analogous to Handford (1988), where (A) represents the suggested geometries across linear shoulder bars, (B) across parabolic bars, and (C) across the apex of a well-developed parabolic bar. The logs relate to the A, B and C, respectively. From Rankey et al., (2006).

ebb-tide dominated with gradual shallowing, and coarsening-upward sequences. Another example of the flood-dominated parabolic bars described by Ball (1967) has basal units of large- or medium-scale cross stratifications in the dip direction.

Joulter's Cay, north of Andros Island (Fig. 2.5) (Wright, 2008), is another modern example of a marine sand belt with extensive leeward sandflats, which cover an area of 40km². Several tidal channels cut through the sandbody (Harris, 1979). Ramsay (1987) interpreted the Holkerian succession (Fig. 2.6) as an ancient sand marine belt dominated by oolitic facies that formed as a linear sandbody parallel to depositional strike, and was cut by ebb-tidal channels preserved only at the upper part of the succession. A linear shoal separated the muddy wackestone, oncolitic sand-flat deposits, which characterise a submerged slope, from storm-influenced lower shoreface and low-energy setting offshore packstone deposits. Ramsay (1987) proposed that the Holkerian succession was deposited as a regressive progradational phase where the tectonic subsidence was the major control.

An additional example of an ancient marine sand belt, described by Handford (1988), comes from the St. Louis Limestone of the Damme Field in Kansas (Fig. 2.7) in a ramp-like setting. This sandbody, formed parallel to the strike of deposition, made of oolitic grainstone. With the sandbody are spillover lobes, bankward, showing a dominant large-to-medium cross-stratifications overlain by small-scale cross-stratifications, with variation in palaeocurrent directions between the ramp and shield units.

2.2.3 Tidal Deltas

Sandbodies of this type relate to tidal inlets, and are controlled by tidal flooding and ebbing (Gonzalez and Eberli, 1997). Usually, the upper part of the sandwaves or the crest is characterised by small 2-D and 3-D dunes with well-sorted

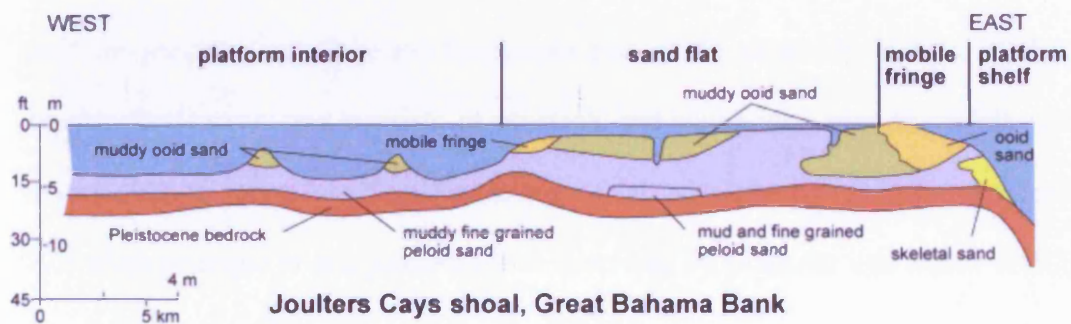
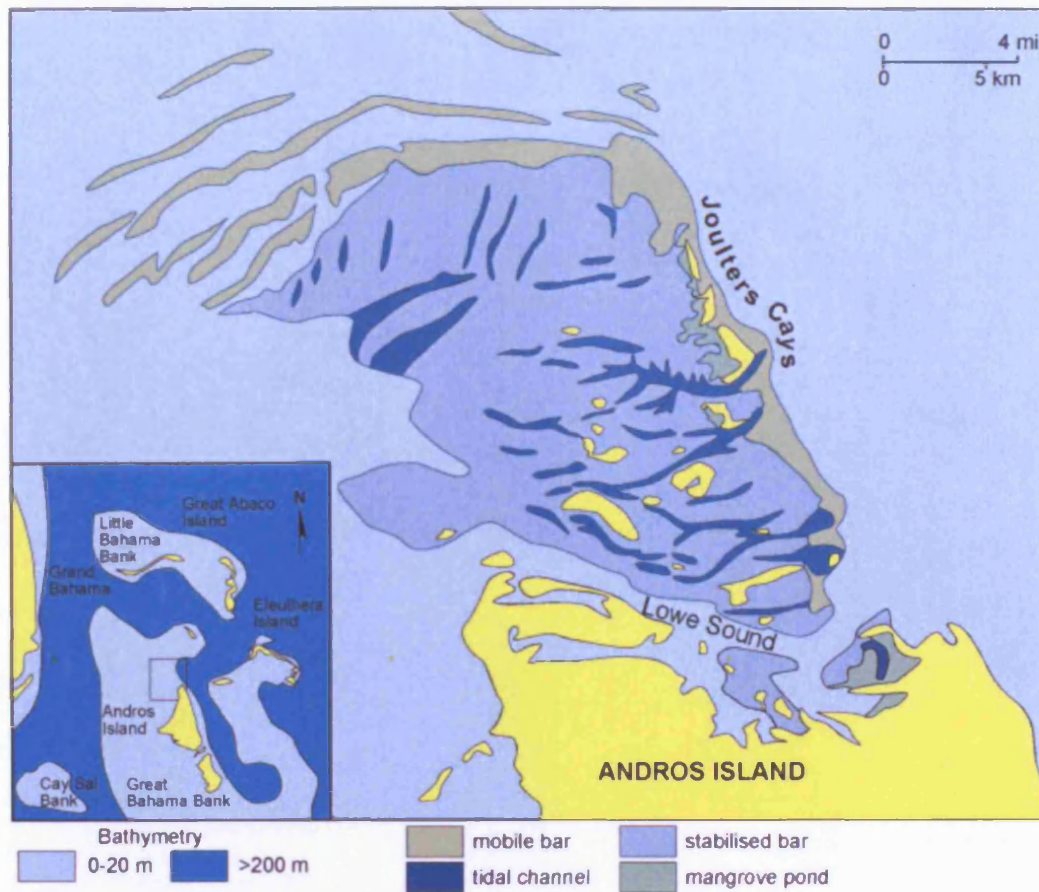


Figure 2.5. Top: a map showing the Joulter's Cays ooid shoal. Below: a cross-section of the north of the Joulter's Cay marine sand belt from East-West. From Wright (2008).

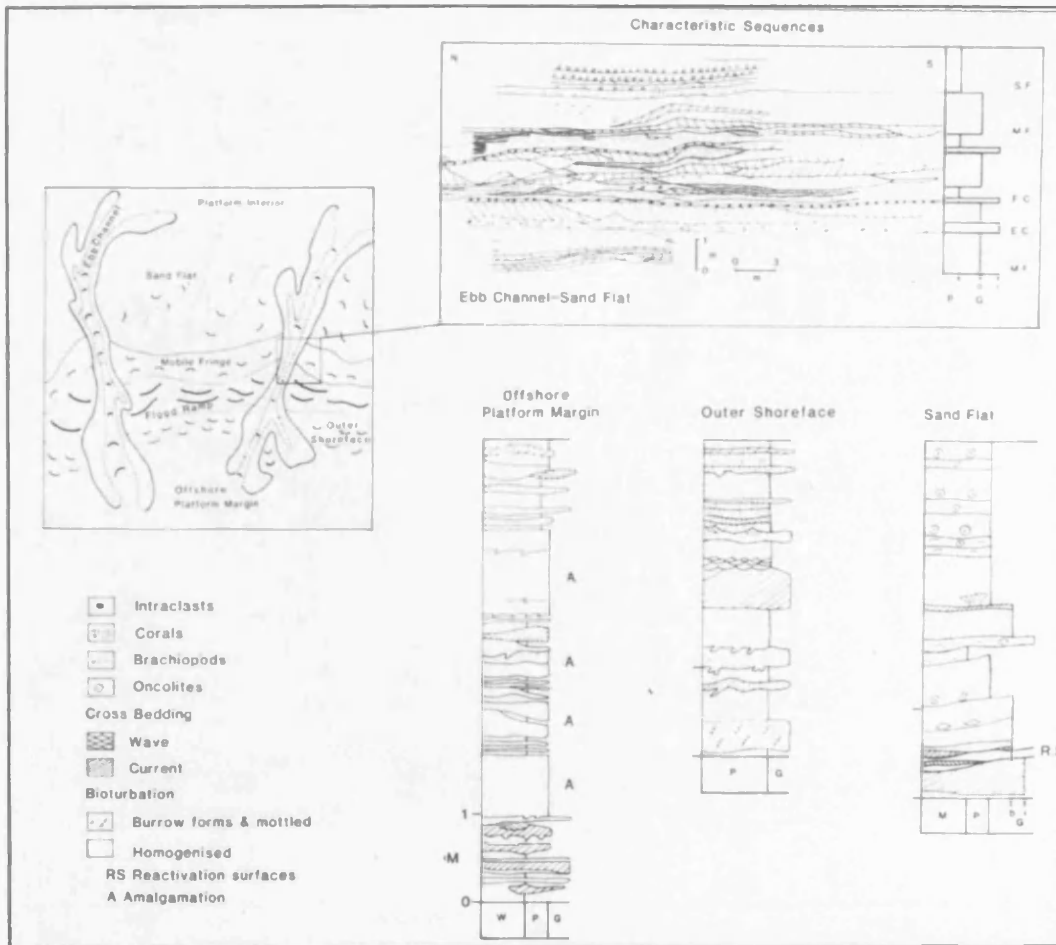


Figure 2.6. Suggested Holkerian depositional model from Ramsay (1987), that is dominated by a parallel oolitic marine sand belt traversed with ebb-tidal channels.

medium-grained ooids, whereas the deeper part of the sandbody is dominated by bipolar sand waves and consists of bioclasts and intraclasts plus the ooids. The associated tidal ranges are classified as microtidal, with a current velocity of 0.6m/s. A modern example of this sandbody was described by Gonzalez and Eberli (1997), from Lee Stocking Island in the Bahamas (Fig. 2.8).

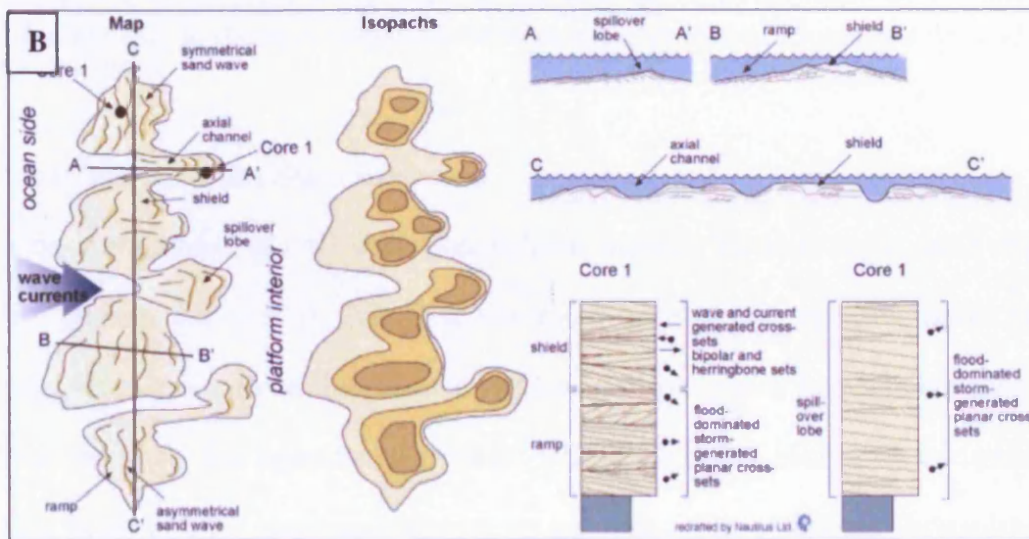
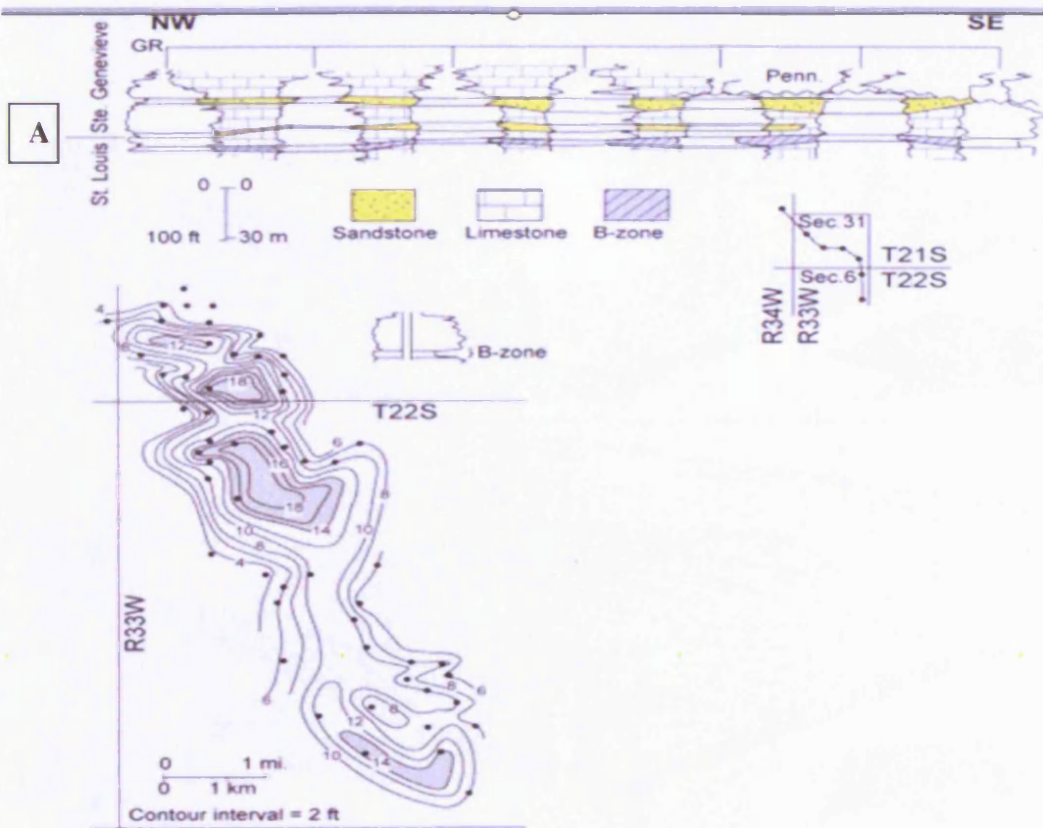


Figure 2.7. A) Example of an ancient marine sand belt, described by Handford (1988), from the St. Louis Limestone of the Damme Field in Kansas.
 B) Idealised model by Handford (1988) shows important characteristics of a marine sand belt.

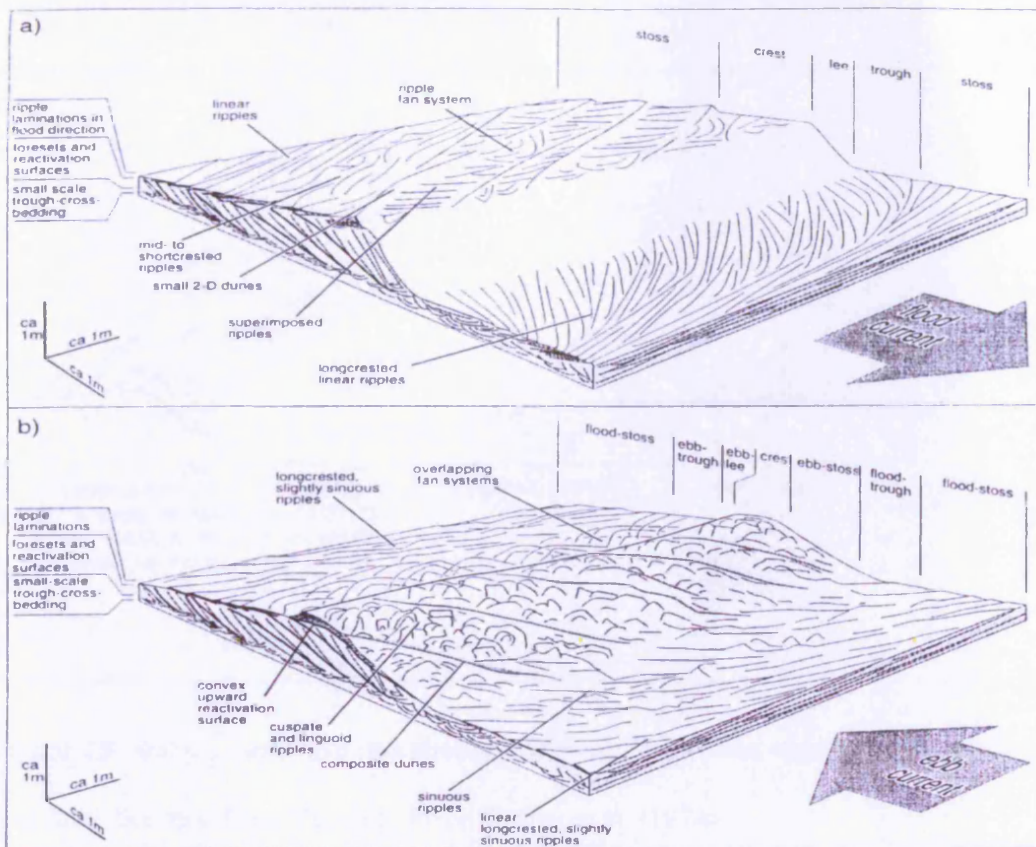


Figure 2.8. Two models of Lee Stocking Island: a) shows the sandwave architecture after flooding; b) shows the sandwave architecture after ebbing. From Gonzalez and Eberli (1997).

2.2.4 Tidal and Long Shore sandwaves

A modern example of tidal sandwaves is found north of Yucatan, in the Strait (Fig. 2.9) (Harms et al., 1974). This area, dominated by stacks of sandwave layers and subaqueous dunes, has carbonate sand that has been transported from adjoining areas from the south; it is approximately 10km^2 with a 5-6m thick blanket of sandwaves. Ideal sandwaves are composed of two main sediment grains, which are distinguished clearly by their sizes. The finer grains, almost all are ooids, are well sorted and greatly polished, and formed within very active wave areas and high energy settings, then migrate northwards. Where the coarser grains are dominated by bioclastic sediments,

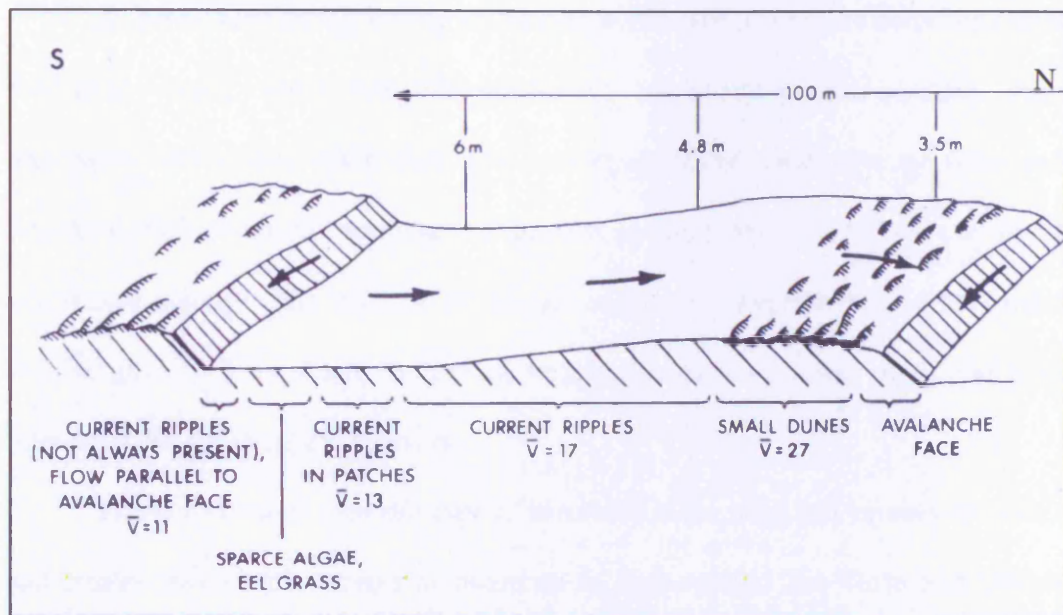


Figure 2.9. Simple sandwave morphology, showing bed forms, depth, crestal spacing, and flow direction from Yucatan. From Harms et al. (1974).

with variation in their shapes and internal pore spaces, they show a range of sources and different hydraulic processes. The structures of this sandbody are characterised by several features typical of such a carbonate system. Each sandwave, ranging from 1m to 3m in thickness, in a transverse direction to the current, represents a tongue shape and is strongly asymmetrical. In the central area of the Strait, the beds are flattened and banded with light- and dark-coloured sediments. The light-coloured bands are characterised by small sand waves and dunes, centimetres in thickness, covered with ripples, and described as active transport sand or active rout. The dark-coloured bands are more stabilised by algae, almost flat topped, and composed of fine-grained sand and silt-sized carbonate.

2.2.5 Barrier and Beach Sandbodies

As mentioned earlier in this section, carbonate sandbodies are associated with four major types, which are tide dominated, wave and tide dominated, wave dominated, and aeolian sandbodies. The next examples of sandbodies are wave and tide-dominated which are an essential process in ramp successions, as well as in siliciclastic systems. The majority of ancient sandbodies were formed as microtidal with ranges of <2 m, where the typical beach sequence, washover sands and tidal inlet-delta, are the common deposits.

The main control over this type of sandbody is the wind that agitates the water and creates waves and currents of moderate to high energy. The Turks and Caicos sandbody example (Fig. 2.10) of a prograding, beach-fronted strandplain proves that ooids can form in moderate- to high-energy shoreface and beach settings without strong tidal currents. The sandbody at Long Bay (Lloyd et al., 1987) is characterised by sheet-like beds of oolitic sand with a maximum thickness of 5m, in places as thin as 1.5m thick, with a length of 5km. However, details of stratification types are available, but the main sediments are dominated by well-developed, well-sorted and medium-grained beach sand of coated particles of oolitic facies, with some skeletal grains. Within 1km offshore, another oolitic sandbody formed as barlike sands, but is older and less developed than the above sandbody. These barlike build-ups (a series of migrated sand waves) are not laterally continuous and represent migrated sand waves in a westward direction. Their sediments are characterised as fine-to-medium grained, mainly fecal pellets with some oolitic facies. The highest point of this buildup is 1.5m deep in the water, and marked by interference ripples.

Examples of ancient wave-dominated sandbodies come from the Early Carboniferous age in Southwest Britain (Burchette et al., 1990). There are three carbonate sandbodies that are related to barriers in this area. These barriers are formed

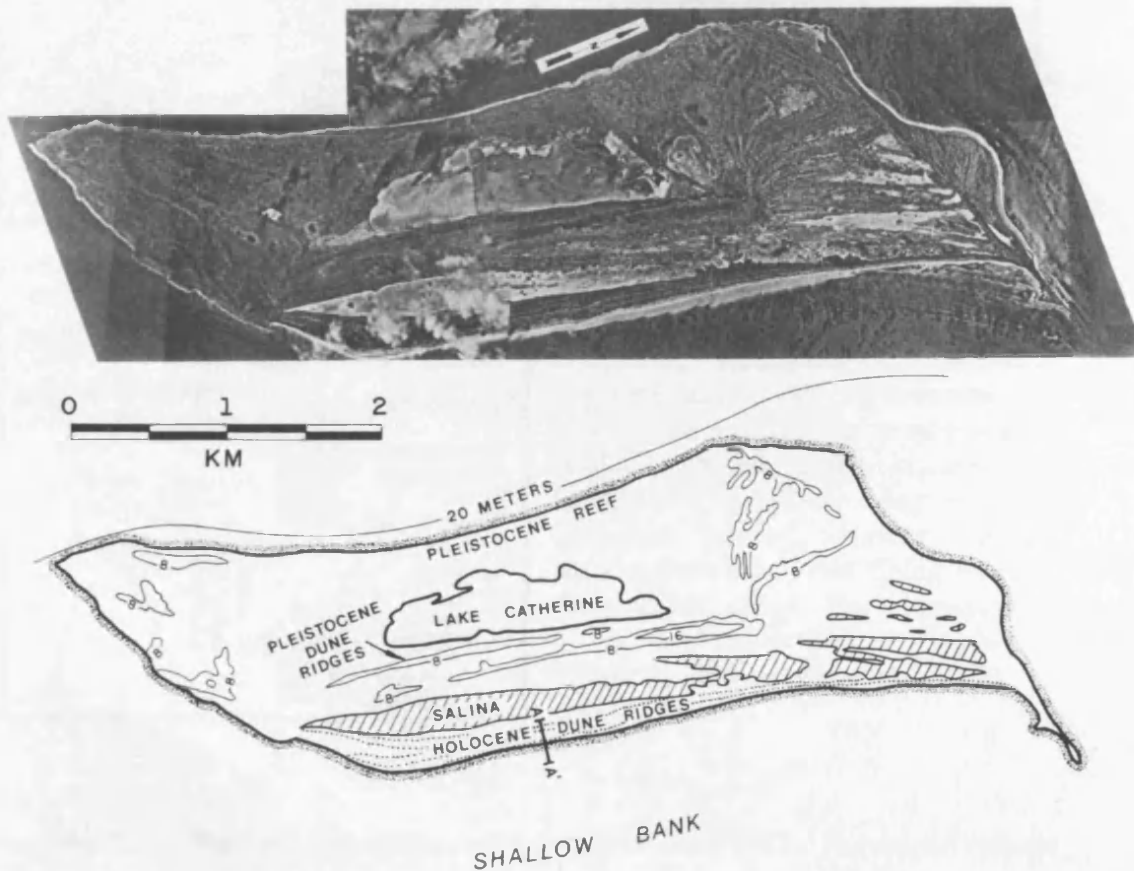


Figure 2.10. Aerial photo showing the morphology of West Caicos Island and the active zone of ooid growth. From Lloyd et al. (1987).

by three episodes related to sea-level behaviour. In the first episode, there is regression of the progradational strandplain the Gully Oolite (Caswell Bay Oolite) (Fig. 2.11), which represents 10-20m thick shallowing- and coarsening-upwards sequences of oolite shoreface, capped by beach deposits and a major exposure surface. These bodies formed at the end of highstand and early lowstand system tracts, extended for more than 30km downdip, and are comparable to the above

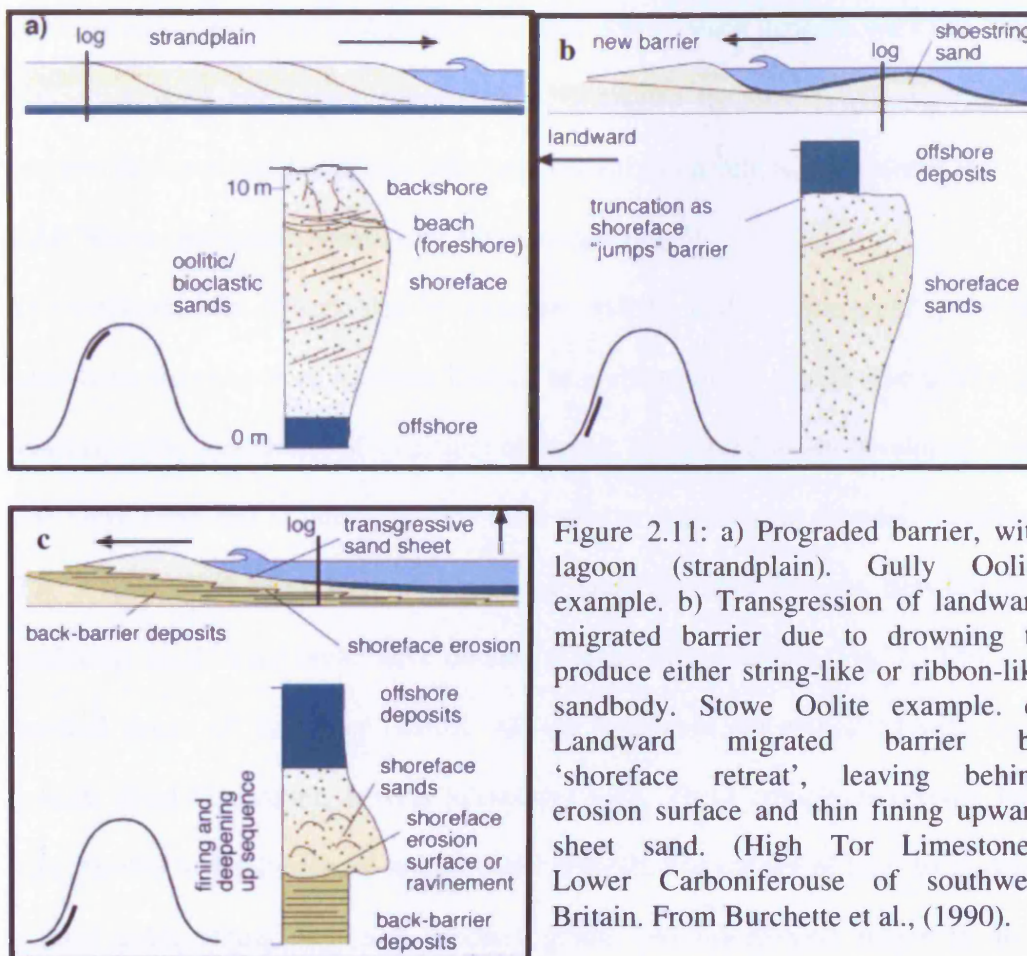


Figure 2.11: a) Prograded barrier, with lagoon (strandplain). Gully Oolite example. b) Transgression of landward migrated barrier due to drowning to produce either string-like or ribbon-like sandbody. Stowe Oolite example. c) Landward migrated barrier by 'shoreface retreat', leaving behind erosion surface and thin fining upward sheet sand. (High Tor Limestone). Lower Carboniferous of southwest Britain. From Burchette et al., (1990).

modern Caicos Platform strandplain example (Lloyd et al., 1987). The second episode occurred when the barriers migrated toward the land during transgression, by drowning of the barrier when the sandbody was covered by offshore deposits. This episode includes the Stowe Oolite in the same area (Burchette et al., 1990). The third example represents the migration of barriers landwards by shoreface retreat and leaving behind an erosion surface or ravinement. The third example is seen in the High Tor Limestone, represented by thin transgressive carbonate sand that formed by the landward movement of the barrier by shoreface retreat, and resulted in fining- and deepening-upwards sheet sand (Burchette et al., 1990). The progradational barriers

are characterised by a trough of cross-laminated oolitic grainstone, coarsening upwards with a presence of hardgrounds, and actual beach deposits with low angle, planar-laminated oolitic grainstone which is capped by an exposure surface that contains structureless grainstone, calcrete crust, rhizoconcretions and palaeokarst.

2.2.6 Wave-dominated Sandbody: Structural Control

This sandbody was documented by Lomando (1999), and is represented by modern inner-ramp deposits from southern Kuwait to northern Saudi Arabia. The sandbodies result from the interaction of structural elements. These sandbodies developed over a very large ramp that is punctuated by three similar north-facing shoreface headlands (Fig. 2.12 a) which rest on major northeast-oriented structural features. Between these headlands, small-scale faults have created a series of re-entrants (Fig. 2.12 b), with seaward slopes of less than 1m/km. All the headlands are associated with major modern shoal complexes, several kilometres long. These complexes contain large bars, parallel to the longshore and oriented NW-SE, and consist of fine- to medium-grained ooids, intraclasts, and bioclast grains. Well-developed ridges in these headlands are composed of a complete ridge-type sequence from basal high energy, coarse-grained and cross-stratifications in the upper shoreface and foreshore units, to finer-grained, well-sorted oolitic aeolianite at the top of the sequence. The re-entrants are characterised by a tidal delta-channel-sabkha complex. The presence of the active ooids in the tidal channels is in response to the contributions of the ebb tidal delta that transports the ooids from the source to the barrier island and spits. The positions of the channels are controlled by the faults, and the oolitic ridges can be up to 7m thick and include some hardgrounds.

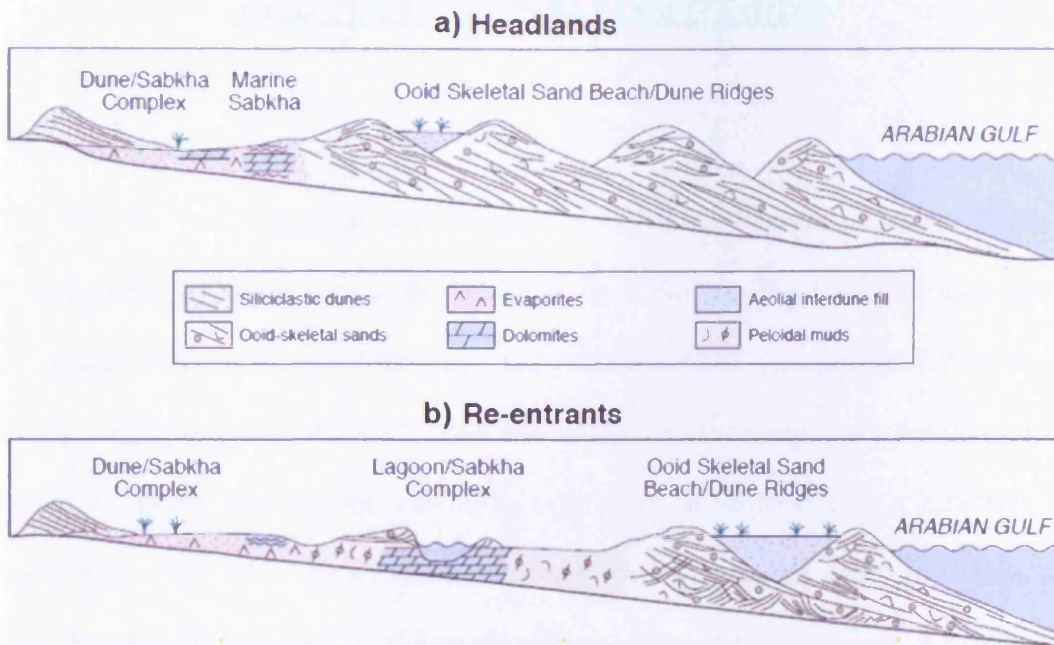


Figure 2.12: a) Profile of the Headlands strandplains. b) Profile of re-entrants coastal ridge. Southern Kuwait to northern Saudi Arabia. From Lomando, (1999).

CHAPTER 3. HUNTS BAY OOLITE (HBO)

3.1 Introduction

The HBO has been logged in three outcrops in the Gower Peninsula, in South Wales. These outcrops, located along the depositional strike, are the Langland Bay (grid reference 635872), Three Cliffs Bay (grid reference 532877), and Port Eynon Bay sections (grid reference 463846), from east to west respectively. They are classified into four major associations and each association is divided into a number of Lithofacies (Fig. 3.1). The overall limestone beds are in slightly different shades of grey, however, they are hardly differentiated from each other on the basis of colour.

The first association (A) is dominated by crinoidal debris and oolitic event beds. The second association (B) is dominated by pure ooid beds which represent part of the main oolitic complex. The third association (C) is represented by coarser grade aggregate oolitic grains such as grapestone-like aggregates and lumps. The fourth association (D) is characterised by very fine-grained bioclastic peloidal grainstone. The above associations are ordered with respect to time of deposition, where A is the oldest and D is the youngest. In this study a number of brown-weathering dykes of late stage dolomite were recorded.

Based on Scott's (1988) work in Gower area, the Cornelly Oolite Formation (in this study represented by Association B & C) and the Stormy Limestone Formation (in this study represented by Association D) are well exposed from base to the top. The Overton Cliff Formation (in this study, the top part of the formation is represented by Association A) represents the base of the Holkerian sequence (in the sense of Scott, 1988).

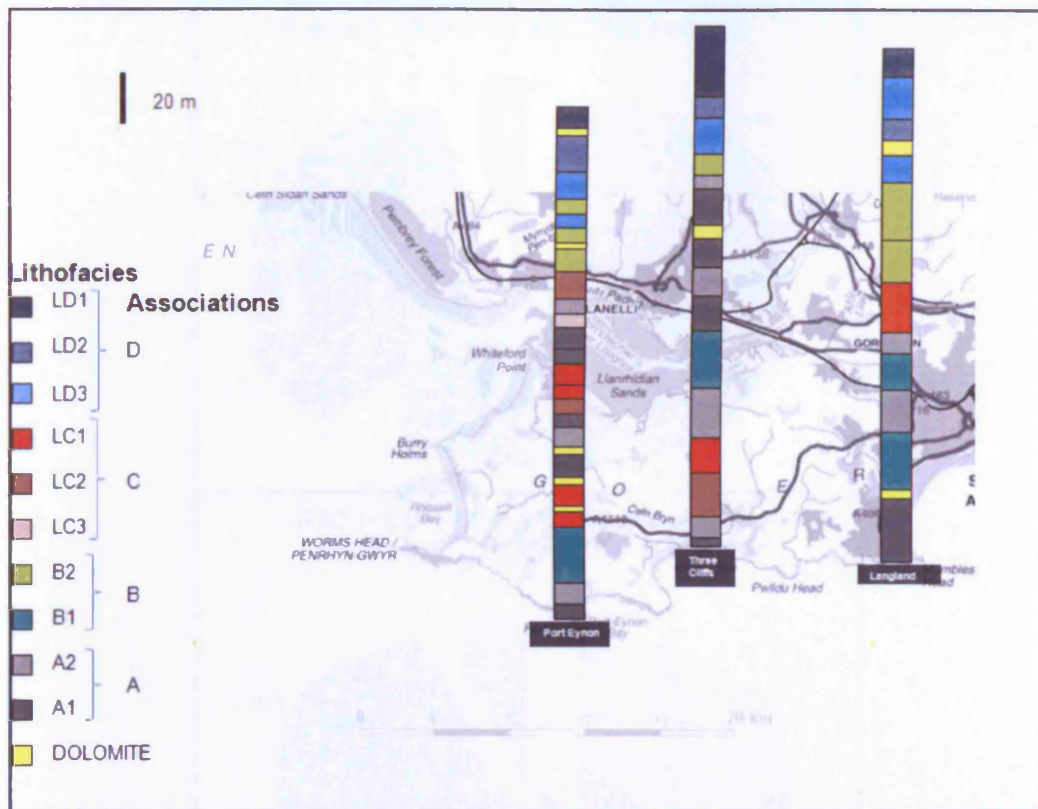


Figure 3.1: Measured sections of the HBO in Gower showing the lateral distribution of lithofacies. The Gower map was extracted from EDINA Digimap.

Each association will be described below, in detail, as follows: introduction, field appearance, association, relative frequency of each (Fig. 3.2), microfacies description and interpretation.

3.2 Very Fine to Fine Crinoidal Association (A)

The association can be subdivided into two stratigraphic lithofacies: crinoidal plate grainstone (LA1), which is more common, and bimodal grainstone (LA2).

3.2.1 Field Appearance of Association (A)

This 65m. to 115m. thick unit crops out extensively, and is well-developed in Three Cliffs Bay. The association thins toward the east (in Langland Bay) and west (in Port Eynon Bay). These beds become darker where fine-grained crinoidal and peloidal grainstone are common, and lighter where oolitic event beds are present.

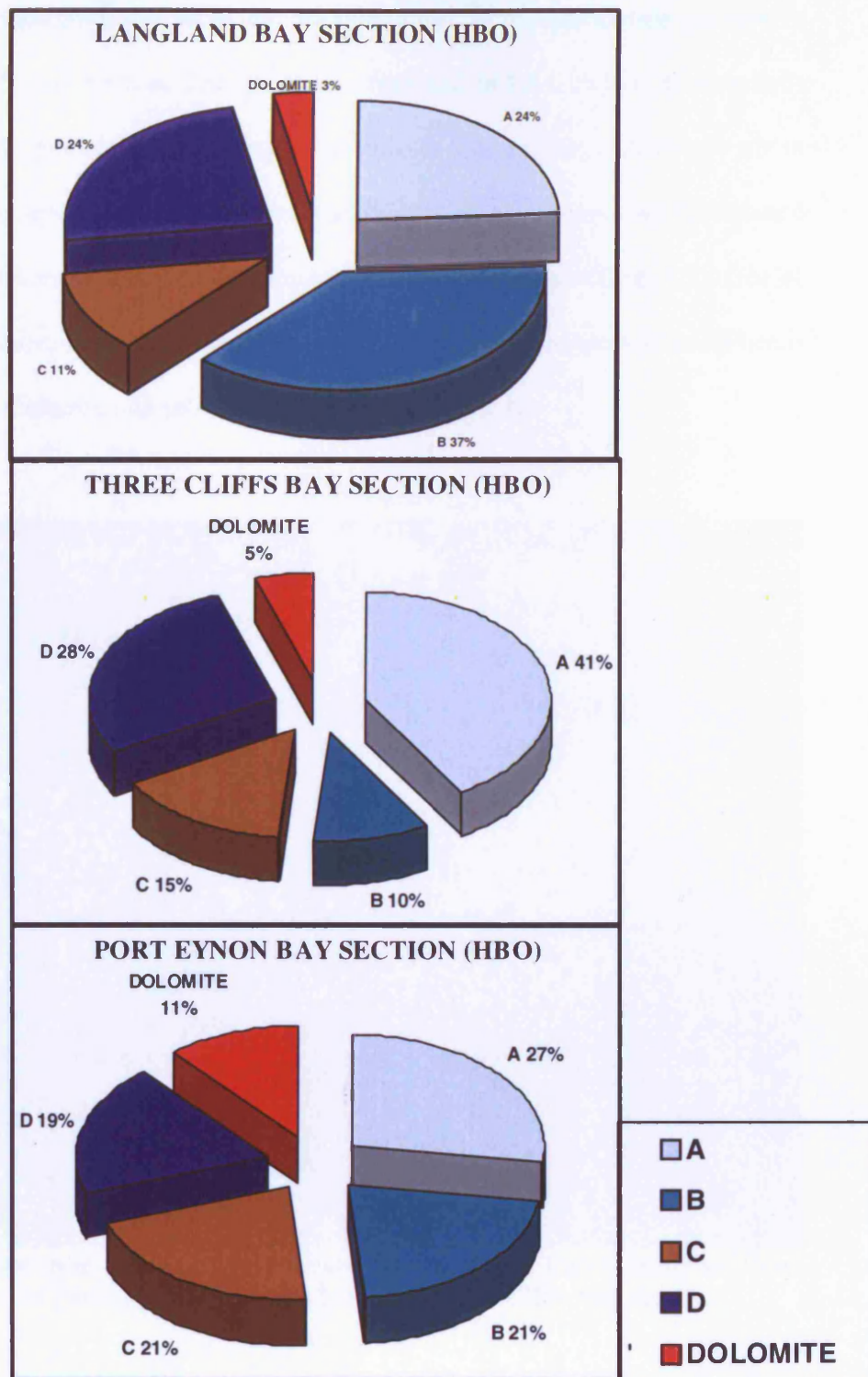


Figure 3.2: Pie charts show the frequency of each association within each logged sections. A) Very Fine to Fine Crinoidal Association. B) Oolitic Association. C) Coarse to Granule Grade Aggregate Oolitic Association. D) Very Fine-to-Fine Bioclastic and Peloidal Association.

Most of the sedimentary structures that are represented in this association are seen in the Three Cliffs Bay section. The structures displayed in LA1 include erosive beds dominated with granule-grade debris of crinoidal lags (average thickness about 10cm), which extend laterally for approximately 10m. The limestones are bioturbated and display *Monocraterion-Skolithos* (escape burrows) type traces (Fig. 3.3). One of the distinct features is the presence of macrofossils, such as *Syringopora* coral heads up to 20cm. in diameter, and solitary corals (3cm. in diameter).

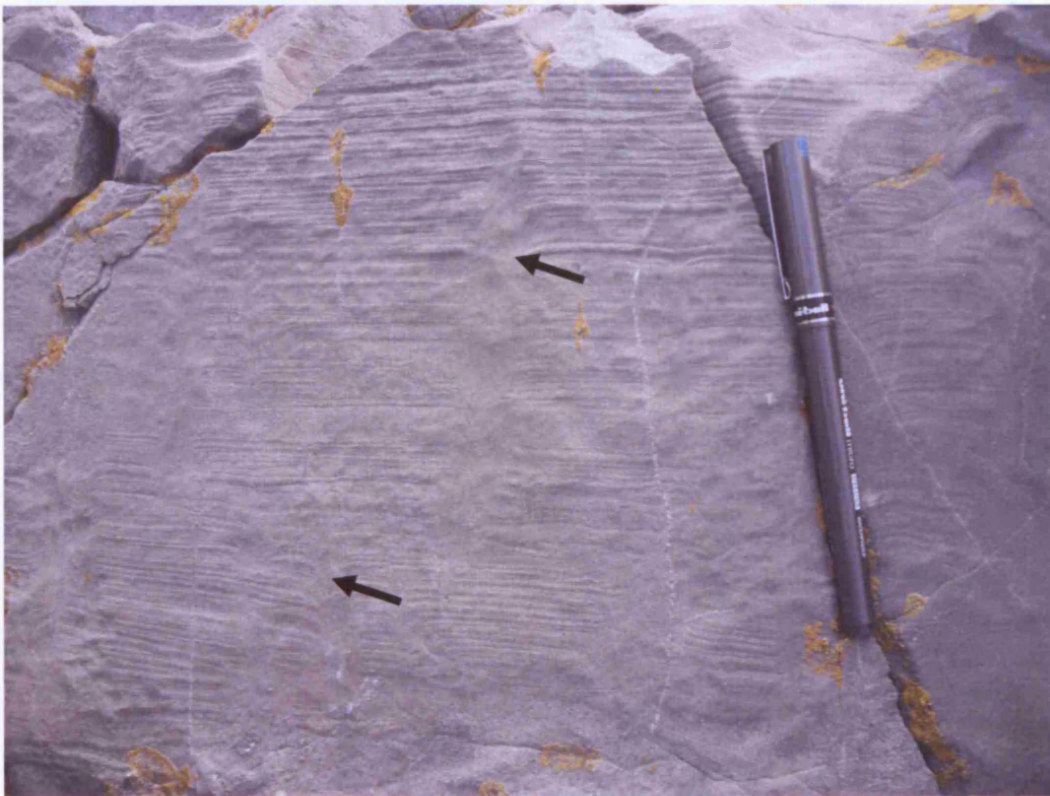


Figure 3.3: Lithofacies LA2, *Monocraterion-Skolithos* type traces (arrows). From 62m above base of HBO. Pen for scale is 15cm long. Three Cliffs Bay section.

The structures exhibited in LA2, which are common in all three sections, are characterised by thin oolitic grainstone event beds with varied thicknesses range between couple of mms and maximum of 15cm. The beds are characterised by

graded, undulating lamination resembling hummocky cross stratification (in sense of Dott and Bourgeois 1982). These oolitic beds also occur as graded, planar laminations within the finer grade beds of crinoidal debris, and the base of these beds is sharp and erosional. Burrows below these beds are filled with the grainstone sediments, resembling tubular tempestites. These tubular tempestites are defined by Wanless et. al., (1988) as “forced fillings of subsurface burrows during storms, are and important to dominant style of sedimentation in environments where large, deep, open burrows are present.” They are *Callianassa*-like burrow structures in modern sediments of Caicos Platform, British West Indies, *Ophiomorpha* and *Thalassinoides* are the ancient example which extends back to Ordovician (Wanless et al., 1988).

The association exhibits chert lenses (or discreet nodules) with an average diameter of 30cm which are laterally discontinuous. These are formed by replacing the original limestone grains with silica.

3.2.2 Distribution and Frequency of Association (A)

This association is the earliest in the HBO, where it is bound by the High Tor Limestone. Usually all three sections start of with lithofacies LA1, then both lithofacies LA1 and LA2 interfinger with the lithofacies of association C in the middle part of the HBO succession. It varies in thicknesses and frequency relative to the other associations. In the Port Eynon Bay section, this association represents approximately 27% of the total section, 41% of the total Three Cliffs Bay section, and 24% of the total Langland Bay section (Fig. 3.2).

3.2.3 Microfacies of Association (A)

Lithofacies LA1 consists of very fine grade crinoidal, peloidal grainstone/packstone, predominantly of non-micritised crinoid plates with very clear cleavage planes (Fig. 3.4). The crinoid ossicles make up over 50% of the skeletal debris throughout the

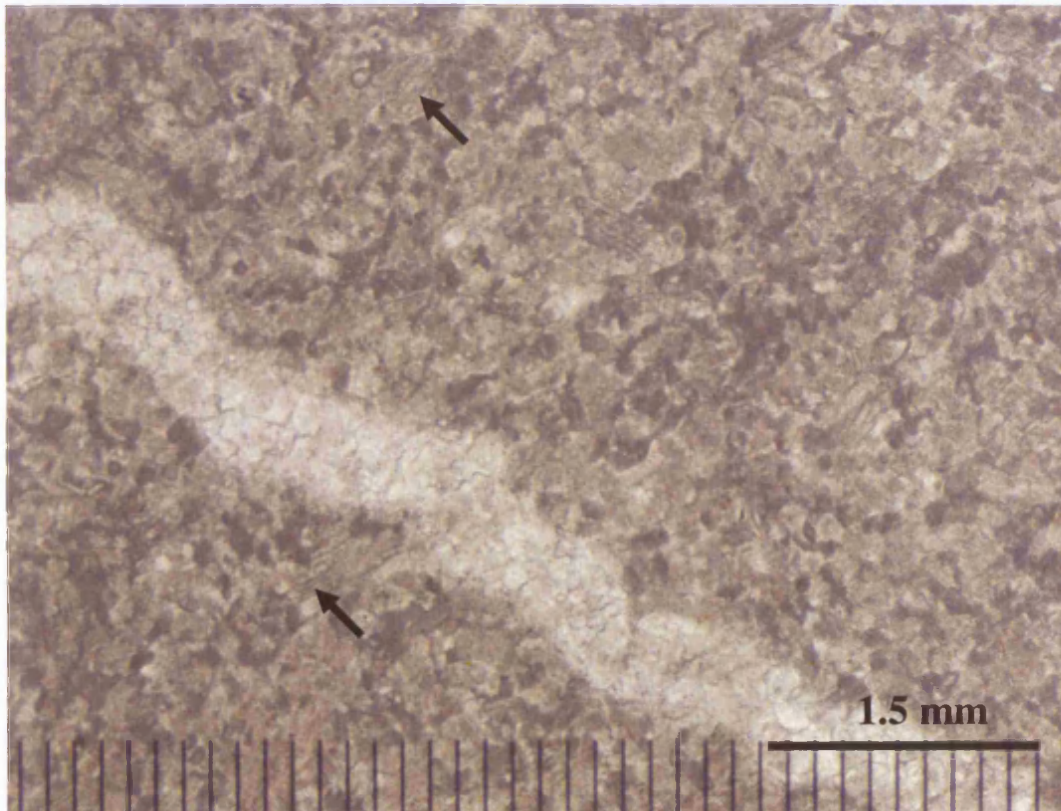


Figure 3.4 Lithofacies LA1, unstained thin section dominated with crinoid plates showing very clear cleavage planes (arrows), a post-compaction fracture cross cuts the sample. Port Eynon Bay, TS# 92.

lithofacies. Other grains, which represent up to 30% of the rock, include very fine peloids, palaeoberesellid tubes, calcispheres, fragments of brachiopod spines, forams, and fragments of the dasycladacean *Koninckopora* (Figs. 3.5, 3.6). The palaeoberesellid tubes are common and represent a characteristic feature of LA1 along with the crinoid plates. These tubes are commonly abundant in wackestones, packstones and grainstones, or with mixed packstone to grainstone facies (Gallagher, 1998). Cloudy neomorphic spar is common, containing outlines of former palaeoberesellid tubes.

Lithofacies LA2 is dominant with crinoidal silt-size debris and coarse sand grade oolitic, aggregate grainstones of shoal complex and intershoal area sediments are representing a bimodal grain-size texture (Fig. 3.6). The bimodal grainstone texture

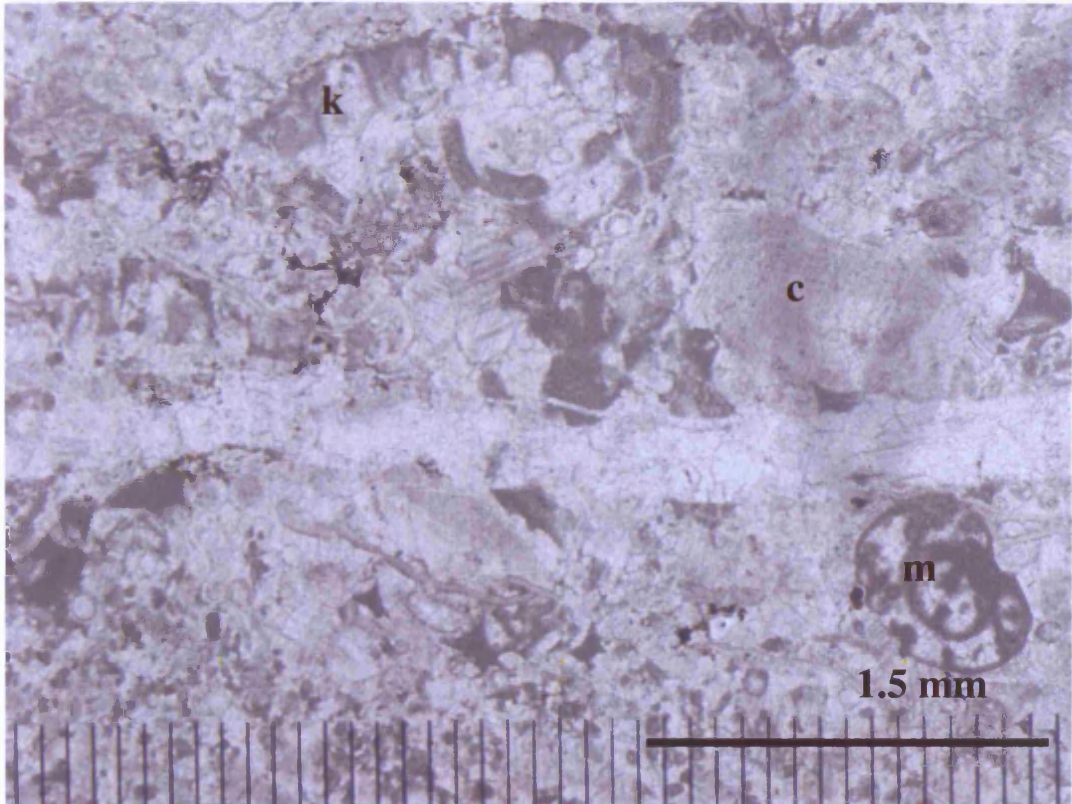


Figure 3.5. Lithofacies LA1, unstained thin section. Very fine crinoid debris with association of forams (m), *Koninckopora* (k), and crinoid plates (c). Three Cliffs Bay, TS# 3.

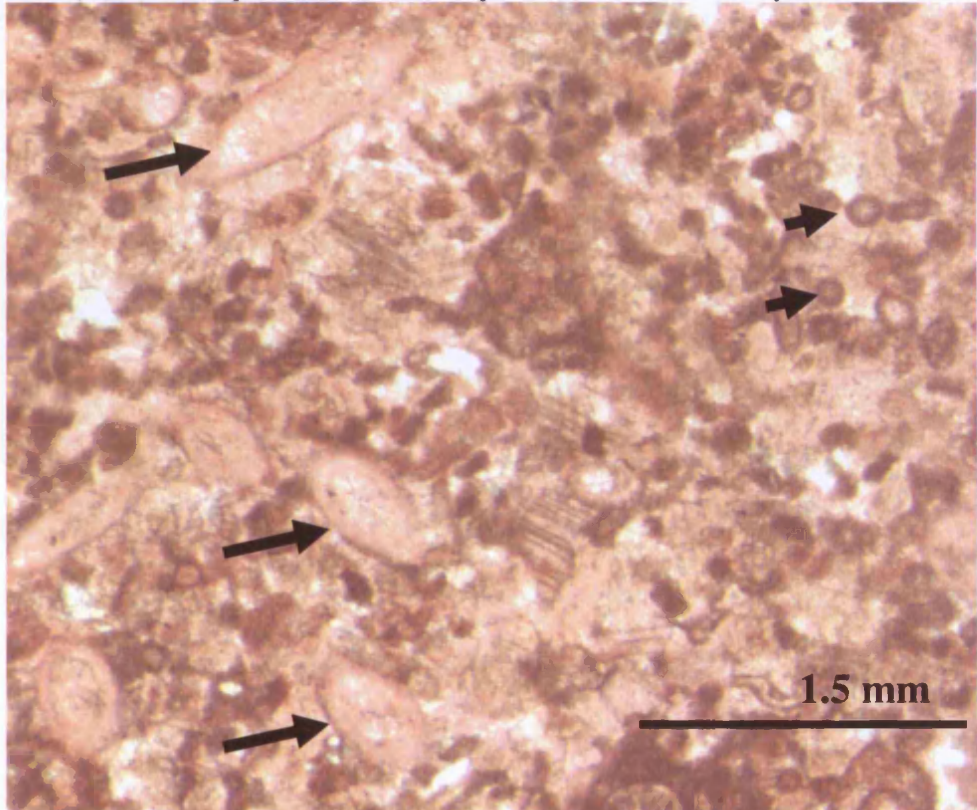


Figure 3.6 Lithofacies LA1, stained thin section. Shows spines of brachiopod (long arrows), and calcispheres (small arrows). Port Eynon Bay, TS# 100.

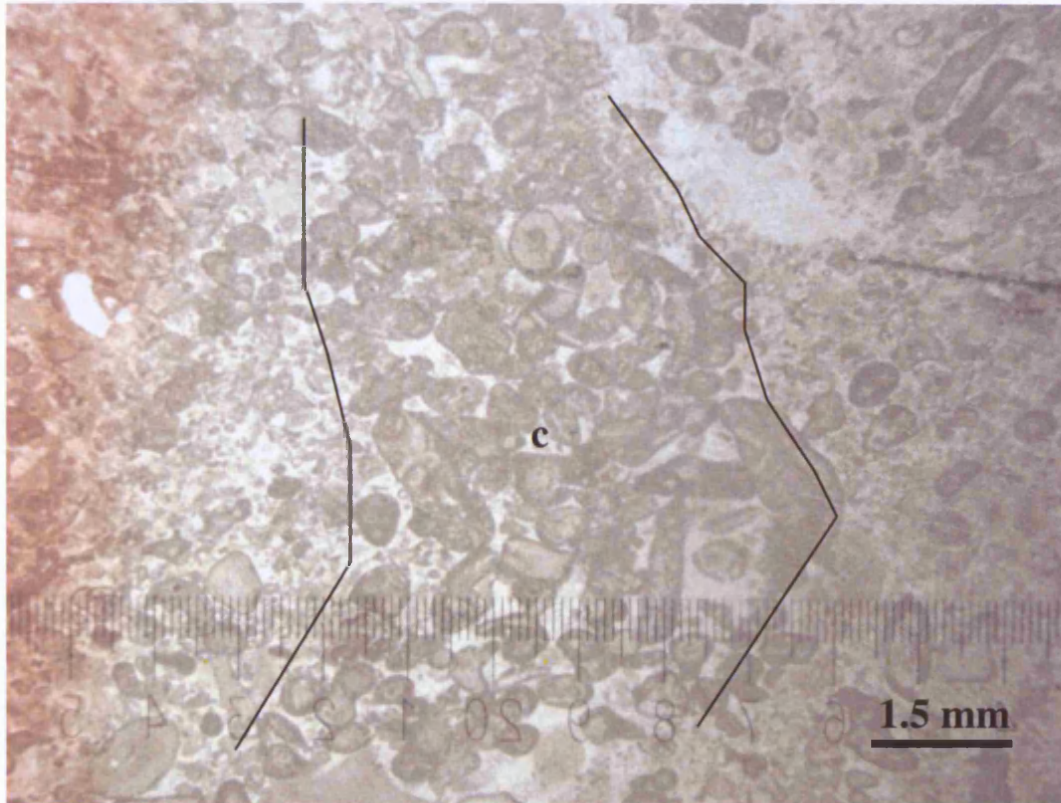


Figure 3.7: Lithofacies LA2, half stained thin section. Possible storm layer of coarser grains (c) interbedded with the crinoidal debris. Three Cliffs Bay, TS# 23.

contains mainly coarse fractions of grapestones, intraclasts of possible hardgrounds (both are discussed in Section 3.4), ooids and lumps (Figs. 3.8, 3.9). The background matrix, which represents the majority of this lithofacies' texture, is similar to LA1.

3.2.4 Interpretation of Association (A)

This association is suggestive of a normal salinity marine environment. The presence of a normal marine fauna and flora such as crinoids, palaeoberesellid tubes which flourished in water depths of approximately 10m (Adams et. Al., 1992; Horbury and Adams, 1996; Gallagher, 1998), brachiopods, forams, and *Koninckopora*. The presence of *Koninckopora* suggests the depositional settings were shallow water <5m deep, as living dasyclads inhabit very shallow water (Flugel, 2004; Wray, 1977). Moreover, these algae found at the top of shallowing upward cycles (Gallagher, 1998).

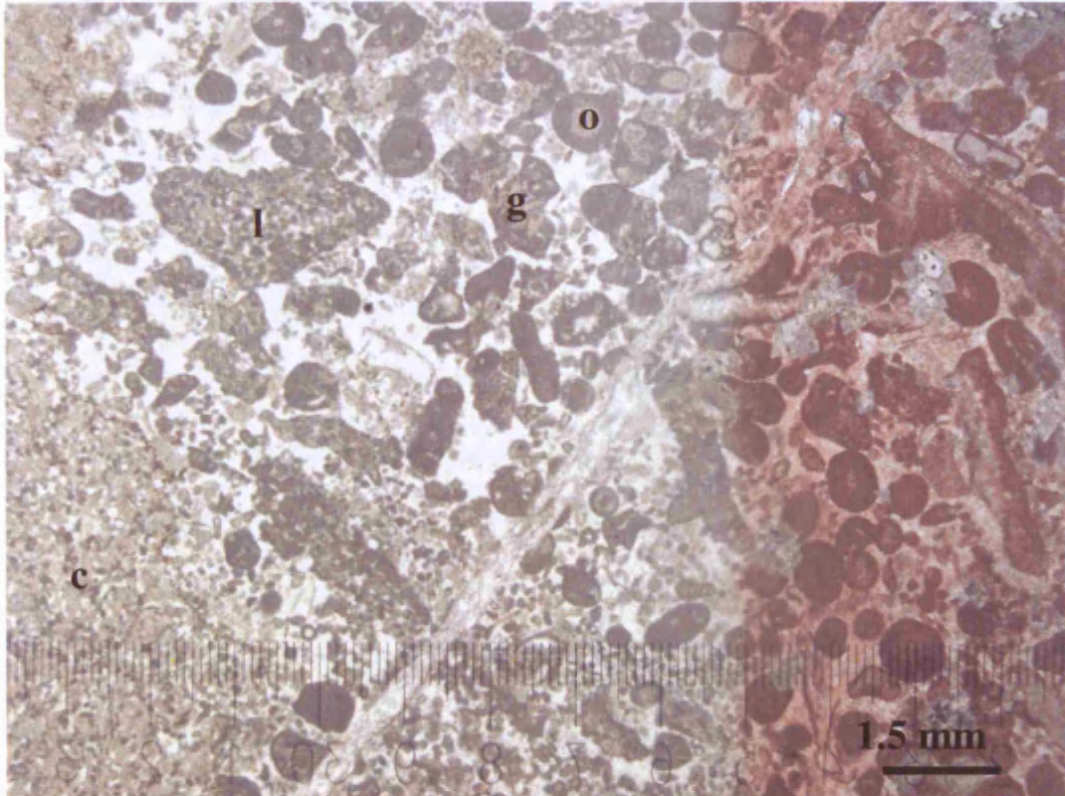


Figure 3.8: Lithofacies LA2, half stained thin section. Typical bimodal texture of very fine crinoidal debris (c), coarse grains of ooids (o), grapestones (g) and intraclasts of possible hardgrounds (l). Three Cliffs Bay, TS# 38.

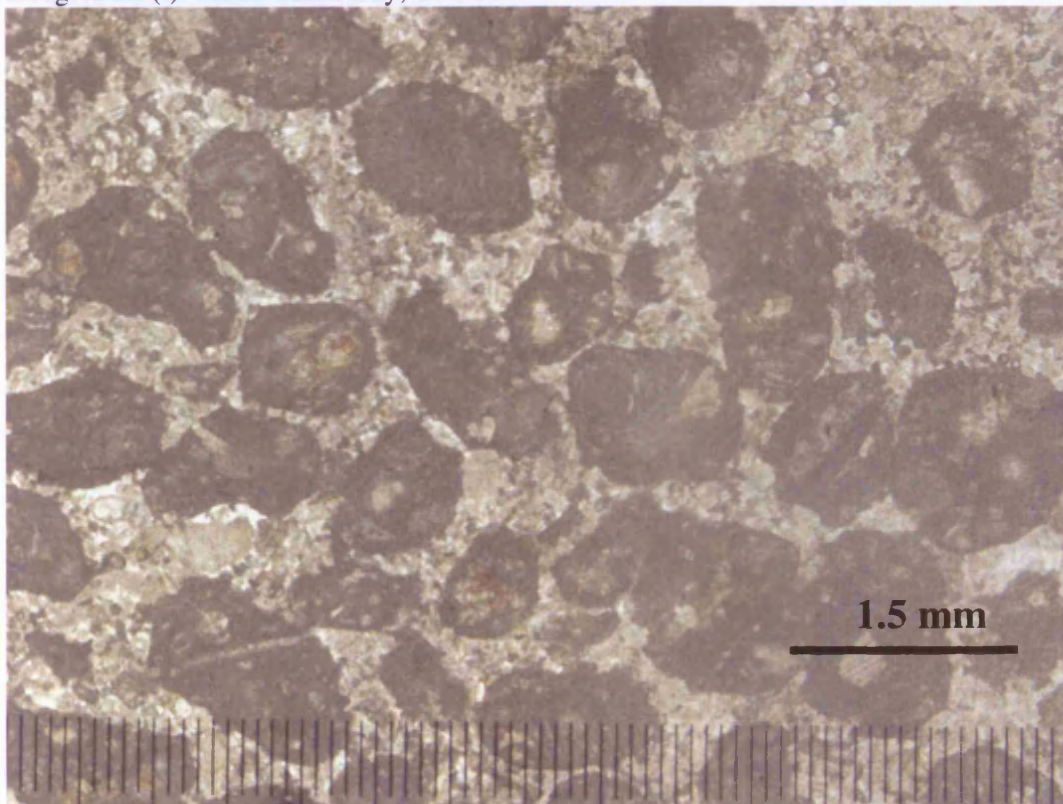


Figure 3.9: Lithofacies LA2, unstained thin section. Shows the lumps and aggregates of coated bioclast (mainly crinoids) associated with the very fine crinoidal debris. The margins of the grains appeared to be etched due to recrystallisation of the palaeoberesellids. Langland Bay, TS# 27.

Where the bimodal texture dominates, it reflects that the depositional environment may have been beyond fair-weather wave-base. Storms can create waves and currents which are able to rework the sediments and redeposit them in area between fair-weather wave-base and storm wave-base. The presence of hummocky cross-stratification is typical of these settings (Dott and Bourgeois, 1982; Tucker and Wright, 1990). Therefore, the bimodal feature possibly resulted from storm activities and/or very strong currents which eroded the sea floor and redeposited the oolitic and aggregate sand offshore of the adjacent settings. Heavily bioturbated beds reflect the obliteration of the original structures and indicates an intermittent deposition.

The variation in the characteristics of these oolitic, aggregate event beds is influenced by their distance from the barrier complex (Aigner and Reineck, 1982), with proximal beds dominated usually with thick and coarse grained grainstones and vice versa with the distal beds.

The “storm filling burrows” are recognised in ancient and modern environments, and associated with ramp-type margins and offbank and onbank lobes of storm-generated sediments associated with shallow carbonate sand banks (Aigner, 1985, Wanless et al., 1988).

In summary the above features suggest the depositional environment was very shallow and within the storm wave base. The oolitic, aggregate deposits and algal remains were washed in and reworked from the adjacent oolitic shoal complex and intershoal areas. In addition, these events were not just resedimentation from oolite shoals but also from the lower energy grapestone facies where the algae also probably lived. Scott (1988) suggested that these sediments were deposited during the mid-Holkerian time in shallow marine water.

3.3 Coarse Grade Oolitic Association (B)

The association is divided into two lithofacies: bioclastic, oolitic grainstone (LB1), and pure ooid grainstone (LB2). LB1 accumulated earlier, usually found in the lower part of the HBO especially in Port Eynon Bay and Langland Bay sections and in the middle part of the HBO in Three Cliffs Bay section, whereas LB2 deposited at the upper part of the HBO.

3.3.1 Field Appearance of Association (B)

LB1 mainly consists of pale-grey massive limestones of by coarse-grained skeletal oolitic grainstone with packages of thin laminations of dark grey, very fine peloidal grainstone with occasional cross bedding. These packages reach thicknesses of around 30-50cm. Examples of this lithofacies is found in all three sections with average thickness of approximately 40m. Overall, these beds contain very few sedimentary structures.

LB2 lithofacies is light grey in colour, massive and are found in all three sections, increasing in thickness from Port Eynon Bay (20m) toward the Langland Bay (50m), with average thickness of approximately 30m. As result of the high degree of sorting, it is rare to find well-pronounced sedimentary structures.

3.3.2 Distribution and Frequency of Association (B)

LB1 usually developed above the Facies Association A in Port Eynon Bay and Langland Bay sections, whereas in the Three Cliffs Bay section LB1 developed within Facie Association A.

Lithofacies LB2 usually overlies coarse to very coarse-grained skeletal grapestone, oolitic grainstone (Lithofacies C1) especially in the Port Eynon Bay and Langland Bay sections. This lithofacies is overlain by LD3 in all three sections.

Figure 3.2. shows the frequencies in percentages of this association relative the entire section of each area. In the Langland Bay section, the association represents approximately 24%, in the Three Cliffs Bay section approximately 10%, and in the Port Eynon Bay section approximately 21% of the total thickness.

3.3.3 Microfacies of Association (B)

In LB1, the grains are mainly up to 30% ooids and up to 60% bioclasts. The ooids have low degree of micritisation and mostly exhibit radial and concentric internal structures. The nuclei can be skeletal fragments or non-skeletal grains. It consists of well-sorted, coarse to very coarse grade skeletal oolitic grainstone (Fig. 3.10). The relatively higher percentages of bioclasts and minor quantity of grapestone distinguish it from LB2 and the Very Coarse Oolitic Aggregate Association (C). Although, the degree of compaction tends to be high in LB1, it shows no open-packed texture like LB2. The general average grain size of the ooids and bioclasts ranges between 300-550 μm , while the superficial ooids range between 100-150 μm . Moreover, superficial ooids with very thin concentric cortices are present and have not been micritised (Fig. 3.10) (Scholle and Ullmor-Scholle, 2003). The mature ooids occur in all section. Their nuclei are dominated by peloids and crinoids fragments, with occasional concentric laminae cortices formed around forams. The dominant components of the bioclasts in this lithofacies are echinoderm fragments (specifically crinoids). Most of the crinoid fragments are partially micritised. The other bioclasts associated with this lithofacies are *Koninckopora* fragments (Fig. 3.12A), bivalve shells, some with constrictive micrite envelopes (Fig. 3.11A), brachiopod fragments, forams, brachiopod and echinoid spines (Fig. 3.11B).

Irregular openings, filled with sparry calcite cement and often larger than the interparticle pores, characterise the fenestral fabric in lithofacies LB1 in very small

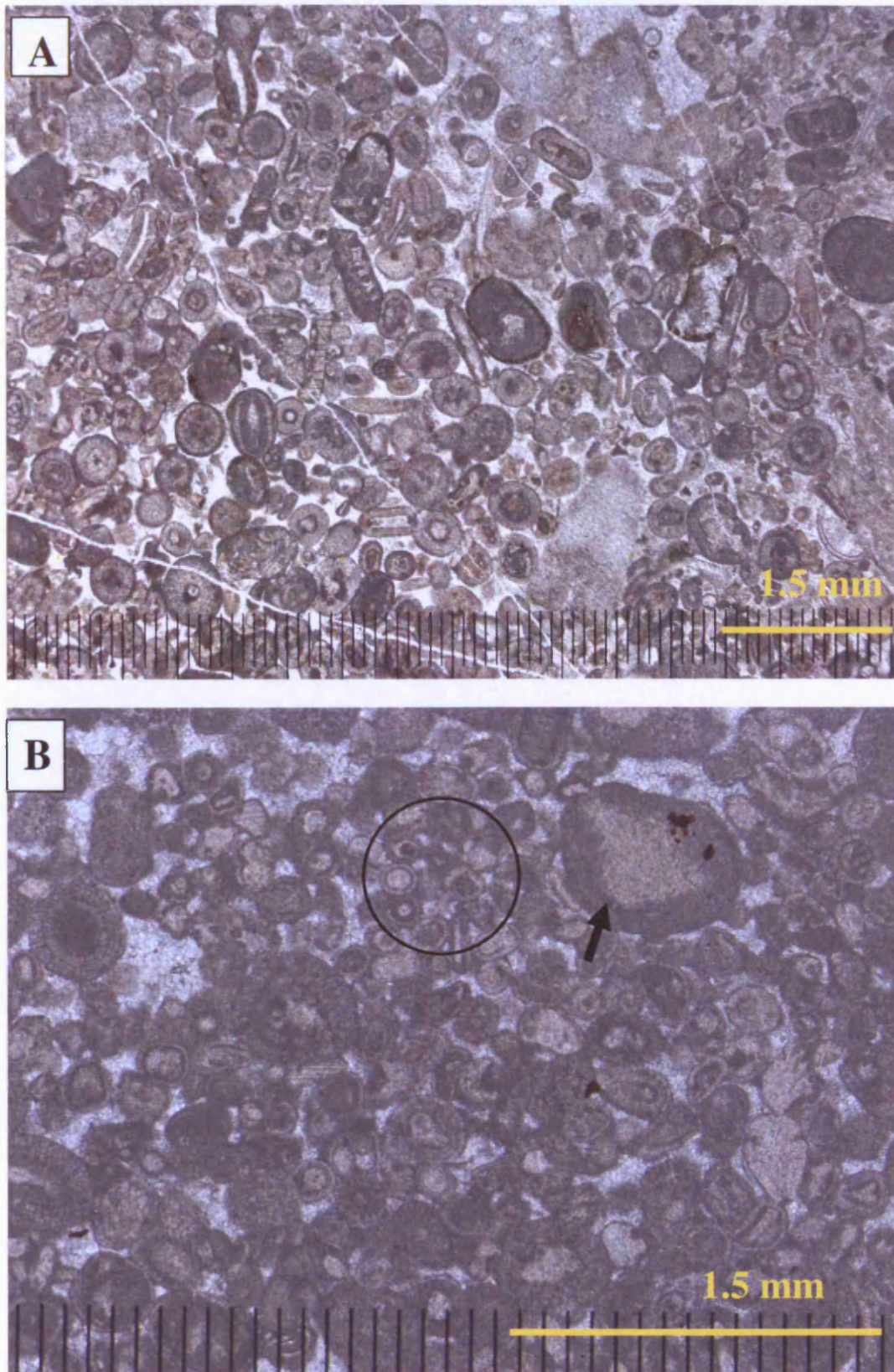


Figure 3.10: Lithofacies LB1, unstained thin sections. A) Gross texture. B) Superficial ooids (circled), and crinoid with destructive micrite envelope (arrow). Port Eynon Bay, TS# 85 & 87.

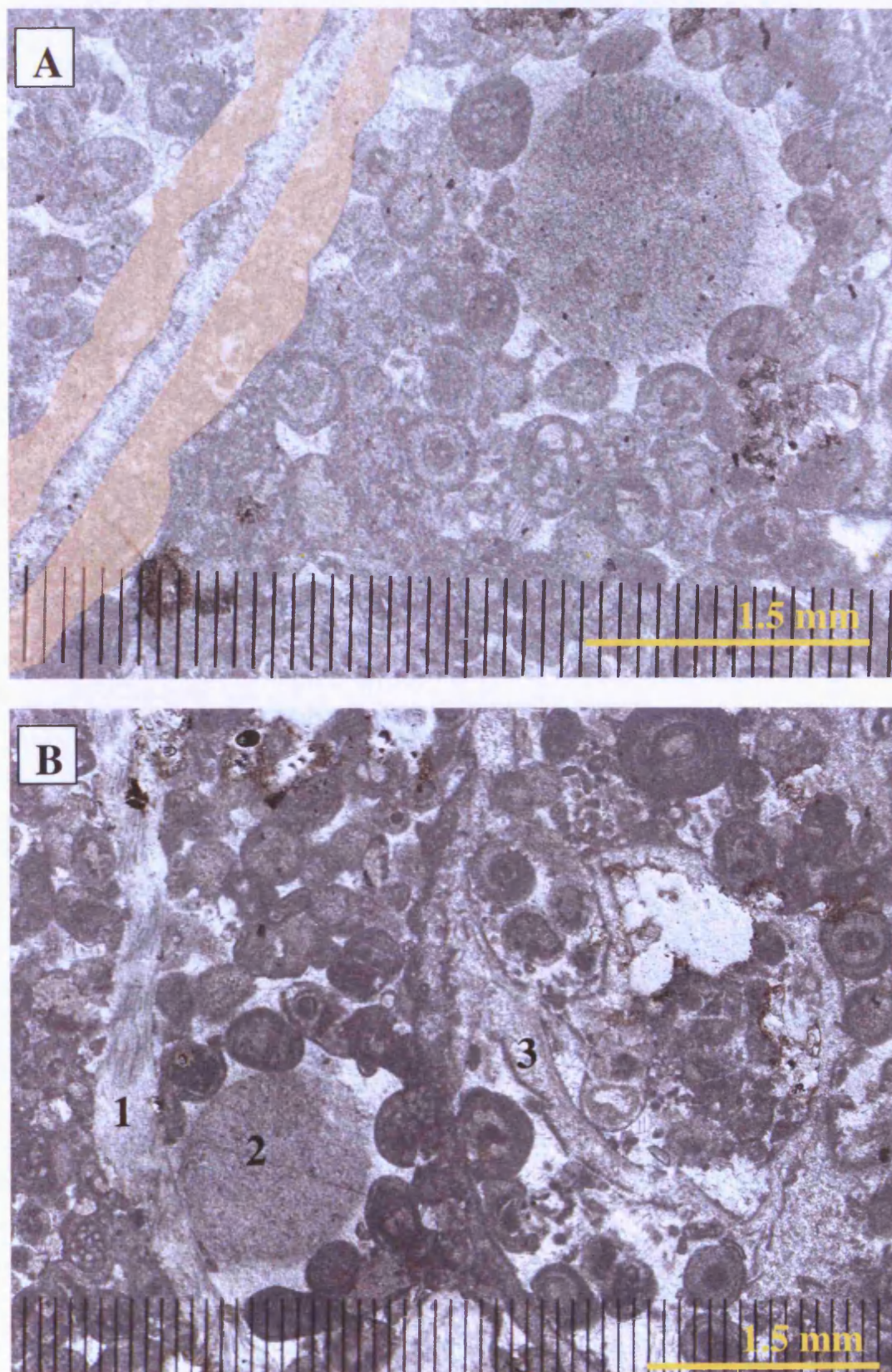


Figure 3.11: Lithofacies LBI, half stained thin section. A) Shows constructive micrite envelope (highlighted) around mollusc fragment. Langland Bay, TS# 28. B) 1. brachiopod, 2. echinoderm, and 3. mollusc fragments in oolitic grainstone. Three Cliffs Bay, TS# 29.

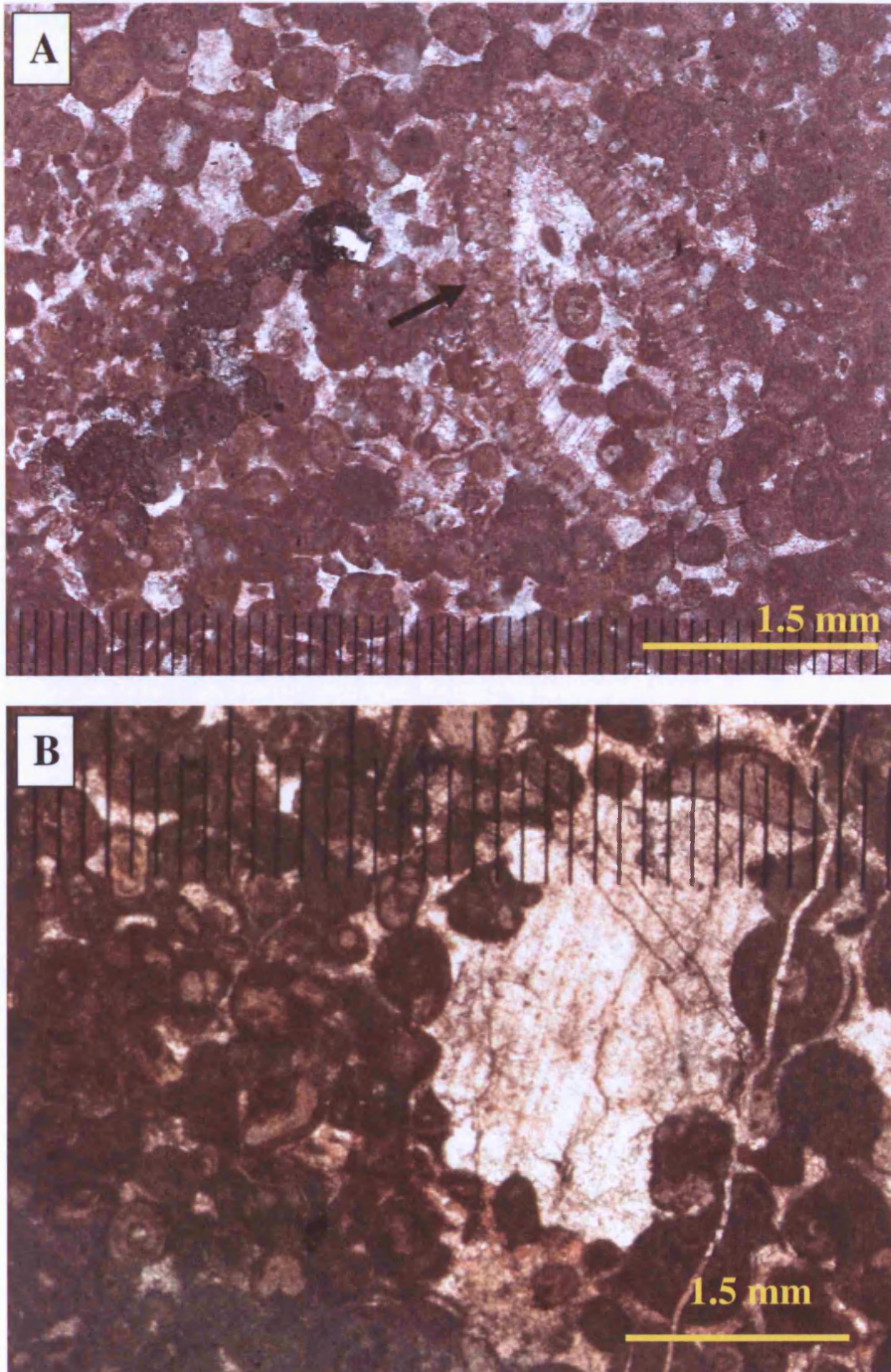


Figure 3.12: Lithofacies LBI, unstained thin sections. A) Slightly oblique transverse section of *Koninckopora* fragment (arrow). B) Sparry calcite-filled fenestral pore. Port Eynon Bay, TS# 89 & 87.

amounts (Fig. 3.12B). Where the fenestral fabric exists, meniscus type cement is also found but it is poorly developed. Dolomite crystals are rare with planar-e (euhedral) rhombs. Some of these rhombs have been calcitised ('dedolomitisation').

The grains of LB2 are mainly up to 90% ooids. This lithofacies is well to moderately sorted, very coarse-grained oolitic grainstone, with minor grapestones (Fig. 3.13A). The texture is mostly open packed and the grains appear to be floating in the sparry calcite, due to palaeoberesellid recrystallisation, but can be compacted, with drusy (Fig. 3.13B) calcite cement, as well as being blocky; this being the common cement type present. However, localised fibrous fringing calcite cement was recorded in the Langland Bay section. Occasionally, LB2 contains fine peloidal clusters near pore throats that resemble microbial hardgrounds which are represented by intraclasts (Fig. 3.14A) (Folk and Lynch 2001). The grains in such modern hardgrounds are coated together by mucilage and endolithic, epilithic and chasmolithic organisms, where they bind the loose grains, and are associated with enhanced filament calcification and micrite trapping (Hillgartner et al., 2001). Moreover, here in this lithofacies ooids are connected together by a meniscus, and in the modern environment this meniscus is initially produced by microbial mucilage and forms a layer of inorganic aragonite crystals (Folk and Lynch, 2001). The ooids have an average diameter of 200-600 μm , with higher degree of micritisation than the ooids of LB1 and have well-developed concentric and/or radial cortices; most common nuclei are peloids and echinoderm plates (Fig. 3.14B). Some opaque grains represent micritisation by endoliths where the micrite tends to preserve the concentric structure (Adams and MacKenzie, 1998). However, some other ooids show a clear radial structure, where the grains have not been micritised by endoliths.

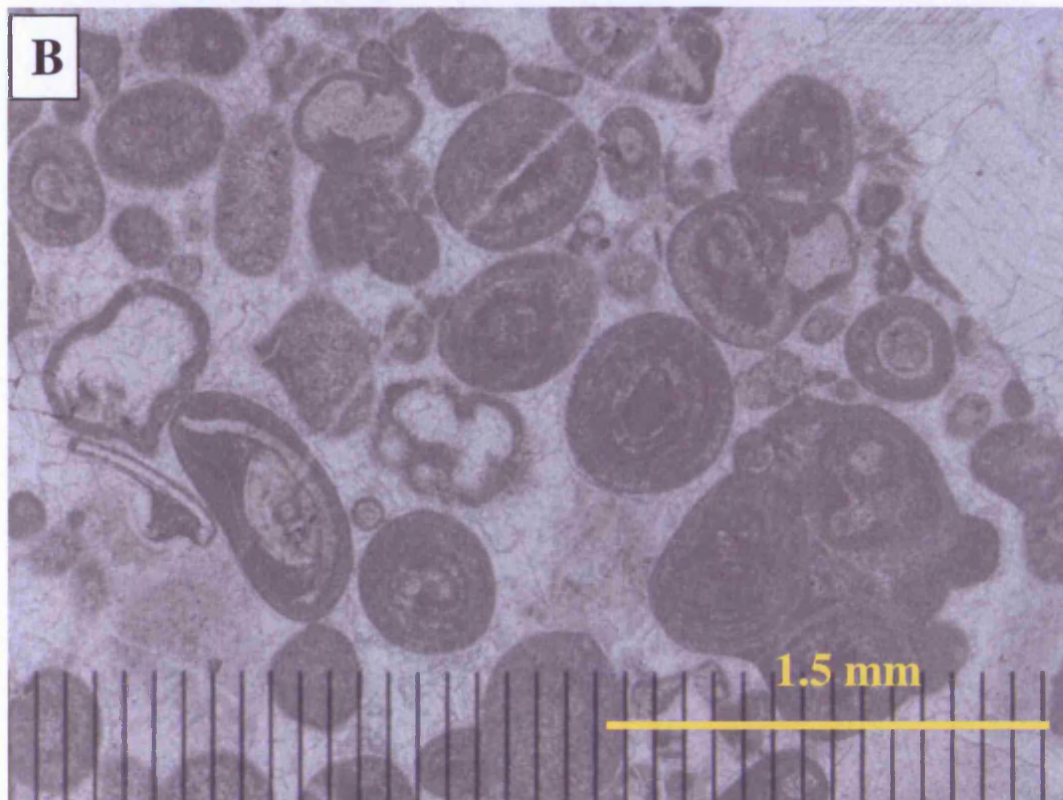
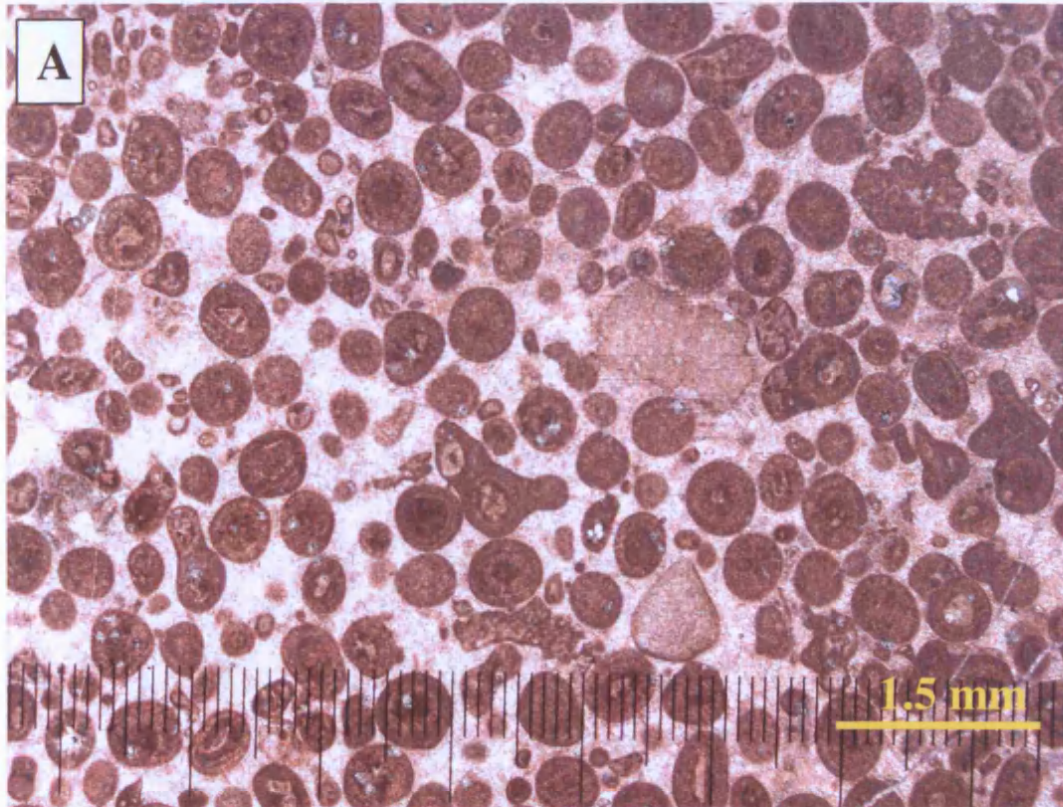


Figure 3.13: Lithofacies LB2 half stained thin section A&B. Open packed with blocky calcite cement gross texture. Langland Bay, TS# 18 & 11.

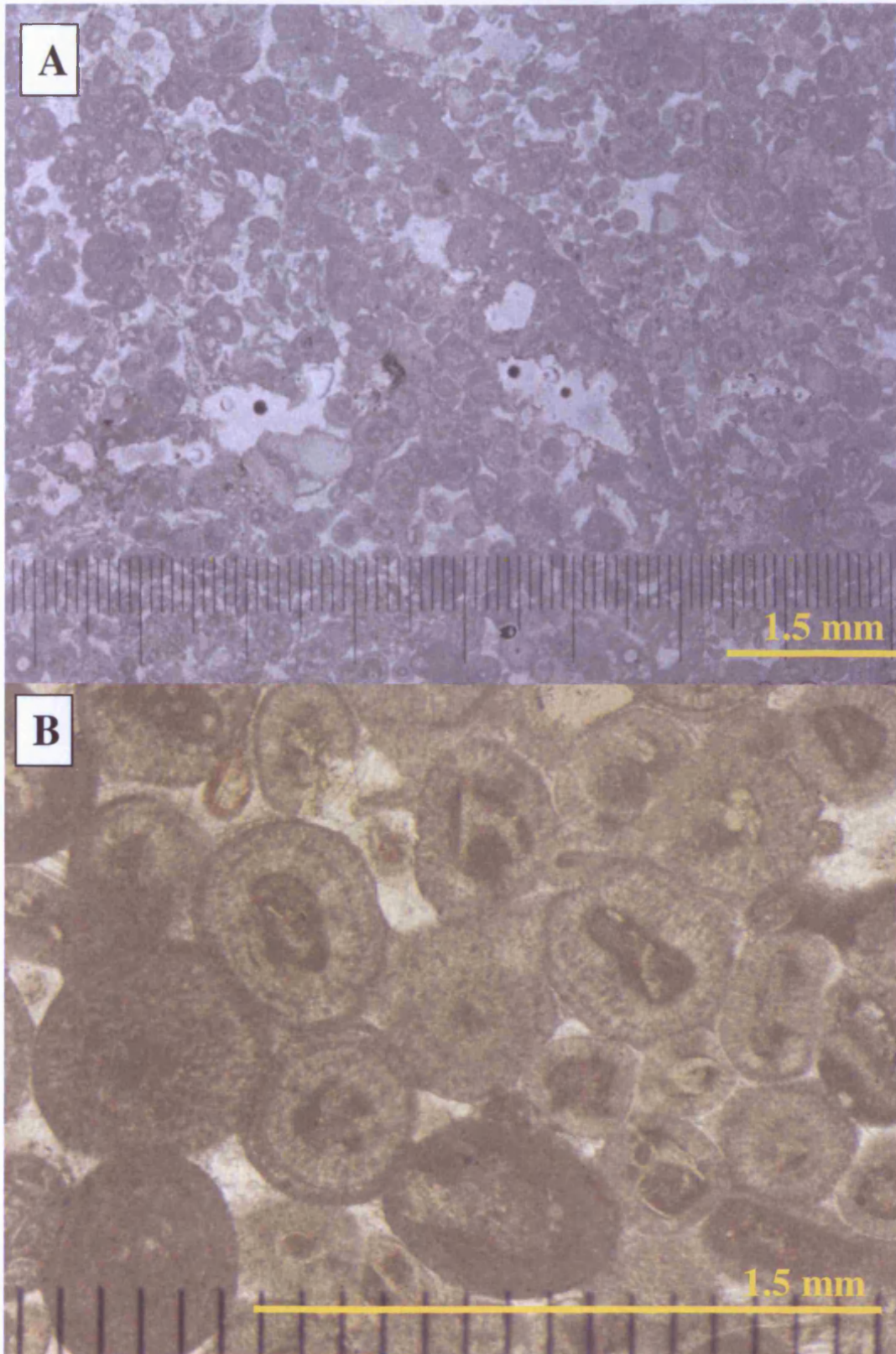


Figure. 3.14. Lithofacies LB2, unstained thin sections. A) Intraclasts with ooids joined together by peloidal cement. The surface of the intraclasts shows an erosion feature that is characterised by micritic layer of peloidal texture. Langland Bay, TS# 16. B) Radial cortices of the ooids. Port Eynon Bay, TS# 39.

The other grains include peloids, palaeoberesellid fragments, echinoderm plates with micrite envelopes and rare gastropod fragments, and make up, on average, <10% of the overall texture. They share some characteristics with ooids grains, e.g. they are well to moderately sorted.

Zoned dolomite occurs as planar-e (euhedral rhombs) (Fig. 3.15) or xenotopic fabrics (Sibley and Gregg, 1987). The crystals are inclusion-rich and vary in size. Some baroque dolomite occurs.

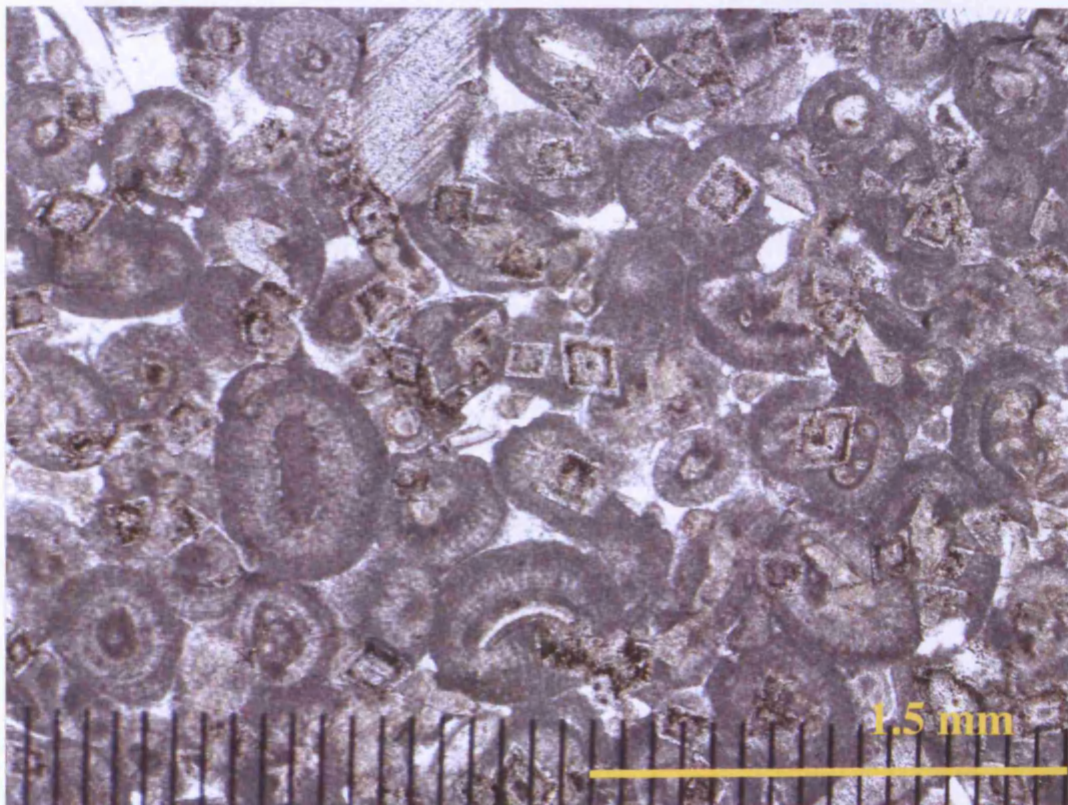


Figure 3.15. Lithofacies LB2, an unstained thin section. Zoned dolomite rhombs in oolitic grainstone. Langland Bay, TS# 16.

3.3.4 Interpretation of Association (B)

The bioclasts in LB1 represent shallow marine fauna, associated with oolitic sediments. The ooids were formed within the active oolitic shoal settings prior to stabilisation, and later micritised by endoliths, which formed the envelopes within and around the bioclasts.

These lithofacies have variable amount of superficial ooids, which are common in the Port Eynon Bay section. Their presence could be interpreted in two ways, firstly these ooids could be brought up from the adjacent area because of their light weight, and secondly they were at their site of deposition.

The alternating (destructive) micrite envelopes, which form during early diagenesis, are usually created by microendoliths. They are distinguishable from the constructive micrite envelope type by the micrite that fills the microborings within the shell fragments. However, the other type of micritisation (constructive micrite envelope) (Fig. 3.12B) has been found within the grainstones, but in small amounts, which leads to the idea of material transported from the adjacent areas such as vegetated areas where a stabilisation mode dominated and caused micritisation processes by endoliths and/or grass-bed (Perry, 1998). In this case, these fragments, with their micrite constructive envelopes, may have been transported from Facies Association D, and specifically from LD2 or LD3, where they are common during the ebb flow.

Ooid formation in LB2 was likely localised in high-energy settings, where shallow water currents and waves provided agitation (Tucker and Wright, 1990). Such a setting is typified by well-sorted oolitic grains with minor micritisation (Dravis, 1979), hence the preservation of the original internal radial structure within the ooids. These equivalent LB2 facies were part of an active sandbody of oolitic sand and are differentiated from the LB1 by the low percentages of skeletal grains. Therefore, they are almost purely non-skeletal oolitic shoal. Modern pure ooid sand occurs in water depths of <2m (Newell et al., 1960) in the Bahamas. The associated fenestral fabric with LB2 reflects that the possible short lived exposure of shoals.

Scott (1988) implied that the absence of isopachous marine fringe cements in the HBO was due to rapid burial in the active oolitic shoal after formation. However, it has been noticed that there are localised fringe cements.

However, the intraclasts (from reworked hardgrounds) involved cryptocrystalline peloidal cement which formed at or near the sea floor with cemented zones being an average of thickness no more than a couple of centimetres. Hardgrounds are early diagenetic feature that are formed in subtidal zones (Hillgartner et al., 2001). This feature occurs in areas prone to microbial activity by mainly three processes; grains binding, microbial calcification and trapping sediments. Hardgrounds are discontinuous surfaces and lack any feature of subaerial exposure (Hillgartner et al., 2001). They usually indicate that the rate of sedimentation was reduced, variable energy settings, and could relate to a stratigraphical disconformity (Scholle and Ullmor-Scholle, 2003).

There is similarity in the formation process of hardgrounds and grapestones, and hardgrounds and intraclasts (Dravis 1979). The former formation occurs when the constituents require binding and cementation that is caused by surficial microbial mats. In the second process, storm events rework the subtidal sediments.

Facies Association B represents an active oolitic shoal by characterised stabilised areas producing hardgrounds which are now reworked intraclasts, minor short lived exposures, ebb flow influence and variability in the skeletal content, degree of micritisation and compaction.

3.4 Coarse to Very Coarse Grade Aggregate Oolitic Association (C)

This association, together with the Facies Association B are the main characteristics of HBO. The average total thickness in all the studied sections is approximately 44m and divided into three major lithofacies.

The first lithofacies is LC1, which are dominated by typical grapestone grains. Lithofacies LC2 contains common grains of aggregate and lumps plus grapestone. Lithofacies LC3 has dominant grapestone, with ooids, and immature aggregates where ooids and bioclasts are coated with irregular microbial rims at the stage of lump formation.

3.4.1 Field Appearance of Association (C)

While this association dominates the HBO succession, all three lithofacies have similar sedimentary field appearances. In the hand specimen, it is easy to see the individual grains because of the very coarse size, producing the lightest-grey colour throughout the whole succession. Where fine materials interfinger with coarser grains, the colour of the limestone turns a darker grey.

These lithofacies exhibit few sedimentary features such as a poorly-developed small scale trough cross-bedding (up to 20cm. thick, 10m. lateral extension), which overlies erosional beds that are marked by bioclastic lags, and bioturbation features that usually appear at the top of each bed. These features occur in repeated beds with average thickness of about 1-2m. Clusters of brachiopod shells are also common in this association.

3.4.2 Distribution and Frequency of Association (C)

Almost all the sections show interfingering of this association with the Facies Association A, but the associated lithofacies do not occur in the same stratigraphic order. For example, in the Three Cliffs Bay section, LC2 was deposited first; and in the Port Eynon and Langland Bay sections, LC1 accumulated first. LC3 was found in the middle part of the Port Eynon Bay section.

As mentioned above, these aggregate oolitic and oolitic associations characterise the bulk of the HBO, and represent a relatively large thickness compared

with the other associations. Therefore, the frequencies of the association itself within each sections are; 21% in the Port Eynon, 15% in the Three Cliffs Bay, and 11% in the Langland Bay (Fig. 3.2).

3.4.3 Microfacies of Lithofacies of Association (C)

Lithofacies LC1 is a heavily-micritised, well-rounded grapestone grainstone. These aggregates, the characteristic of this association, represent encrusted recrystallised ooids formed by a binding action, probably by microbes, algae and forams, encrusting in the substrate as is seen today in the Bahama Islands (Winland and Matthews, 1974). The shape of these grapestone-like aggregates occurs as botryoidal lumps resembling clusters of grapes, and sometimes represents eroded lumps (abrasion-derived botryoidal lumps) (Wilson, 1967). The outlines of these aggregates are quite clear (Fig. 3.16). There is no genetic difference between grapestones and lumps, where the micritised interstices are bound together by filamentous micro-organisms or cementation (Wright, 1990; Gebelein, 1974; Winland and Matthews, 1974; Fabricius, 1977; Kobluk and Risk, 1977; Cros, 1979).

These coarse granule-grade grains vary in their sizes, but their average size is 1-3mm in diameter. Such grains represent about 30-35% on average of the total grains in this lithofacies; however, locally they reach up to 80%. Moreover, ooid grains also occur, but in low percentages, making up about 15% of the total constituents. The average size of these single ooids is <0.5mm in diameter. Fine grade peloids are normally present, not only in this lithofacies but also in the whole association.

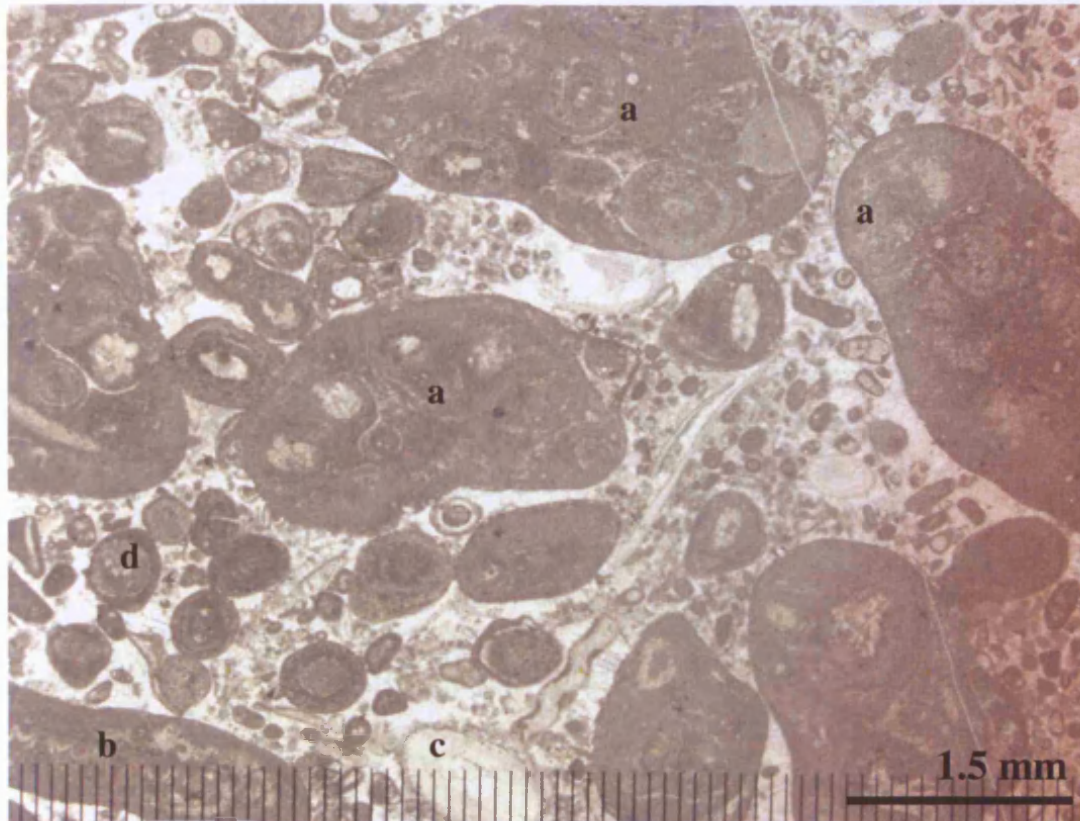


Figure 3.16: Lithofacies LC1, half stained thin section. (a) botryoidal lump of grapestone, (b) coated dasycladacean *Koninckopora*, (c) echinoderm fragment, and (d) ooid. Three Cliffs Bay, TS# 17.

This association, as with most of the other lithofacies within this association, commonly shows a range of percentages of bioclastic grains (Fig. 3.17), such as echinoderm debris including echinoid spines, crinoid plates, algal fragments including the dasycladacean algae *Koninckopora*, brachiopod spines, and palaeoberesellid tubes. Most of these grains have been discussed in other lithofacies where they exhibit almost the same characteristics; however, the palaeoberesellid tubes are very abundant in this association. The presence of palaeoberesellid algae has influenced diagenesis (Section 5). Their influence is characterised by recrystallisation.

The palaeoberesellids (Fig. 3.18) are septate, tubular fragments (Adams and Al-Zahrani, 2000), were important sediment producer during the Carboniferous (Adams et al., 1992). Most workers on the Carboniferous refer to it as a sponge (e.g.

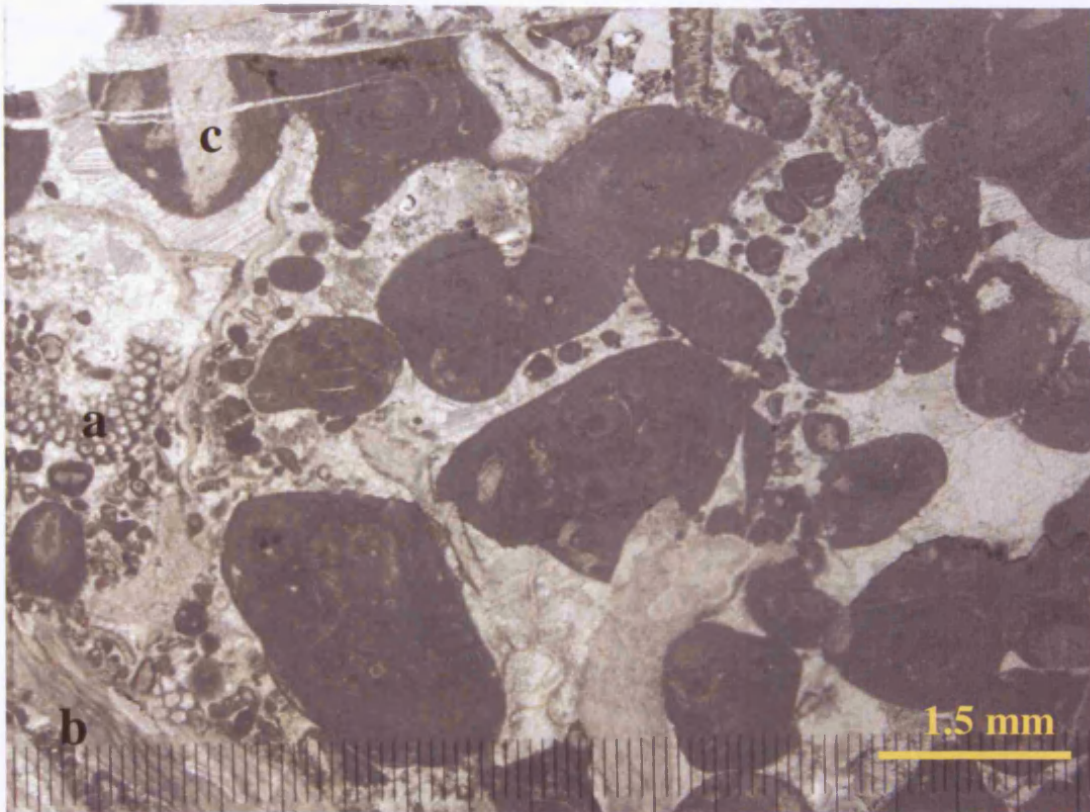


Figure 3.17: Lithofacies LC1, half stained thin section. Associated bioclasts; a. *Koninckopora* fragment, b. brachiopod shell, c. coated crinoid fragment. Three Cliffs Bay, TS# 16.

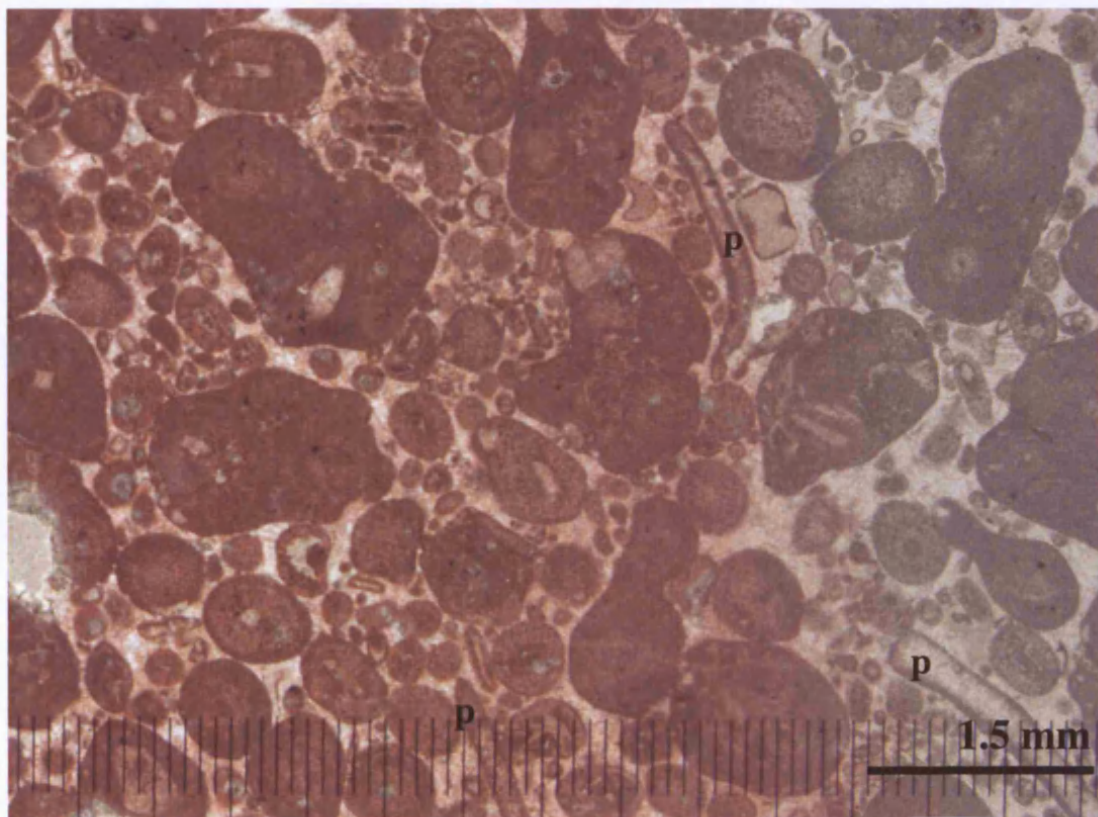


Figure 3.18: Lithofacies LC1, half stained thin section. Palaeoberesellid tubes (p). Three Cliffs Bay, TS# 17.

Dehantschutter and Lees, 1996), due to its occurrence within sediments inferred to be sub-photoc zone (200-300m. water depth) (Lees and Miller, 1985; Lees et al., 1985). The most convincing classification was done by Skompski (1987), who introduced the new Family Beresellaceae and Tribe Palaeobereselleae for these dasycladacean algae. There is a similarity between palaeoberesellid and echinoderm fragments, which can be confusing to distinguish. The difference between them is exhibited where the algal tubes show undulose extinction and may have been aragonite in origin (Mamet and Roux, 1975), while the echinoderm fragments show a sharp extinction. However, both bioclasts can develop syntaxial rim cements (Adams and Al-Zahrani, 2000). These algal may comprise up 80% of the grains in a thin section (Adams et al., 1992; Gallagher, 1996), and they are abundant in wackestones, packstones and grainstones (Gallagher, 1998).

Lithofacies LC2 consists mainly of moderately sorted and sub-rounded to rounded, grainstone, and less commonly packstone, characterised by lumps (or aggregates), and intraclasts of completely micritised grapestones, aggregates or reworked hardgrounds (Fig. 3.19). The lump grains do not contain a single nucleus, rather they formed as aggregate grains, mainly incorporating numbers of skeletal fragments and/or peloids. The encrusted coatings are made of cryptocrystalline calcite, which could be microbial circumcrusts in the sense of Wolf (1965) or, as Bathurst (1964) suggested, be micrite envelopes.

Lithofacies LC3 is poorly developed in the Port Eynon Bay section. It is distinguished by the following features: the limestones are poorly sorted, and coarse to very coarse grade bioclastic oolitic grapestone grainstone (Figs. 3.20-3.21). Ooids

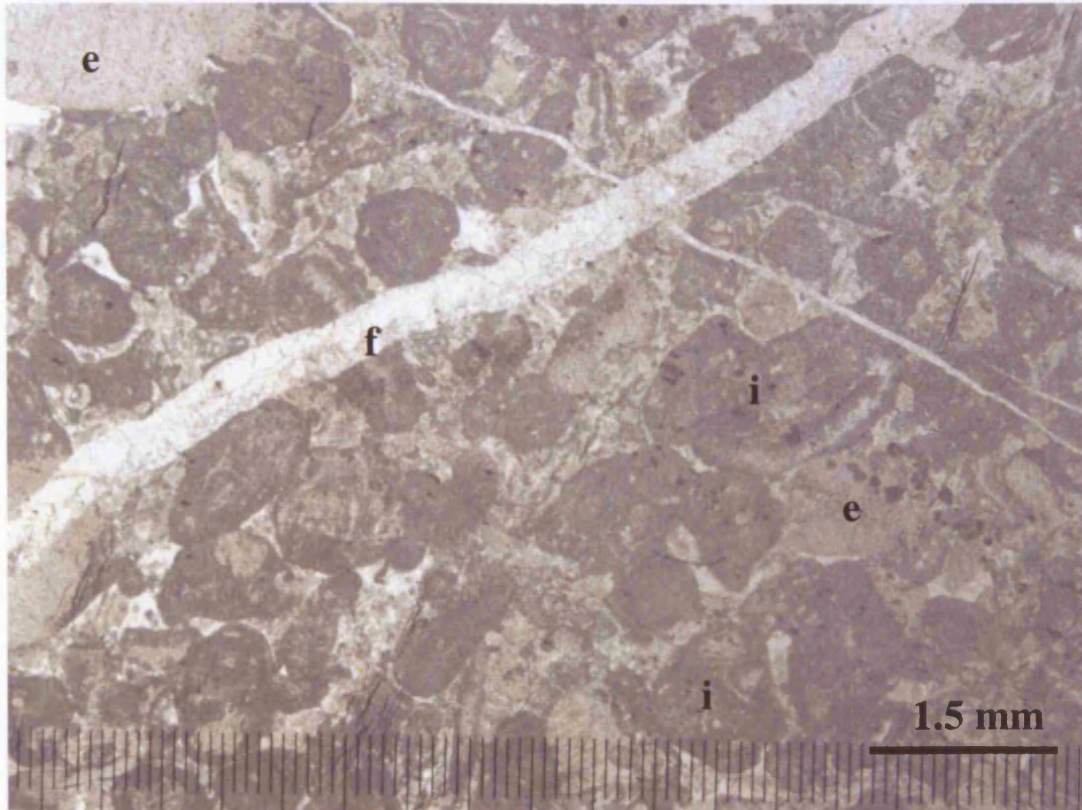


Figure 3.19: Lithofacies LC2, unstained thin section. Intraclasts of micritised grapestones and lump grains (i), echinoderm fragments (e), and post-compaction fracture with spar calcite cement (f). Langland Bay, TS# 22.

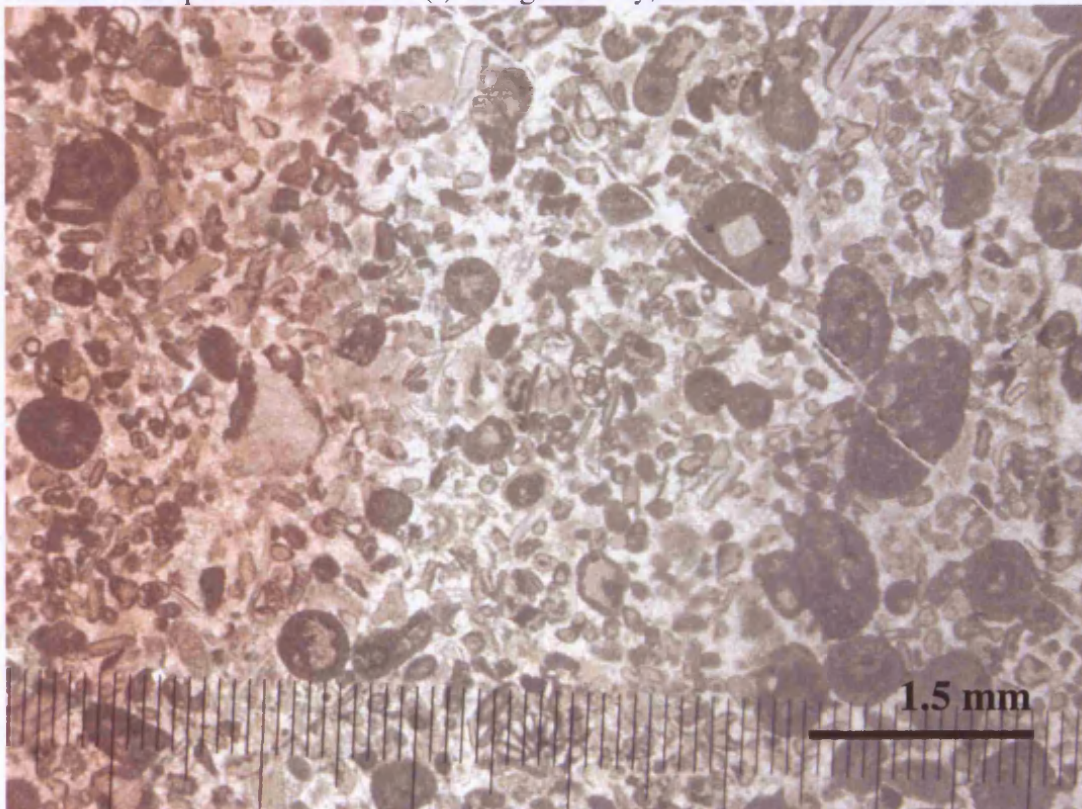


Figure 3.20: Lithofacies LC3, half stained thin section, dominated by bioclasts (some with micrite rims) and ooid grains. Three Cliffs Bay, TS# 11.

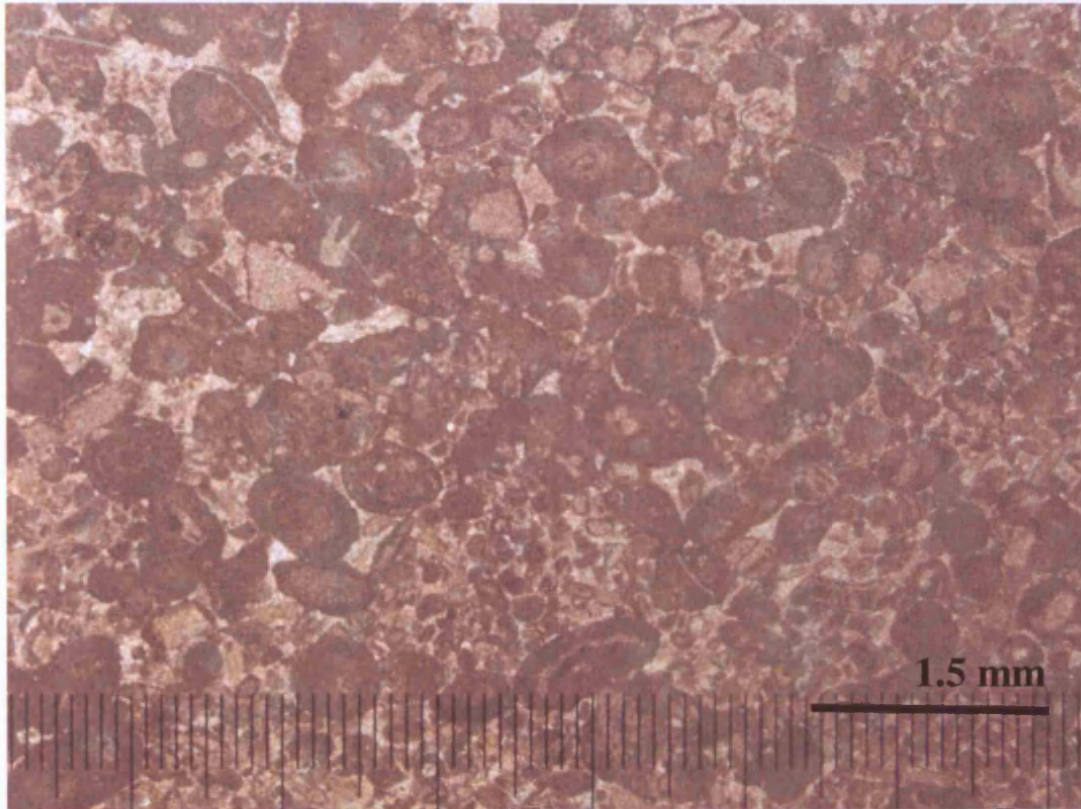


Figure 3.21: Lithofacies LC3, a stained thin section. General texture, with coarse ooids and grapestones, and fine to medium grade bioclasts and peloids. Langeland Bay, TS# 22.

are more abundant than grapestone and bioclasts, but the characteristic feature of these ooids is their irregular cortices due to heavy recrystallisation and/or they represent a 'pre-grapestone stage' (in the sense of Fabricius, 1977).

3.4.4 Interpretation of Association (C)

Grainstone texture occurs where the rate of sedimentation decreases and stabilisation or cementation processes dominate. However, a packstone texture reflects a decrease in the energy level (Hillgartner et al., 2001; Scott, 1988).

The levels of sorting reflect the level of energy (Flügel, 2004), therefore, through the association, the sorting ranges from well sorted in higher energy settings of LC1, to moderately sorted in relatively lower energy areas of LC2 to poorly sorted in LC3.

The presence of palaeoberesellid tube fragments is interpreted by Adams and Al-Zahrani (2000) as deposits in deeper water off the shelf sea which was shallow. Adams et al. (1992) suggested that packstone was deposited below the wave-base on a ramp in the Craven Basin, and in the shallows upwards at the base of the late Dinantian sequences. These algae thrived in water depth of approximately 10m (Adams et al., 1992; Horbury and Adams, 1996; Gallagher, 1998).

The general depositional settings of these lithofacies are shallow environments, which were adjacent to the active oolitic shoal where a fraction of ooids were washed in by periodic high energy currents from the shoal area, as described by Purdy (1963), from Bahama Bank.

The Great Bahama Bank platform (such as Joulter's Cay, described by Harris, 1979) is the modern analogue of grapestone formation. The distribution of such grains covers a range of energy levels, where it varies from just off the very active ooid shoal areas to protected mud environments with a maximum water depth of 15m. However, such energy levels have to be capable of preventing the deposition of lime mud content and leaving grainy fractions behind (Flügel, 2004). The formation of grapestone resulted from marine diagenesis processes by biofilms that bind the ooids together (Tucker and Wright, 1990). However, grapestone and heavy micritisation always develop in areas with unequal wave and current energy conditions, with infrequent sediment movement or quiet water, commonly due to the protection of the oolitic shoal (Winland and Matthews, 1974). The whole process occurs on the undisturbed bottom of a subtidal area over a long time in order to allow the microbial biofilm to cover the grains (Fabricius, 1977). Therefore, the grapestones formed in environments with predominantly stable substrates, low sedimentation rates and intermittent erosional events (Hillgartner et al., 2001).

The grains in LC2 (lumps and intraclasts) are either have been reworked from the hardgrounds surface as discussed in section (3.3), which are derived from the erosion of the adjacent areas and resedimented within the same area. Lithofacies of LC3 represents the transition zone, which is halfway between the formation of the ooids and grapestone in quiet water (Fabricius, 1977).

Scott (1988) interpreted the presence of trough cross-bedding by the deposition of migrated megaripples. He also recorded a beach sequence within the LC2 in the Hunt Bay section that was not logged in this study. However, there might be other beach sequences within the logged sections but they are not well developed and are difficult to identify.

In summary this association represents back barrier lower energy level settings relative to the Facies Association B. it is characterised by different type of aggregate grains mainly grapestones, and the abundance of the algal palaeoberesellid tubes. Its modern analogue example had been described by Harris (1979) in Joulter's Cay in the Bahama Bank.

3.5 Very Fine-to-Fine Grade Bioclastic and Peloidal Association (D)

The strata of this association have been divided into three lithofacies: very fine grade bioclastic and peloidal grainstone as lithofacies LD1, constructively coated sponge packstone plus the facies of LD1 as lithofacies LD2, and oolitic grainstone along with facies of LD2 as lithofacies LD3. All the above lithofacies have a similar field appearance, including colour and sedimentary structures, and have brachiopod shell clusters present. However, the change between these lithofacies is transitional with no marked abrupt changes or erosional surfaces.

3.5.1 Field Appearance of Association (D)

These lithofacies are associated with massive units that range in thickness from 50m to approximately 80m, but outcrop as 1-2m layers of massive limestone without any distinct sedimentary structures. Occasionally, very thin lamination is seen in the very fine-grained examples. These beds are pale grey in colour but are, in general, darker than the beds associated with coarser-grade grainstones. However, this association shows a clearly defined sequence with LD3 in the bottom of the association with the coarser materials and a gradual change to the finer grains of LD2 to even finer grains of LD1. It is difficult to notice a change in colour. Clusters of brachiopod shells occur with a variety of thicknesses, averaging between 20-50cm. These shell concentrations exhibit no distinct orientation, but they extend laterally for tens of meters.

3.5.2 Distribution and Frequency of Association (D)

These lithofacies occur at the top of HBO successions. Ramsay (1987) recorded that all these successions are capped by erosional surfaces and soil features which were not recorded in this study. LD3, which is usually found in the base of Facies Association D, is gradually mixed up with LB2.

This association varies in thickness and frequency among the other associations. In the Port Eynon Bay section, this association represents approximately 19% of the total section, 28% in the Three Cliffs Bay section total, and 24% for Langland Bay (Fig. 3.2).

3.5.3 Microfacies of Lithofacies of Association (D)

The limestones in lithofacies LD1 are dominated by very fine to fine-grade bioclastic peloidal grainstone, and consist of a range of grain sizes and textures. Grains are dominated by rounded peloids with an average of 30%, and a variety of small foraminifera (i.e. *Endothyranopsis crassa*, etc.), dasycladacean algae *Uraloporella*

Korde, calcispheres, and minor crinoid and brachiopod fragments (Fig. 3.22). This lithofacies exhibits neomorphic textures, where the relics of some peloids or bioclasts are distinguishable in the sparry calcite groundmass.

The lithofacies LD2 is dominated by packstone and grainstone, with fine to medium grade bioclasts and peloids. In addition to the components of LD1, this lithofacies are characterised by micritic coatings (encrusting shell fragments), including coatings of what appear to have been sponges, with calcified tubes that resemble canals (Fig. 3.23). These canals were enlarged and formed cavities similar to fenestral fabric. Another characteristic feature that appears in this lithofacies and continues in the subsequent lithofacies are dasycladacean algal (*Koninckopora*) fragments.

The constituents and texture of LD3 are similar to LD2, but the presence of single ooids are the clear characteristic of this lithofacies. The ooids are small superficial, averaging 100µm. However, LD3 includes packstone and grainstone textures, and the grains are coarser in the grainstone texture. Coarser grains include simple ooids, peloids and fragments of *Koninckopora* and crinoid debris (Fig. 3.24).

3.5.4 Interpretation of Lithofacies of Association (D)

A variety of skeletal and non-skeletal grains is distributed in this association with different percentages. Some of the skeletal grains indicate very shallow depositional environments such as *Koninckopora* algae. Another example of the skeletal grains is *Uraloporella* Korde, which consists of thick micritised walls of cylindrical tubes up to 1mm long. Because of their tendency to be easily recrystallised, it is difficult to distinguish brachiopod spines from *Uraloporella* tubes. The recrystallisation has influenced the surrounding areas of these tubes (Wright, 1982; Riding and Jansa, 1974). These microfossils belong to either dasycladacean

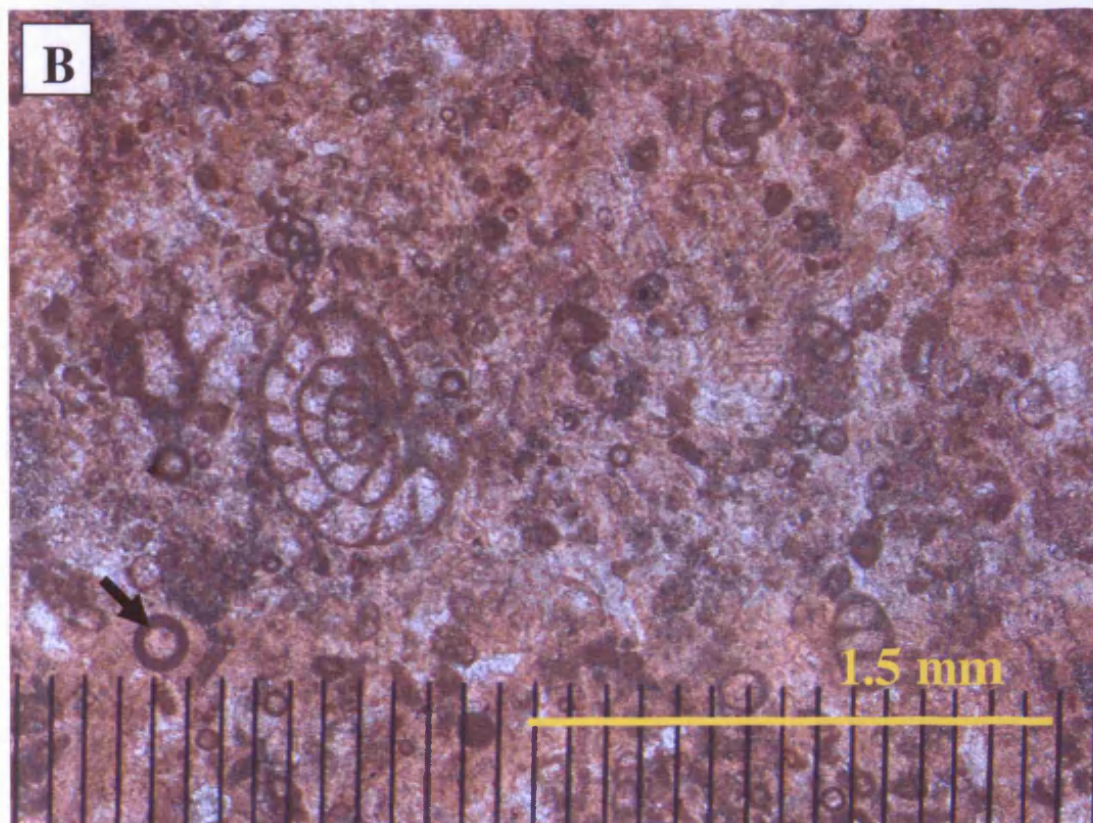
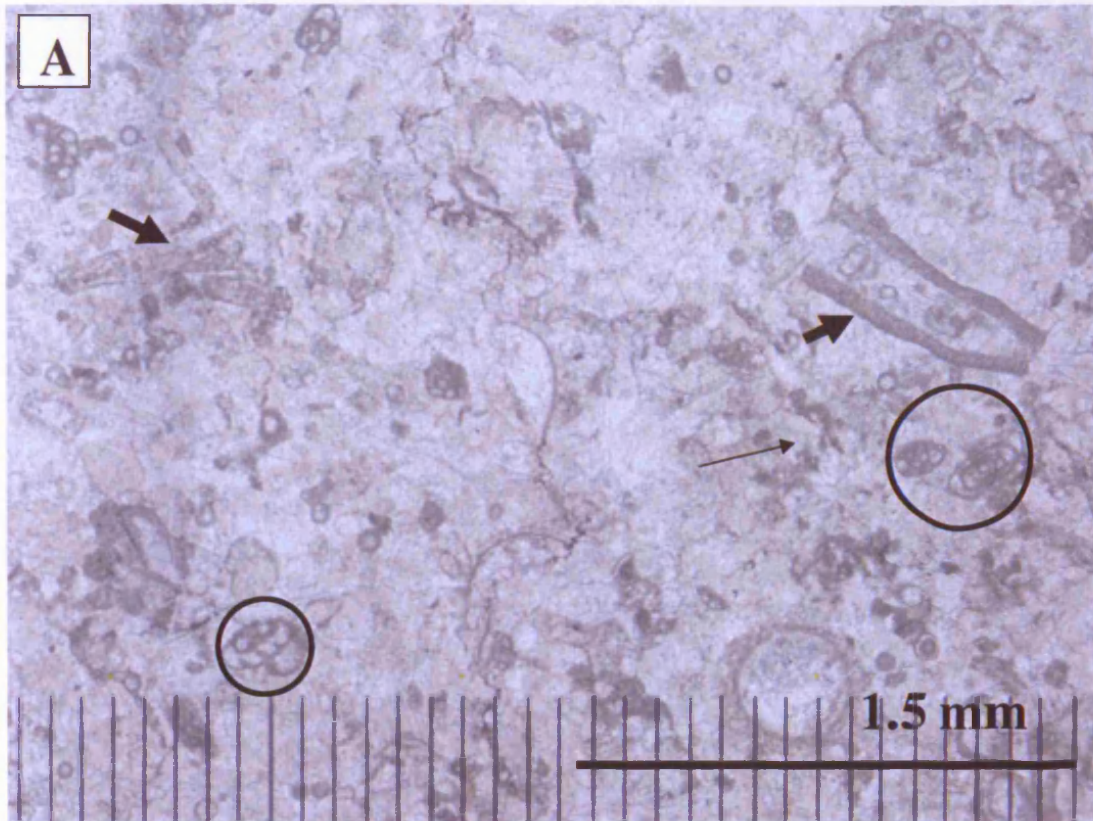


Figure 3.22: Lithofacies LD1, half stained thin section. A) Gross texture with *Uraloporella Korde* (arrow), forams (circled), and pale brown nomorphism relics. Three Cliffs Bay, TS# 65. B) Dominated by forams, calcispheres (arrow), and very fine peloids. Port Eynon Bay, TS# 5.

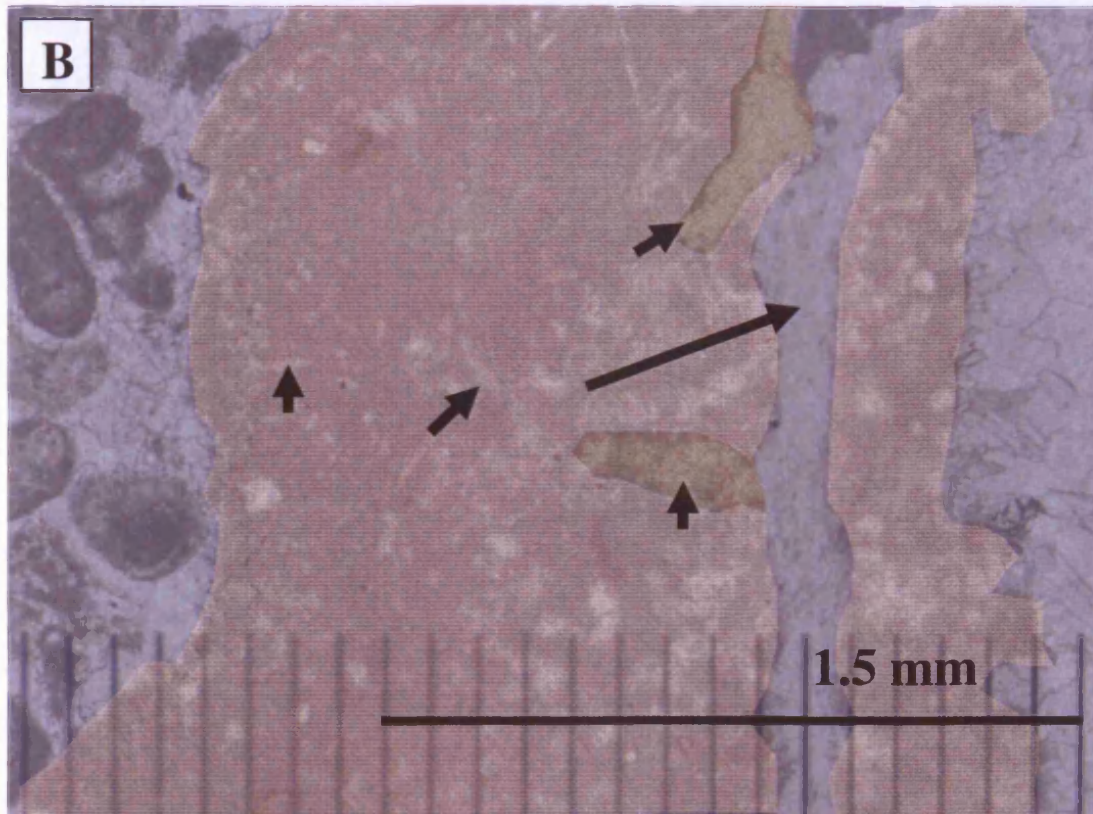
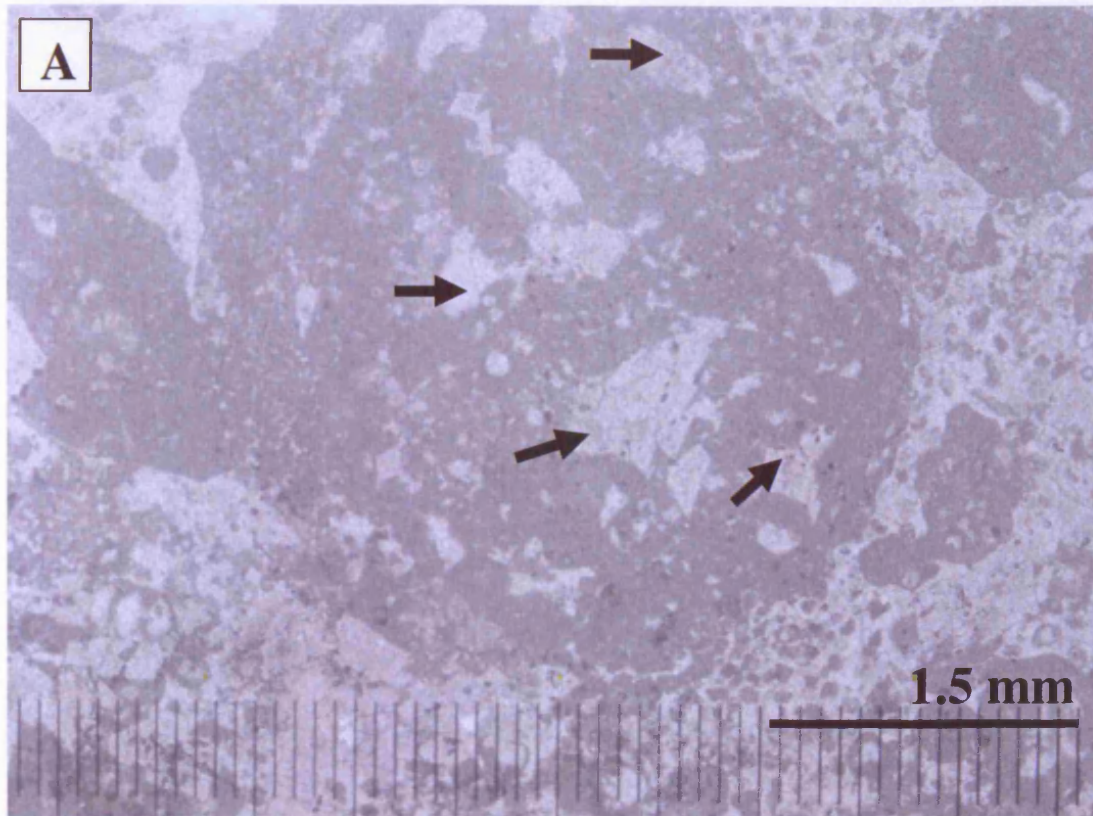


Figure 3.23: Lithofacies LD2, an unstained thin section. A) Individual sponge material with fenestral fabrics filled with sparry calcite (arrows). Three Cliffs Bay, TS# 61. B) Sponge encrusting (pale orange highlight) brachiopod fragments (long arrow) with calcified sponge canals (dark orange highlight and small arrows). Langland Bay, TS# 3.

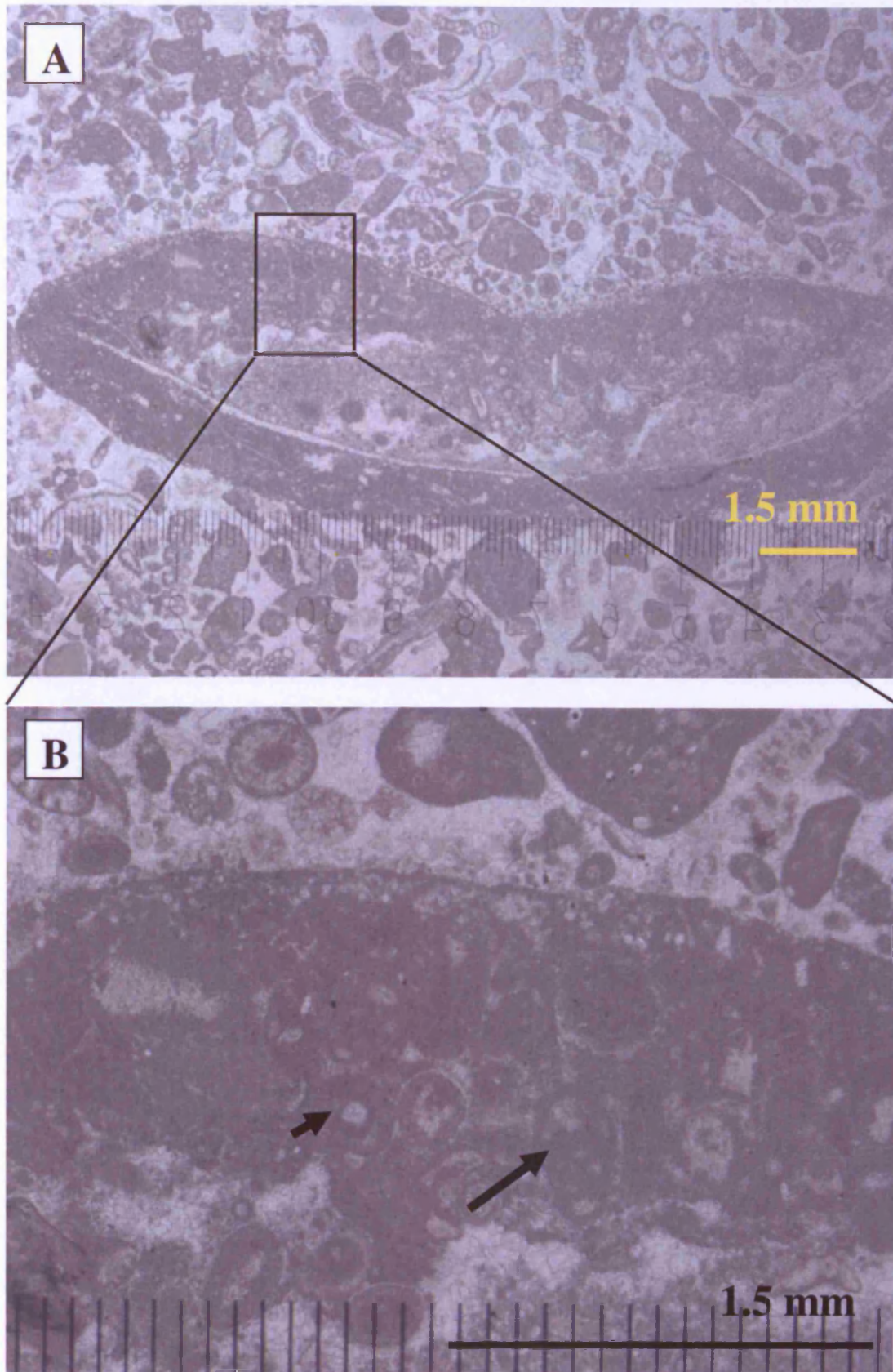


Figure 3.24: Lithofacies LD3, an unstained thin section. A) Gross texture. B) Magnification of A shows constructive micrite envelope, that bound different types of grains such as ooids (small arrow) and forams (long arrow). Langland Bay, TS# 6.

algae as interpreted by Korde (1950), or probably foraminifera as interpreted by Riding and Jansa (1974). The microfossils are usually distributed in back-reef and restricted lagoonal settings (Riding and Jansa, 1974, 1976; Kazmierczak and Goldring, 1978; Faber and Riding, 1979); however, their association with brachiopods and crinoids suggests open marine conditions (Wright, 1981). Therefore, as concluded by Faber and Riding (1979), these microfossils occur in protected lagoonal settings, but are not a good indicator of the specific depositional environment, and may of course have been reworked.

As mentioned in LD2-3, the presence of individual grains of sponge and/or encrusting shell fragments with very clear calcified canals and sometimes fenestral fabrics filled with sparry calcite that resemble the examples of 'calcified siliceous sponges' (Fig. 3.23) discussed by Warnke (1995) from the Lower Carboniferous in northwest Ireland. He concluded that these types of grains are in the first phase of mud mound formation.

Some of the fragments of brachiopods and crinoids have both types of micrite envelopes, destructive and constructive. However, the constructive type formed around the limestone grains without disturbing the internal structure of the shells. Today micrite constructive envelopes occur in grass-bed settings (Perry, 1998). The sponge grains discussed above would be classified as constructive micrite envelopes where they encrust shell fragments. Figure 3.24 shows a constructive micrite envelope which has coated adjacent distributed grains.

The different types of grains imply that the settings around this association vary with barrier and lagoonal settings. The dominated peloids may be sourced from faecal pellets, and the increase in micritisation reflects the higher degree of stabilisation with low agitation currents. The superficial ooids are very shallow (a few

meters of water depth), and their presence suggests either that they are at their site of deposition, or that they are being transported from the adjacent oolitic shoal.

The general association suggests their being deposited in a low-energy environment, probably in a back-barrier setting which was deposited in a low-energy environment unlikely to have been deeper offshore and likely lagoonal, probably a more open embayment, but not a restricted lagoon. There are two reasons supporting this idea; first is the presence of the coarser grains that need higher energy to be deposited, second is the interfingering with LB2 in the Three Cliffs Bay section.

3.6 Summary

* The HBO has been logged in three sections south of Gower area, and these are from east to west respectively Langland Bay, Three Cliffs Bay and Port Eynon Bay.

* All three sections contains the following associations and lithofacies:

- Facies Association A represents open marine deposits and it is the deepest part of the HBO. It is divided into two lithofacies; crinoidal plate grainstone LA1 and bimodal grainstone LA2.

- Facies Association B is the main oolitic factory that had been deposited in an active shoal setting. This association have two main lithofacies; bioclastic, oolitic grainstone LB1 and pure ooid grainstone LB2.

- Facies Association C is dominated with grapestones, lumps and aggregates having been deposited in a back barrier environment. It has three lithofacies; the main and most common typical grapestone grainstone (LC1), lumps and aggregate grainstone and packstone (LC2) and the less common immature grains of “pre-stage” aggregates and grapestones (LC3).

-Facies Association D represents very shallow lagoonal facies and has three lithofacies which are very fine grade bioclastic and peloidal grainstone (LD1),

constructively coated sponge packstone including facies (LD1) as lithofacies (LD2), and the above lithofacies plus ooid grains as (LD3).

* All the above associations fit into simple model from offshore toward the lagoonal areas.

3.7 Depositional Model of the HBO

The stratigraphical successions in the logged sections have quite similar thicknesses where the exposed thickness of the HBO in the Port Eynon Bay is around 274m, in the Three Cliffs Bay is around 280m and in the Langland Bay is around 271m. However, the facies associations show variations in the thickness as shown in the fence diagram (Fig. 3.25). There is thickening trend from the Port Eynon Bay toward the Langland Bay. For example, the main oolitic factory Association B in the upper part of the HBO has a thickness of around 28m in the Port Eynon Bay, and in Langland Bay to the east of around 50m. The thickness variation was reflected the slow rate of subsidence to relatively the high rate of sedimentation.

Three minor cycles are distinguished within the HBO in south Gower area (Fig. 3.26), if the deep mid-ramp dominated Association A is used as a marker to define the bases of these cycles. These cycles (discussed in detail in section 4.1) are shallowing upward, but still have lateral variability. After all, the HBO is a range of small sandbodies that were shifting up and down, and formed as a complicated shifting structure of large sandbodies and associated facies around them. Block diagram (Fig. 3.26) of the HBO shows the ideal distribution of these facies from the deepest middle ramp facies through oolitic shoal complex and back shoal grapestone facies to more restricted very shallow lagoonal facies. So, Association B or C, which

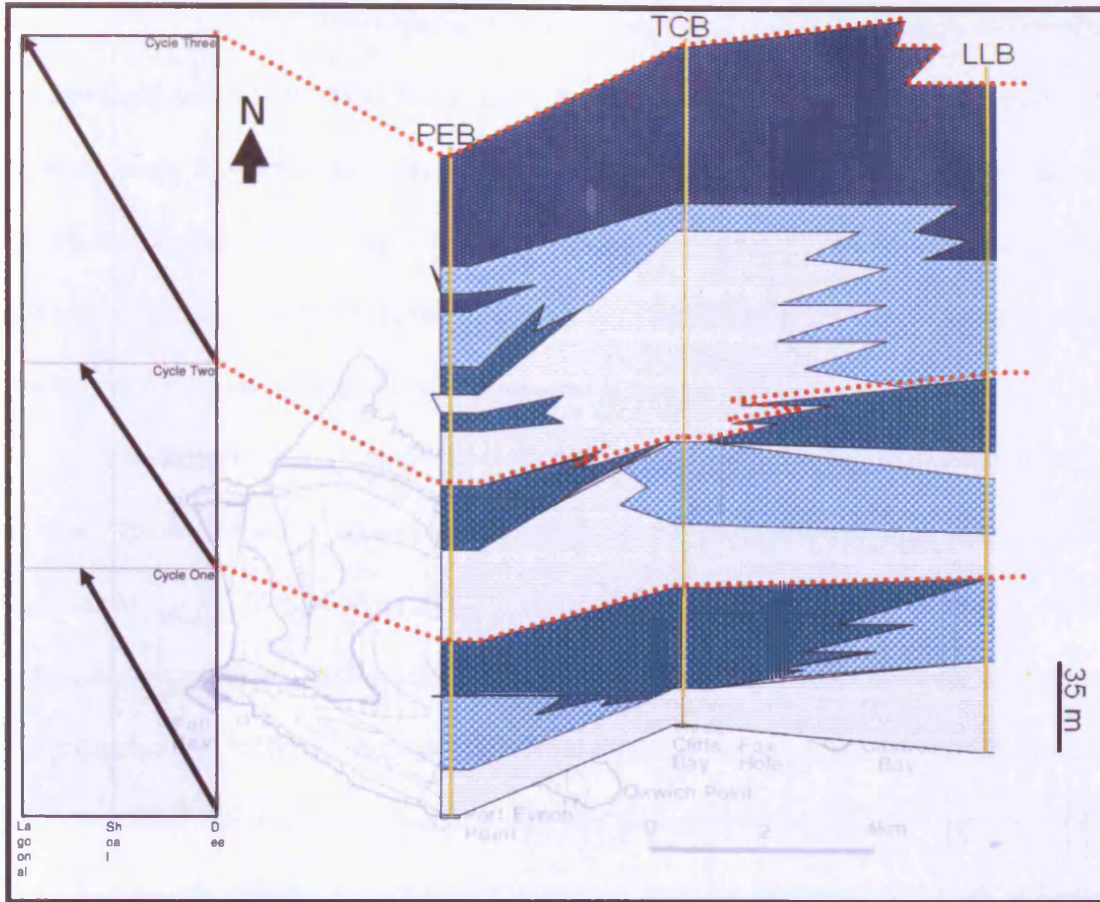


Figure 3.25: HBO fence diagram is reflecting the W-E barely increase in thickness trend in a complex mosaic sandbody, also the recognised cycles are shown to the left of the diagram. (Figure's key, see Fig. 3.25 below)

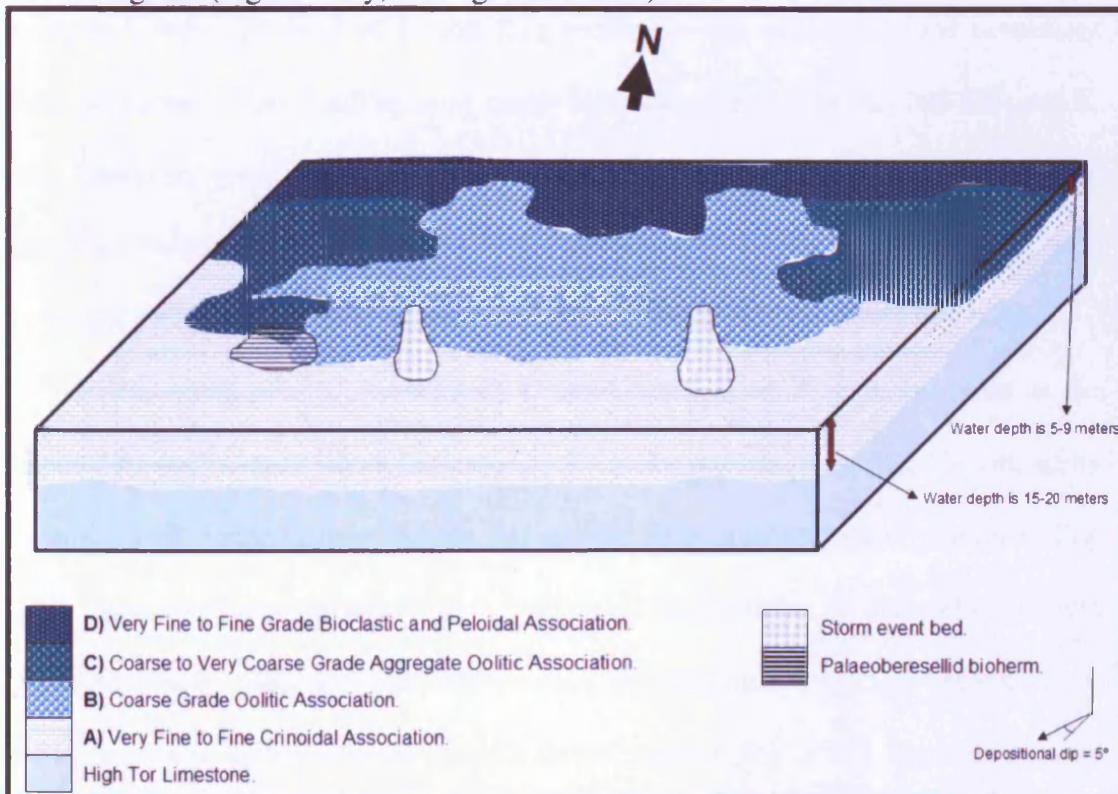


Figure 3.26: Suggested block diagram of the HBO.

are closely related and likely represented water depths of only a few meters difference accumulated adjacent to Association D or A. However, Association A is not expected to have been deposited adjacent to D. The mosaic-like distribution of the facies, unlike the model of the migration or stacking of linear facies, illustrated in the thickness decrease with a linear increase in facies unit thickness (exponential thickness-frequency relationships; Wright and Burgess, 2005).

The depositional orientation (whether strike- or dip-oriented) is not clearly defined, because the key characteristics such as the palaeocurrent data and isopach map could not be identified in this study. However, Ramsay (1987) provided some palaeocurrent readings for the HBO of S. Wales. He did not provide mean values for the palaeocurrent readings, though just visual analysis was done on his rose diagrams. The conclusion of the visualisation is that the majority of the readings are ebb-tidal flow dominated, oblique to seaward (southwest and southeast), if the E-W palaeo-shoreline was preferred. There are some readings toward the northwest, found in the Port Eynon Bay section, which represent flood dominated flow. Moreover, minor readings may imply bimodal pattern (NW-SE, NE-SW, and E-W). However, some other readings are confusing and do not reflect a preferred direction, while there should be well pronounced bidirectional pattern (N-S) perpendicular to the shoreline in order for HBO to fit marine sandbody belt model.

The occurrence of Association C over Association A is problematic as the intervening oolite shoal facies (Association B) is not present. This might be caused by extensions of Association A within the oolitic shoal and intershoal complex (Fig. 3.26). This could have arisen if the oolite shoals (Association B) were elongate and partly or wholly detached and separated by Association A. Such a setting might reflect extensive spits produced by long shore currents (Fig. 3.27). There extensions

of Association A were not isolated enough to become lagoonal but were in open connection with the main marine basin.

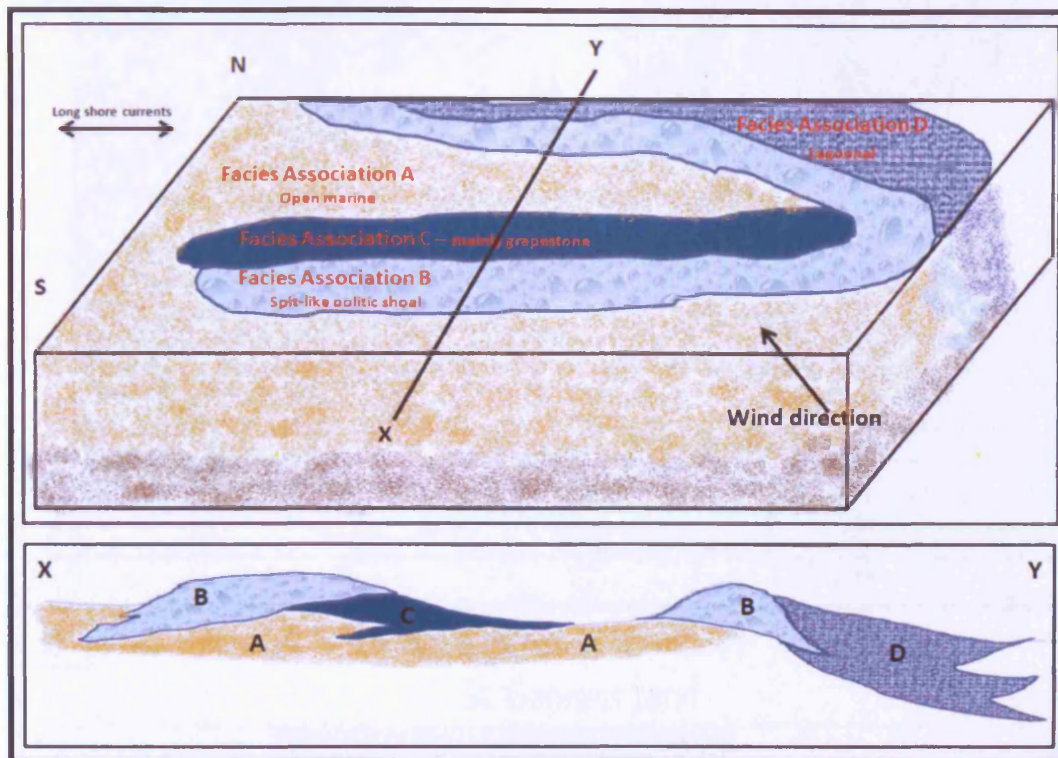


Figure 3.27: Spit-like model of suggested HBO sandbody in Gower area, and below is a NS cross-section within the area.

Although no specific spit-like facies have been identified, a setting consisting of a mosaic of shifting, stacking oolitic shoals, connected (spit-like) and detached, could explain the thick development of oolitic and grapestone facies (Fig. 3.28).

Ramsay (1987) (Table 3.1) and Scott (1988) (Table 3.2) had emphasised that HBO is comparable with the marine sand belt model in the Bahama Bank Platform of Hine (1977) and Ball (1967), respectively. Therefore, there are diagnostic criteria that need to be well represented in any sandbody if it is to be classified as a marine sand belt deposit. Based on Handford (1988), there are criteria associated with marine sand belts accumulated in windward areas and others with ones accumulated in leeward areas. Some of these criteria are similar in both areas and the most important

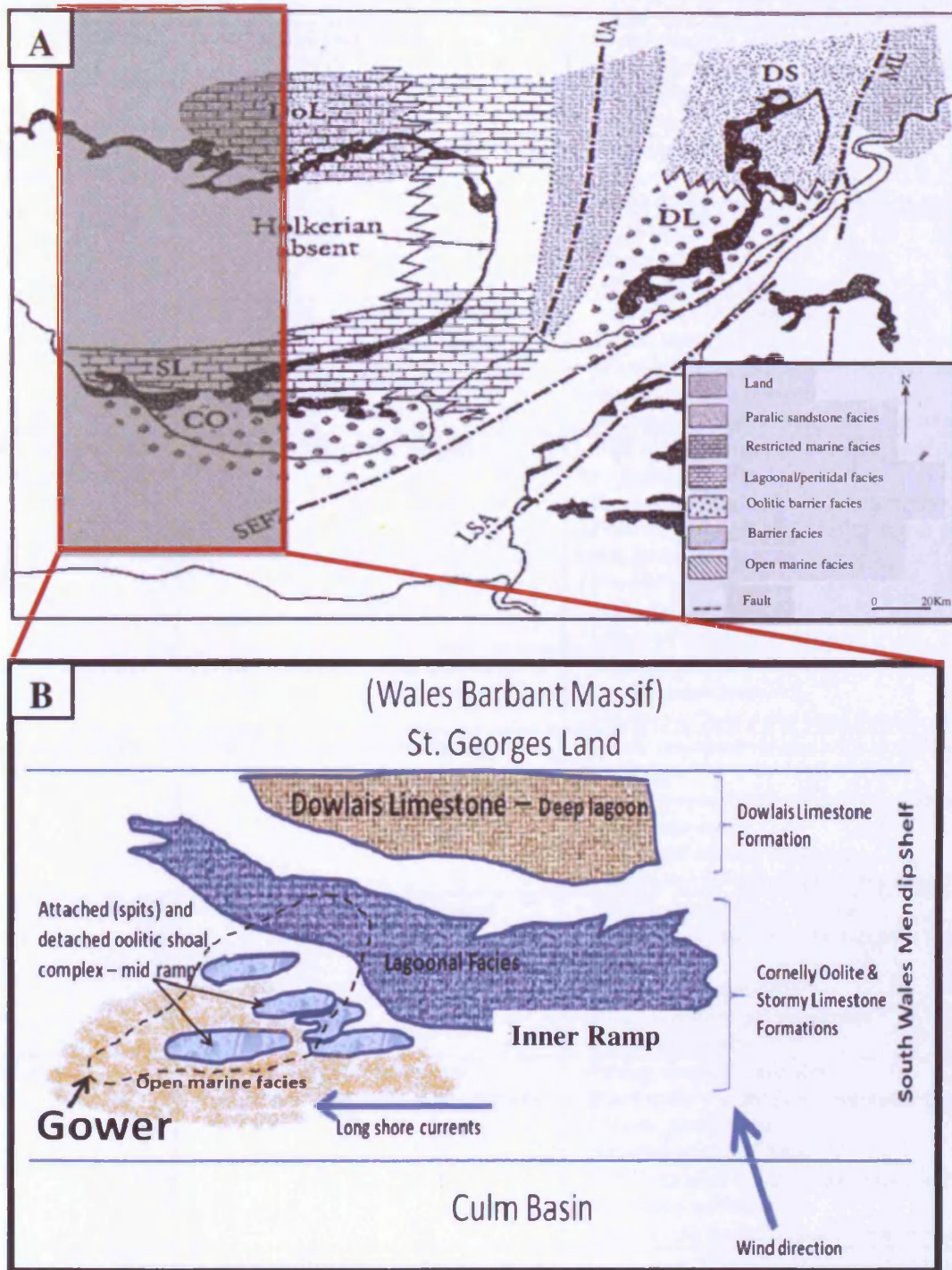


Figure 3.28: A. Palaeogeography map for south-east Wales and part of southern England during the Holkerian. (DoL: Dowlais Limestone, DS: Drybrook Sandstone, DL: Drybrook Limestone, SL: Stormy Limestone, CO: Cornelly Oolite, CDL: Clifton Down Limestone, UA: Usk Axis, ML: Malvern Line, SEFZ: Severn Estuary Fault Zone, LSA: Lower Severn Axis). Based on Burchette (1987) and Wilson et al. (1988). B. Speculative facies distribution for Holkerian times. (dominant wind direction during early Carboniferous monsoonal system, Wright 1990).

Chapter 3

Deposits of	Texture	Sedimentary features and/or structures
Storm-wave dominated offshore	Poorly sorted packstones	<ul style="list-style-type: none"> - Bioturbation. - Coarse lenses and discontinuous layers - Grainstones with structures. - <i>Zoophycos and Thalassinoides burrows.</i>
Shoreface, adjacent to oolitic marine sand belt	Oolitic grainstone	<ul style="list-style-type: none"> - Featureless - Burrow mottled - 10-50 cm planar or trough cross sets
	Bioclastic limestone	<ul style="list-style-type: none"> - Featureless - Planar laminated - Trough cross-bedded
	Graded units	<ul style="list-style-type: none"> - 5-10 cm trough cross-bedded - Planar lamination within bioclastic grainstone - Wave-knitted cross-sets within bioclastic grainstones to packstones - Bioturbation within bioclastic packstone
Ebb-tidal channels cut across the oolitic sand belt	Fining-upward oolitic grainstone	<ul style="list-style-type: none"> - 5-10 m sequences (from oolitic grainstone to bioclastic packstone) - Erosional bases with coarse intraclasts lags - Dunes and megaripples of 15-50 cm high trough cross-beds - Intensely-bioturbated - Reactivation surfaces - Offshore transport southward
Ebb-spits of flood tidal deltas	Planar-laminated oolitic grainstones	<ul style="list-style-type: none"> - Dipping northward laminations - Small trough cross-sets - Separate a flood ramp from the ebb channel
Migrated sand waves by flood	Coarsening-upward successions	<ul style="list-style-type: none"> - Planar erosional surface with intraclasts and fossils lags - Coarsen-upward from bioclastic packstone to oolitic grainstone - Landward dipping cross-sets - Terminates at landward dipping erosion surface
An emergent, vegetated ebb shield	Well-sorted oolitic grainstones	<ul style="list-style-type: none"> - Trough cross-beds at the base - Intense bioturbation at the top with the oolitic grainstone - Contains rhizcretions - Bimodal pattern palaeocurrent - Planar-lamination
A broad lagoon	Poorly sorted packstones and wackestones with beds of mudstones	<ul style="list-style-type: none"> - Fining-upward sequences - Basal units contain fine intraclastic grainstones or oolitic grainstones - Scoured erosional bases - 20-50 cm high trough cross-beds with reactivation surfaces - Coated fine bioclastic packstone on the surface

Table 3.1: Illustrates the sediments distribution with the depositional environment for HBO. Based on Ramsay (1987).

Chapter 3

Time	Palaeogeography	Dominant	Sedimentary features
Arundian/Holkerian	A shelf barrier with a variable small scale topography	Crinoidal sheet & peloidal sand	Reduced sedimentation rate.
Very early Holkerian	An establishment of oolitic shoal barrier complex	Alternating shale and limestone deposition. At the top peloidal bioclastic sands.	Bioclastic peloidal wackestone and packstone interbedded with calcareous bioturbated shales.
Early Holkerian	Developed shoal barrier complex on the mid-shelf area	Prograded bioclastic sand with thin veneers of oolitic shoal barrier complex during storms.	Chert lenses or discreet nodules. Lags of crinoidal debris. Lenticular structures with bioturbated erosive base. Overlain by wave ripple laminae. Low angle laminae. Parallel laminations. The oolitic lithology contains bioturbated erosive bases, bases are hummocky cross-sets with wave ripple lamination. Cuspate structure found at the base as well as planar. Low angle truncation surfaces.
Mid-Holkerian	Seaward margin of the well-developed shoal barrier	Active ooid shoals flanked by crinoidal bioclastic sediment.	Featureless. Stabilised sediments. Trough cross bedding. Asymptotic foresets at the base. Gradational bases and sharp tops.
	Behind the seaward ridge of the shoal barrier	Stabilised oolitic aggregate sand	
	Protected marginal back barrier area	Peloidal sands and micritic tidal flat deposits.	
	Offshore of the shoal barrier	Crinoidal bioclastic sands with storm introduced, thin veneers of oolitic sediment.	
Late Holkerian	Broad shallow area behind the prograded shoal	A mosaic of deposits including shallow subtidal peloidal and bioclastic sands, ooid shoals, micritic tidal flats and oolitic washovers.	Basal lags and channel fills in tidal inlets/channels. Thin foreshore units of low energy beach sequences.
	Central part of the shelf	Low energy, active (channelized) tidal flats	

Table 3.2: Illustrating the depositional environments throughout the Holkerian time. Based on Scott (1988).

characteristics are that the sandbody has to be parallel to depositional strike, divided into ramp, protection shield and spillover lobes (spillover lobes directed to bankward area) and bipolar large-scale tabular cross-beds in the shield area. Hine's (1977) sandbody model (Lily Bank) accumulated in a windward setting with the following features that are not present in leeward areas, such as flood dominated wide ramps covered with sandwaves, shield covered with symmetrical sandwaves, ebb flow in narrow deep channels with a hierarchy of beds from linear sand ridges to small ripples, and subtidal sandwaves superimposed with ripples and megaripples. Ball's (1967) sandbody model (Cat Cay) accumulated in leeward area with the following characteristics, the surface consists of ripples, sandwaves, and dunes, and one of the important features which is the base is marked by bipolar large-scale tabular cross-beds overlain by smaller scale cross sets.

Both earlier proposed models for HBO (Ramsay, 1987; Scott, 1988) are lacking the differentiation between the main two parts of the marine sand belt the ramp and shield. In this study (Table 3.3) no small scale ramp-shield deposits have been identified. Also in Ramsay's (1987) model the spillover lobes developed in the seaward area where as Handford (1988), Ball (1967) and Hine (1977) had recorded this feature always in the bankward (landward) areas. Although, in the current study the large bipolar cross-stratifications, which are several meters thick, have not been found. A critical feature should be the prominent spill over lobes. In modern systems these can have relief of several meters, occurring as large avalanche-type fore-sets overlying lower energy, protected lagoonal facies. Such features have not been seen in any of the sections in the Gower.

Unfortunately, the sandbody in this study does not compare to any of the Mississippian ones neither to the modern examples described in chapter two. There

Association	environment	Lithofacies	Dominant	Sediment Features
Very Fine to Fine Crinoidal Association (A)	salinity marine environment of shallow water <5m deep.	LA1	crinoidal plate grainstone.	Erosive beds dominated with granule-grade debris of crinoidal lags. Bioturbated. Presence of macrofossils.
		LA2	crinoidal silt-size debris and coarse sand grade oolitic, aggregate grainstones.	Thin oolitic grainstone event beds. Planar and undulating lamination resembling hummocky cross stratification. Tubular tempestites.
Coarse Grade Oolitic Association (B)	active oolitic shoal of high-energy settings.	LB1	bioclastic, oolitic grainstone.	packages of thin laminations of dark grey, very fine peloidal grainstone with occasional cross bedding.
		LB2	pure ooid grainstone.	Massive, rare to find well-pronounced sedimentary structures.
Coarse to Very Coarse Grade Aggregate Oolitic Association (C)	back barrier lower energy level settings, shallow and adjacent to the active oolitic shoal.	LC1	typical grapestone grains	poorly-developed small scale trough cross-bedding. erosional beds that are marked by bioclastic lags. Bioturbation at the top of the units.
		LC2	grains of aggregate and lumps plus grapestone	
		LC3	grapestone, with ooids, and immature aggregates	
Very Fine-to-Fine Grade Bioclastic and Peloidal Association (D)	low-energy environment unlikely to have been deeper offshore and likely lagoonal, probably a more open embayment.	LD1	very fine grade bioclastic and peloidal grainstone	massive units. very thin lamination. No distinct sedimentary structures. Fining upward sequence.
		LD2	constructively coated sponge packstone plus LD1	
		LD3	oolitic grainstone plus LD1 and LD2	

Table 3.3: Illustrating the depositional environments throughout the Holkerian time of the recent study.

are a couple of possible reasons; for example the oolitic, grapestone facies can be distributed for over 100m stratigraphically within the HBO, where there is no major oolite shoal near by to have fed these grapestone facies. Major features of the well-documented sandbody models of the Mississippian and the modern are not have developed in the HBO, such as the ramp, shield and spillover lobes with large-scale bipolar cross-stratifications of the marine sand belts. Large tidal features such as in tidal bar belts; are not present (Ball, 1967; Kelleher and Smosna, 1993). For tidal deltas; bipolar sand waves (Gonzalez and Eberli, 1997) are not seen. For tidal sandwaves; the stacks of sandwave layers and subaqueous dunes, and sandwave beds with 1m to 3m in thickness, in a transverse direction to the current and strongly asymmetrical (Harms et al. 1974) are not seen. Trends in grain size and sedimentary structures indicative of barrier islands such as typical shoreface and beach sequences, washover sands and tidal inlet-delta (Lloyd et al., 1987) are not seen including 10-20m thick shallowing- and coarsening-upwards sequences of oolite shoreface (Burchette et al., 1990). Finally for purely wave-dominated sandbodies, the complete ridge-type sequence from basal high energy, coarse-grained and cross-stratified in the upper shoreface and foreshore units, to finer-grained, well-sorted oolitic aeolianite at the top of the sequence (Lomando, 1999) are not seen.

In conclusion, the ambiguity of the HBO sandbody is still unresolved and it may represent a unique complex model. One possibility is that a sense of attached and detached oolitic shoals occurred, separated by open settings (Association A), with extensive grapestone facies developed on their leeward margins. From original data and by using Ramsay's (1987) palaeocurrent readings, it seems not well integrated with the modern or ancient examples of marine sand belt models. Many of the major

Chapter 3

characteristics, as reviewed in chapter two and summarised above, of the modern or the Mississippian sandbody models are absent within the HBO.

**CHAPTER 4. REVIEW OF SEQUENCE STRATIGRAPHY AND
TECTONICS, AND THE GLOBAL SEA-LEVEL CURVE**

4.1 Sequence Stratigraphy and Tectonics

Ramsay (1991) has offered an integration of tectonic and sequence stratigraphy of the Dinantian, especially the Holkerian of S. Wales. He proposed that the Dinantian accumulated on a south-dipping hanging wall of a half-graben on a fault zone of the Bristol Channel. Originally Gayer and Jones (1989) proposed that the South Wales area during the early Carboniferous was deposited on a subsiding set of half grabens whose faults (probably re-activated pre-Caledonide structures) dipped to the south. Ramsay (1989 & 1991) also invoked such a setting. Asymmetrical subsidence and an E-W oriented rifting phase caused the changes in the basin-margin floor architecture. The slopes of the depositional settings (basin floor topography) of all the Dinantian successions were controlled by movements on concealed basement faults which resulted in active high-hinge lines. These lines, along with basement structures, affected the thickness and erosion features and may have controlled the development of cyclic nature of the successions. The ramp itself was formed by the asymmetrical subsidence and the hinge lines. Cyclicity within the Holkerian of the Gower area was a product of a regressively prograded and migrated barrier, due to a tectonic fluctuation in sea-level (Ramsay, 1987).

Ramsay (1991) identified and correlated three cycles, from North Crop to the Gower area, which are characterised by three upward-shoaling cycles. Briefly, these cycles were described thus: cycle one is a sequence of upward shoaling from storm-dominated offshore ramp deposits which, in the present study, are represented by Association A, through shoreface sediments, to oolitic intraclast grainstone; cycle two is the result of barrier retreat, extension, subsidence and sea-level rise followed by



progradational phase; and cycle three is characterised by the dynamic regime of a shoaling-upward transgressive phase where *Lithostrotion* bioherms accumulated in North Gower. The sequence in cycle three started with barrier retreat and penetration of interfingered oolitic grainstones, and bioclastic packstone grainstone; both represent the oolite shoal, and end with lagoonal deposits. This sequence is the product of progradation and seaward migration of the barrier, and is controlled by relative sea-level rise and a rate of sedimentation that allows the barrier to have prograded and aggraded, and developed a major lagoonal area. At the end of the Holkerian, the HBO was capped at the basin-wide erosion surface that is associated with palaeokarst platforms which mark the Holkerian-Asbian boundary (Ramsay, 1991).

Two suggested models have been applied in this study, the autocyclic and allocyclic models. The former is associated with static sea-level and shoreline progradation, which can be summarised as an asymmetrical cycle initiated by subtidal deposits, followed by sediments possibly including subaerial exposure and soil development, followed by a lag time where sediments are reworked until subtidal settings are initiated again and shallow upwards in a new cycle (Wright and Burchette, 1996). However, this model is less attractive because the thickness of each cycle in the HBO is larger and non-uniform as would be expected in an autocyclic model which typically invokes subsidence as the control on accommodation space creation.

Cycles of the allocyclic model are found in areas that are influenced either eustatically or tectonically (Wright and Burchette, 1996). The first control is neglected in this case study for three reasons; the first is thickness. With the average Carboniferous-cycle post-Holkerian glacio-eustatic cycle thickness is around 3-30m

(most are in the range 3-10m), so the HBO cycles are too thick to be glacio-eustatic. Secondly, the HBO lacks any exposure surfaces which are a key element in glacio-eustatic cycles. Thirdly, Holkerian time lasted 3 million years, and the HBO in the Gower area exhibits three cycles, each of probably 1 million years duration. However, the glacio-eustatic cycles in the post-Holkerian are generally 100-120 ky long (Wright and Burchette, 1996), in some cases 200-400 ky (e.g. Tucker and Wright, 1990). The tectonic-influenced cycles are likely locally controlled. For example, normal faulting would affect small areas, and the associated cycles would not contain prominent exposure surfaces (Wright and Burchette, 1996). This is the most likely scenario to describe the cyclicity of the HBO in the Gower area, as Ramsay (1991) suggested.

The present study describes three non-glacio-eustatic shallowing-upward allocycles. All the cycles consist of the same associations (here called units). These units (Fig. 4.1) are distributed in the same hierarchy but they show lateral variations, and are, respectively, from old to young: a very fine to fine crinoidal unit (**A**: offshore deposits), a coarse grade oolitic unit (**B**: shoal complex deposits), a coarse to very coarse grade aggregate oolitic unit (**C**: back shoal deposits), and a very fine to fine grade bioclastic and peloidal unit (**D**: lagoon deposits). The latter unit is found only in the third cycle. Cycle one has an average thickness of about 75m, cycle two is around 85-90m, and cycle three about 132m.

According to the depositional model of the HBO in this study (Fig. 3.25), the cycles were controlled by sea-level changes caused by tectonic effects, as Ramsay (1991) proposed. These cycles have not been detected before in any other nearby areas, such as the Vale of Glamorgan (Wilson, 1990), which proves that these cycles may be formed in a locally influenced area by tectonics. Ramsay (1991) identified the possible influence of the Port Eynon thrust as the lowest cycle in the Gower (Fig. 4.2)

(Ramsay, 1991). He speculated that this structures and the hinge line along the present Cefn Bryn anticline could have influenced thickness changes in the Holkerian. It is very difficult to prove or disprove such proposals gives the limitations of outcrops. It is also difficult to identify the exact effects of these pre-Hercynian structures after later compression took place and they were likely re-activated and possibly inverted. What can be stated is that as the Holkerian sediments mainly represent deposition in very shallow waters, even small scale changes in subsidence rates may have influenced short term and longer term accommodation space and facies distribution.

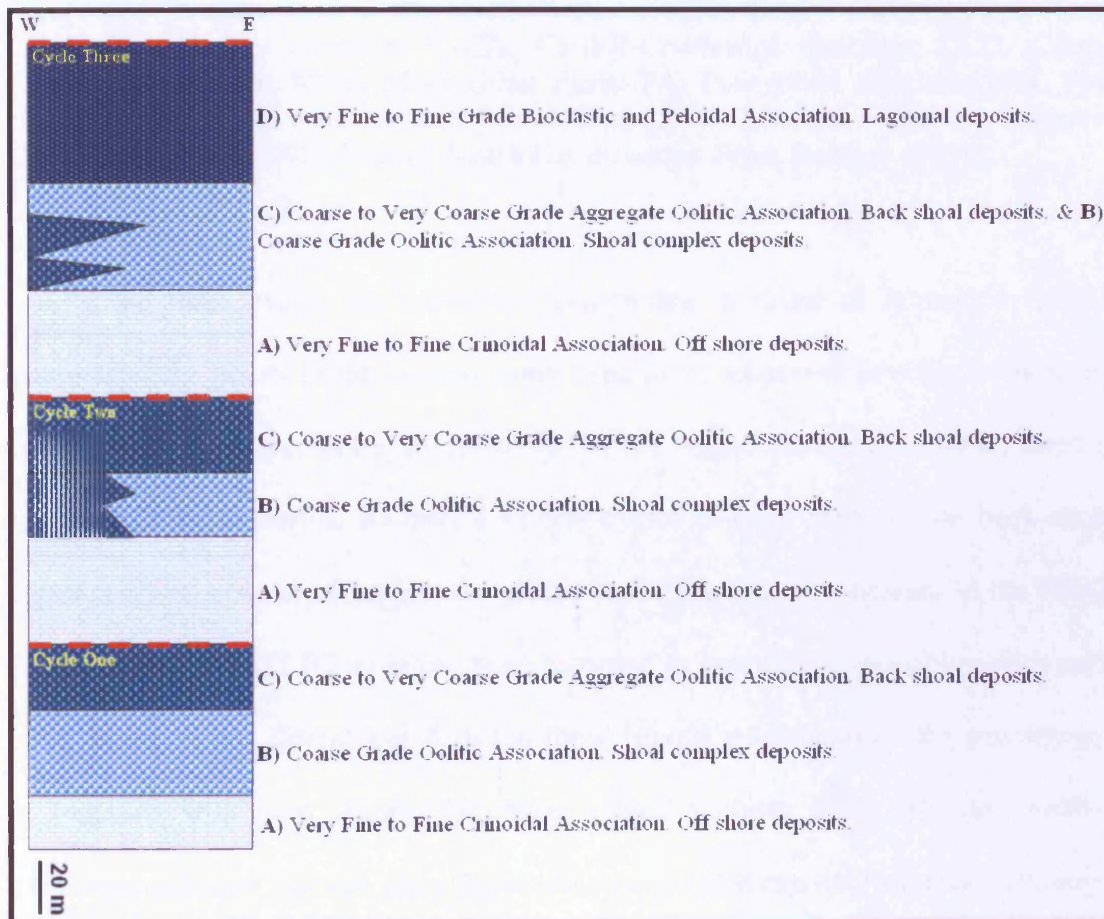


Figure 4.1: Cycles within the HBO identified in the present study.

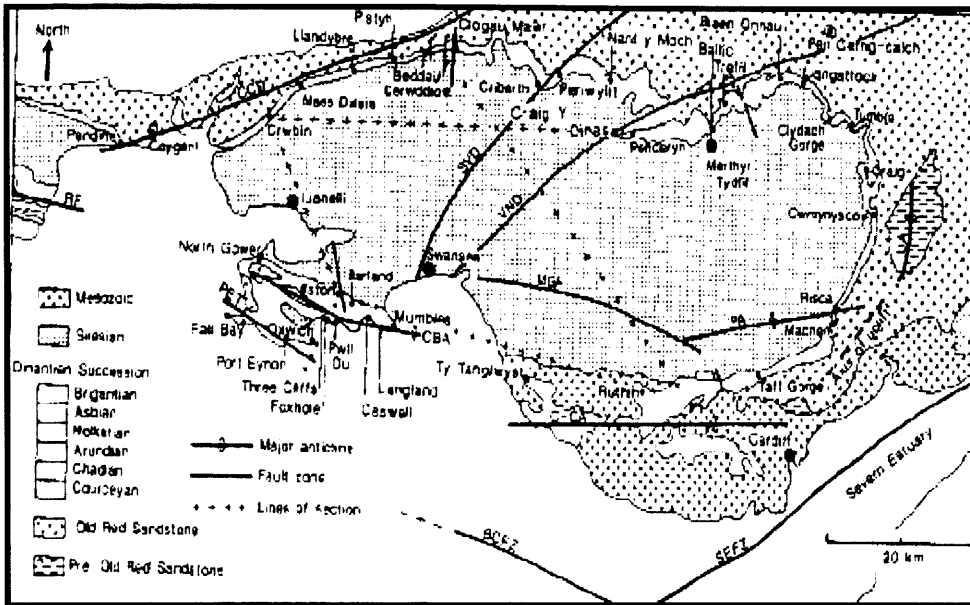


Figure 4.2: Structure map of the South Wales. (BCFZ, Bristol Channel Fault Zone; CBA, Caswell Bay anticline; C-CA, Cardiff-Cowbridge anticline; CCD, Carreg Cennen Disturbance; MGF, Moel Gilau Fault; PA, Pontypridd anticline; PET, Port Eynon Thrust; SEFZ, Severn Estuary Fault Zone; SVD, Swansea Valley Disturbance; UA, Usk anticline; VND, Vale of Neath Disturbance). From Ramsay (1991).

The three cycles are somewhat compatible to those of Ramsay's (1991), however, some points in the current study need to be addressed in order to integrate both studies. All three cycles are identified in the logged sections; however, there is no presence of bioherms. Ramsay's (1991) cycles did not mention the back-shoal deposits which consist of grapestone grains that are major constituents in the HBO. Lithofacies LB1 and LB2 have not been recorded as being in juxtaposition with each other, however, the differences between these lithofacies depend on the percentages of bioclasts with ooid grains. All three logged sections have exhibited neither prominent exposure surfaces nor palaeokarst surfaces that cap the Holkerian, although there is no evidence of peritidal limestones within the studied area, where the absence of such features reflects the rapid fill of the back-barrier areas in the progradational phase (Wright, 1986). Therefore, both sets of cycles (Ramsay's, 1991; and present study) display many common features and could be comparable to each other.

The HBO is capped by a subaerial exposure surface (Ramsay, 1987) that could be seen as the end of the regressive phase, which deposited Association D over the Gower. However, this upper most 'lagoonal' dominated unit (up to 50m thick) must have been deposited during an interval of net accommodation space creation to maintain a persistent lagoonal area. This correlates well with the main eustatic curves for the Holkerian (Fig. 4.3), which identify a net transgression throughout the stage.

4.2 Global Sea-level Curve During the Holkerian

Most workers, worldwide, on the Holkerian are agreed on one sea-level behaviour (Fig. 4.3), that the associated strata lack any presence of glacio-eustasy and any exposure surfaces. The sea-level fluctuation curve was constructed after reviewing a number of significant previous works that were done from different parts of the world, and it is comparable to Ross and Ross's (1988). However, work such as Ramsay's (1987) and Scott's (1988) has not integrated the global sea-level curve with their stratigraphic sections. This section will discuss the similarities of Holkerian sea-level behaviour, comparing the previous studies and the present study. The Holkerian cycle lasted for about 3.0 My (Menning et al., 2000), to 4.5 My (Jones, 1995).

Ramsbottom (1981) calculated the net eustatic sea-level rise for each stage in the Palaeozoic, and ended up with a eustatic rise of sea level during the Dinantian of about 227m. He also indicated that the preliminary factor in the deposition of the Dinantian was eustasy, where the subsidence and isostasy influences were local to the basinal areas.

Ross and Ross's (1988) work identified around 60 transgressive-regressive worldwide depositional sequences in the Late Palaeozoic that were controlled mainly by eustatic sea-level changes. These sequences have an average duration of 2 million years. Ramsbottom (1973, 1977, 1979, 1981) studied the effects of early

Carboniferous sea-level changes in Great Britain in detail, and ended up with 11 transgressive-regressive depositional cycles based on the facies and depositional history. The Holkerian of S. Wales was used to construct the eustatic sea-level curve in Ross and Ross (1988), are based on Ramsbottom's work (1973, 1977, 1979, 1981). Also, the Holkerian cycle (about 3.0 million years in duration) falls into Ramsbottom's (1977) D4 cycle. Ross and Ross's (1988) eustatic sea-level curve was based on the studying of depositional environments, biostratigraphic zonations, facies changes and unconformities. Moreover, tectonic activities and climatic changes, which were evident during the Late Palaeozoic, influenced the eustatic sea-level fluctuations.

Late Palaeozoic glaciation was active in the late Tournaisian and in the mid-late Viséan (Bruckschen and Veizer, 1997) (in early Asbian about 330 Ma; Wright and Vanstone, 2001). However, there are no prior indications of this event before the Asbian (within the Holkerian) of glacioeustatic sea-level fluctuations. Studies of the Holkerian shallow-water successions in Southwest Britain indicate that the sea-level oscillations are not related to glacioeustatic phases. The former successions in South Wales do not contain any evidence of prominent cyclothems or subaerial exposure surfaces (Wright and Vanstone, 2001).

Haq and Schutter (2008) produced a long-term sea-level oscillation curve was based on stratigraphic successions from preicratonic and cratonic basins. They realised 172 short-term third-order cycles which range in duration from about 0.5 to 3.0 My in general, and up to about 6.0 My, i.e. long cycle duration, especially for the Early to middle Mississippian. The Holkerian lies within an interval with a gradual drop in the long-term sea-level. Glaciation, which is not the only cause of sea-level

fluctuation, is believed to have started in late Viséan, post-Holkerian time and represents a fourth-order cycle.

Rygel et al. (2008) believed the Late Palaeozoic is, overall, an icehouse phase. Their review referred to assumptions from over a hundred published papers on Palaeozoic glacioeustasy where the modest size of the fluctuations is a good indicator of the fluctuation processes. The middle Mississippian, which includes the Holkerian, is considered a non-glacial (free glaciation deposits) interval with moderate glacioeustatic fluctuation of <25m, unlike previous and subsequent intervals. The shallow-water sediments of the interval show a paucity of coeval pronounced exposure surfaces, and their stratigraphic architecture is not related to glacioeustasy behaviour (Wright and Vanstone, 2001).

In the present study, the Holkerian sea-level curve is not applicable to the studies cited. It represents three large cycles in terms of thickness and duration. These cycles are not caused by waxing and waning ice sheets, rather, they are the result of local tectonically-influenced sea-level oscillations.

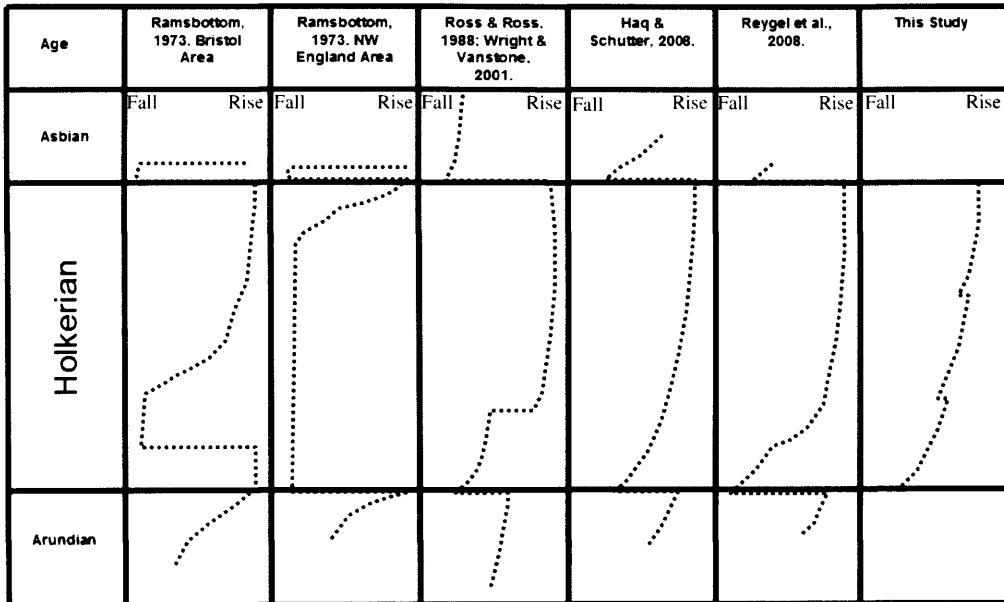


Figure 4.3: Correlation of coastal onlap curves from this study and previous studies for the Lower Viséan successions.

CHAPTER 5. DIAGENESIS OF HUNTS BAY OOLITE

5.1 Introduction

This chapter reviews the diagenesis and porosity evolution of HBO, focusing on two main aspects. Firstly, the origin of the cements is discussed, considering whether they are marine or meteoric. Secondly, evidence of sub-aerial exposure surfaces within HBO is reviewed. The diagenetic events (Table 5.1), are classified, in part, relative to compaction, as eogenetic, mesogenetic or telogenetic (Choquette and Pray 1970), and include: grain micritisation (peloids) and micrite envelopes, fenestral porosity, peloidal cements, fibrous (fringe) cement, aragonite dissolution, non-ferroan calcite cements (blocky and drusy), early dolomitisation, syntaxial cement, neomorphism/recrystallisation, compaction/pressure solution, late-stage dolomitisation, dedolomitisation, fractures with non-ferroan and ferroan calcite.

The HBO in the Gower area was buried relatively rapidly after deposition to a depth of 7km. (Fig. 5.1), then, during the Triassic, the HBO was uplifted (Dickson 1985). Burial by Cretaceous strata probably exerted some effect on the HBO, and later erosion took place in the Oligocene. Overburden pressure and temperature are the main controls on diagenetic effects for any rock types, however, due to rapid burial and uplift, the carbonates may not have reached equilibrium. These movements resulted in an excess pressure solution in confined beds, and underpressuring, respectively (Dickson, 1985).

5.2 Grain Micritisation (Peloids) and Micrite Envelopes

Grain micritisation is considered an early marine diagenetic process that is common in stable shallow water settings at the sediment water interface (Kobluk and Risk, 1977). This type of diagenesis, occurs in stages. Figure 5.2 shows crinoid debris, with altered

margins as well as *Koninckopora* fragments. Micritisation is caused by microborings, due to algae and other micro-organisms, into the surface of the ooids and bioclasts; these microborings later become filled by micritic carbonate, fine-grained sediment or cement, and form destructive micrite envelopes that represent a stage in the formation of peloids (Bathurst, 1966). However, the bioclasts or ooids will alter to peloids if the microorganism activity is intense and completely micritises the whole grains. They can be distinguished from faecal pellets by their irregular shape, and it is often difficult to recognise the original grain after micritisation (Tucker and Wright, 1990). These features occur in almost all associations, but they are intense in Association C.

Figure 3.23 and 3.22B (in section 3.5.3) illustrate constructive micrite envelopes where the organisms trapped some ooids, forams and peloids on the surface of the brachiopod fragment. Constructive micrite envelopes represent the opposite process to destructive micritisation, where micritic sediments accrete on, rather than in, the surface of the grains. They typically form as algae, and microbial filaments induce cementation on the surface without disturbing the internal structure of the grains. Moreover, these envelopes, in modern settings, occur in vegetated areas where microbial biofilms occur within seagrass-beds (Perry, 1998). Such envelopes would not be preserved in agitated settings if there were very active currents and wave energy. They are absent in oolitic shoal areas unless these areas had quiescence periods to allow calcification of the micro-organism (Kobluk and Risk, 1977). Also, the constructive envelope causes reduction in the grains mobility which become more stable (Kobluk and Risk, 1977). This feature is common in lithofacies LD2 and LD3. another mechanism for producing constructive micrite envelopes is encrustation by sponges, although identifying sponge remains is difficult. Warnke (1995), also

Events	Eogenetic	Mesogenetic	Telogenetic
Micritisation (Peloids)	■		
Micrite Envelopes (constructive & alteration)	■		
Fenestrae	■		
Peloidal Cements		■	
Fringe Cements		■	
Aragonite Dissolution		■	
Non-ferroan Calcite Cements (blocky & drusy)		■	
Early Dolomitisation		■	
Syntaxial Overgrowth Calcite Cement		■	
Neomorphism/Recrystallisation		■ ■ ■	
Compaction / pressure solution		■ ■ ■	
Late Stage Dolomitisation			■ ■
Dedolomitisation			■ ■ ■
Fractures with Non-ferroan Calcite			■ ■ ■
Fractures with Ferroan Calcite			■ ■ ■

Table 5.1: Paragenetic sequence for the HBO rocks. Choquette & Pray (1970) proposed the terms: the early burial stage "eogenetic," the late stage "telogenetic," and the normally very long intermediate stage "mesogenetic."

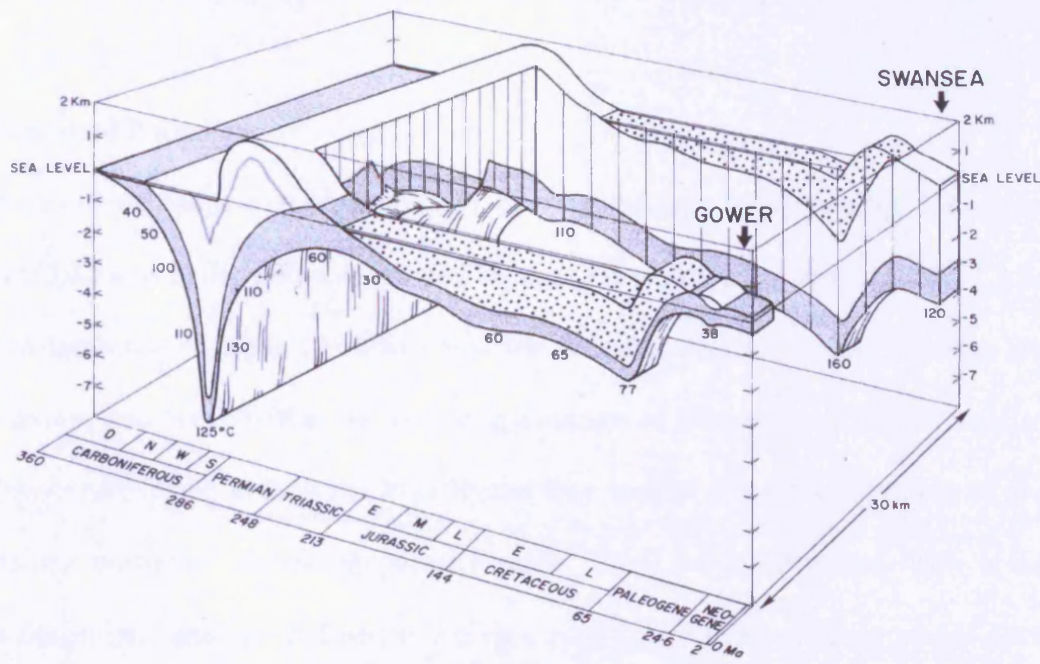


Figure 5.1 Burial curve (Dinantian sediments shown in fine stipple; Mesozoic sediments in coarse stipple; Temperatures shown at base of Dinantian in degrees Celsius; time-scale from Harland et al. 1982) from Early Carboniferous to Recent in the Gower and Swansea areas. From Dickson (1985).

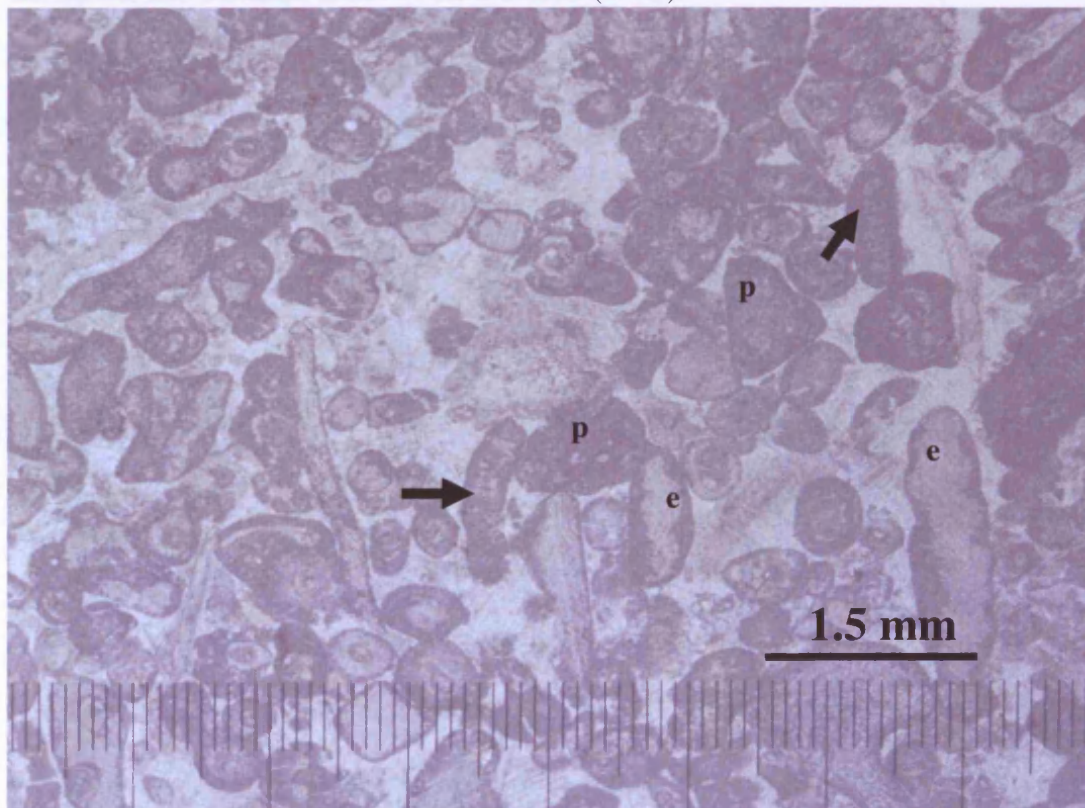


Figure 5.2: Photomicrograph of an unstained thin section. Micritisation effect as with peloids (p), and destructive micrite envelopes (e), around crinoids and *Koninckopora* (arrowed). Langland Bay, TS# 25.

reported this form of micritisation, especially around brachiopod or mollusc shells (Fig. 5.3, Fig. 3.22 B).

5.3 Fenestral Porosity

In this example, there is a small number of irregular type fenestrae (Fig. 3.11 B in section 3.3.2), as defined by Grover and Read (1978), with an average length of 1.5-2.5mm and height of 1mm, filled with non-ferroan calcite cement. These fenestrae are very minor, and occur within the oolitic grainstones of lithofacies (LB1), as seen at the lower part of the unit in the Port Eynon Bay section. Fenestrae (Tebbutt et al., 1965) and birdseyes (shrinkage pores: Fischer, 1964) are synonymous. This is an early diagenetic structure defined as being a pore larger than an intergranular pore space. It represents one of the minor porosity types that are formed in supratidal, intertidal and sometimes in subtidal environments (Hanley and Steidtmann, 1973). The pore, if not empty, is usually filled by calcite cement, evaporites or other sediment. This fabric is the main outcome of periodic wetting and drying. In this study, however, fenestrae in oolitic grainstone facies would suggest two possible environmental interpretations: intertidal exposure or subtidal hardgrounds. In order to decide which model is most appropriate, there are certain criteria that need to be considered. Shinn (1983) listed some petrographic reasons for the subtidal origin of Holocene fenestral voids formed in subtidal hardgrounds: acicular aragonite cement, isopachous acicular cements (eliminating meniscus cement) and marine bioclasts. Bain and Kindler (1993) indicate that the presence of fenestrae with meniscus cements is characteristic of intertidal and supratidal settings, such as the beachrock on San Salvador Island, Bahamas. Based on that, the HBO examples could possibly be interpreted as due to exposure, as meniscus cements are present (Fig. 5.4).

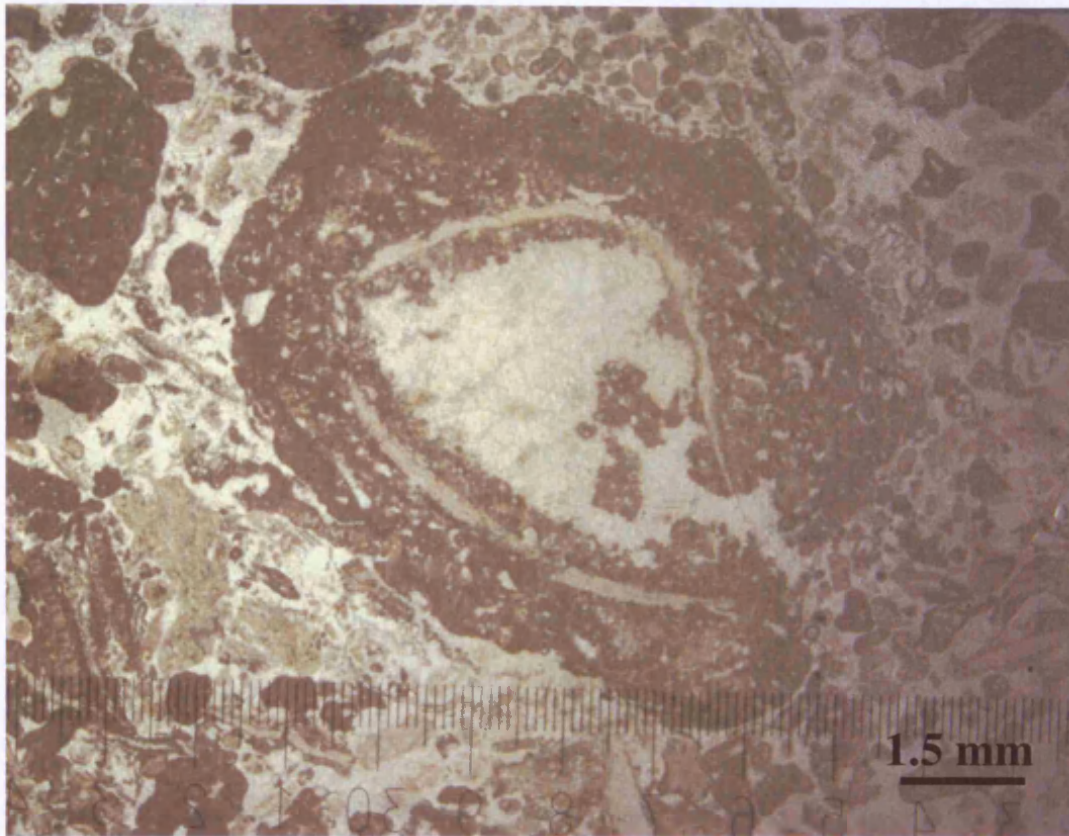


Figure 5.3: Photomicrograph of an unstained thin section. A constructive micrite envelope (at the centre) developed on the surface of a brachiopod fragment, possibly by sponges. Port Eynon Bay, TS# 17.

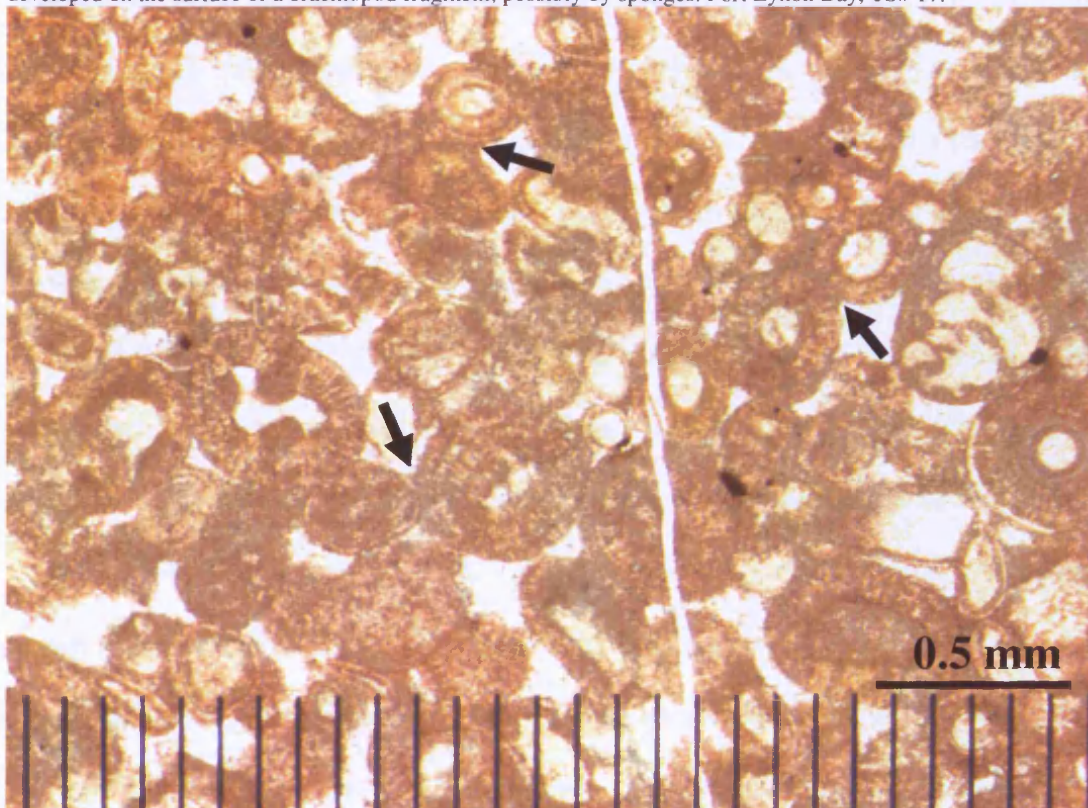


Figure 5.4: Photomicrograph of stained thin sections. This is the same thin section in Figure 3.11 B in section 3.3.2. Meniscus type cement holds the ooids together within lithofacies LB1. General distribution of the meniscus cement (arrowed). Port Eynon Bay, TS# 85.

However, Grover and Read (1978) mentioned some associated features with exposure-related fenestral, such as pendant calcite cement, vadose silt, and moulds that imply exposure, which are difficult to distinguish in this example. In other words, throughout the logged sections, they show no record of such features within the HBO other than meniscus cements.

5.4 Peloidal Cement

This feature is associated with intraclasts of probable hardgrounds (Fig. 5.5; 5.6) where the bioclasts, ooids and grapestones are bound together by intergranular peloidal cement. These intraclasts were found especially at the top of the unit that is dominated with LB1 and LB2 and predominant in LC2 (7m thick in Port Eynon) at different sizes, up to 2mm. These intraclasts resemble microbial hardgrounds holding together (lithified) minute peloids (hence peloidal cement) and no obvious fringe cement is seen. Such hardgrounds are commonly formed inorganically, and occasionally by microorganic processes. Dravis (1979) recorded cementation of ooids form an active shoal area within the first eleven meters of water depth connected by meniscus-like cement (peloidal cement). In a modern example from Joulter's Cay, there is a mucus-rich solution associated with a fur of aragonite crystals (Folk and Lynch, 2001). These crystals develop over the mucus around the stable active ooids, which they bind together by this process. Folk and Lynch (2001) suggested that the presence of meniscus fabric is a general indicator of vadose (meteoric diagenesis) settings. However, Hillgartner et al. (2001) differentiate between vadose meniscus cements and meniscus-type cements, the latter being formed by filament calcification in subtidal zones. Therefore, meniscus cement in general is not a specific indicator of meteoric or marine diagenesis. The formation of hardgrounds is controlled by three factors: surface topography, local hydrography and

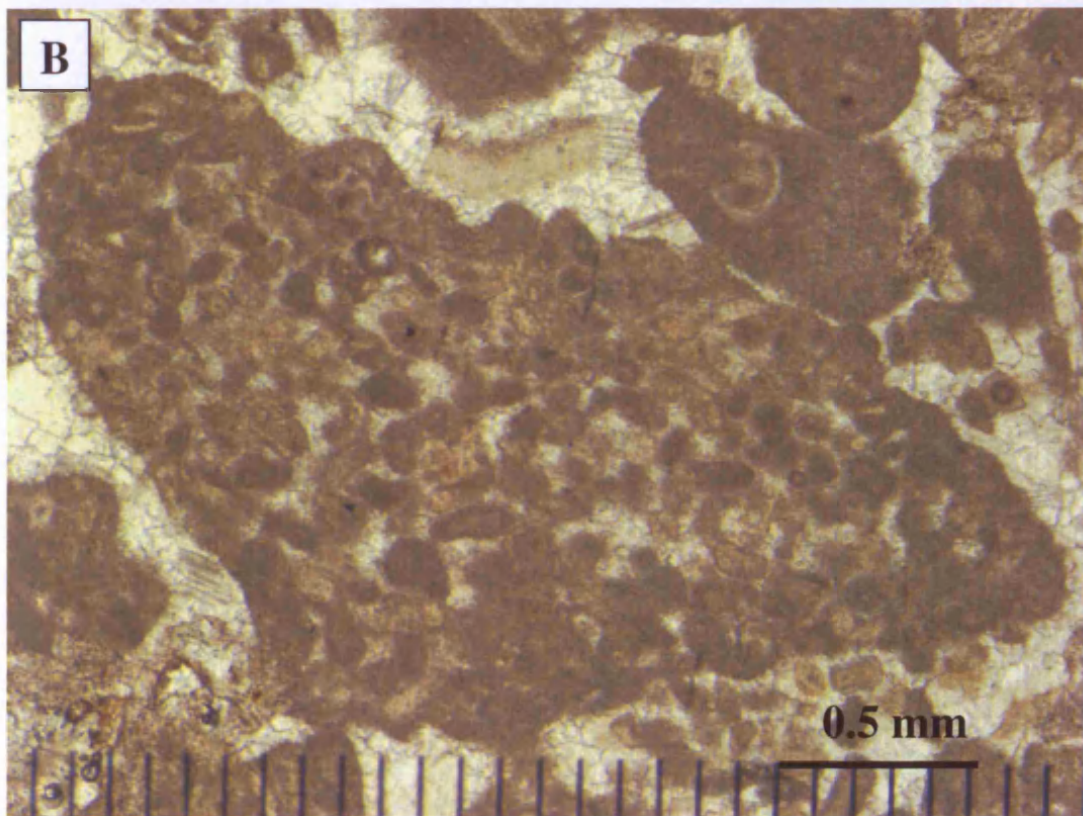
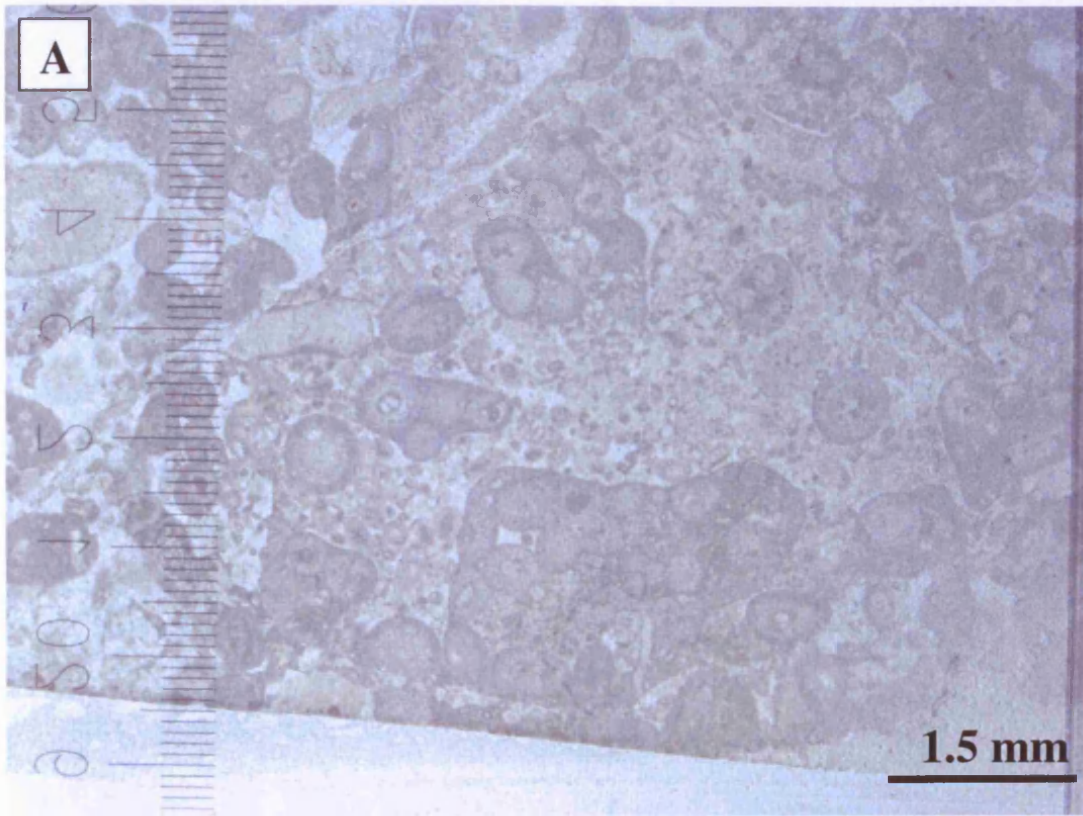


Figure 5.5: Photomicrograph of unstained thin sections. A) Ooids and grapestones joined together by peloidal cement. Port Eynon Bay, TS# 32. B) Very fine-grained peloids bound together by peloidal cement. Three Cliffs Bay, TS# 11.

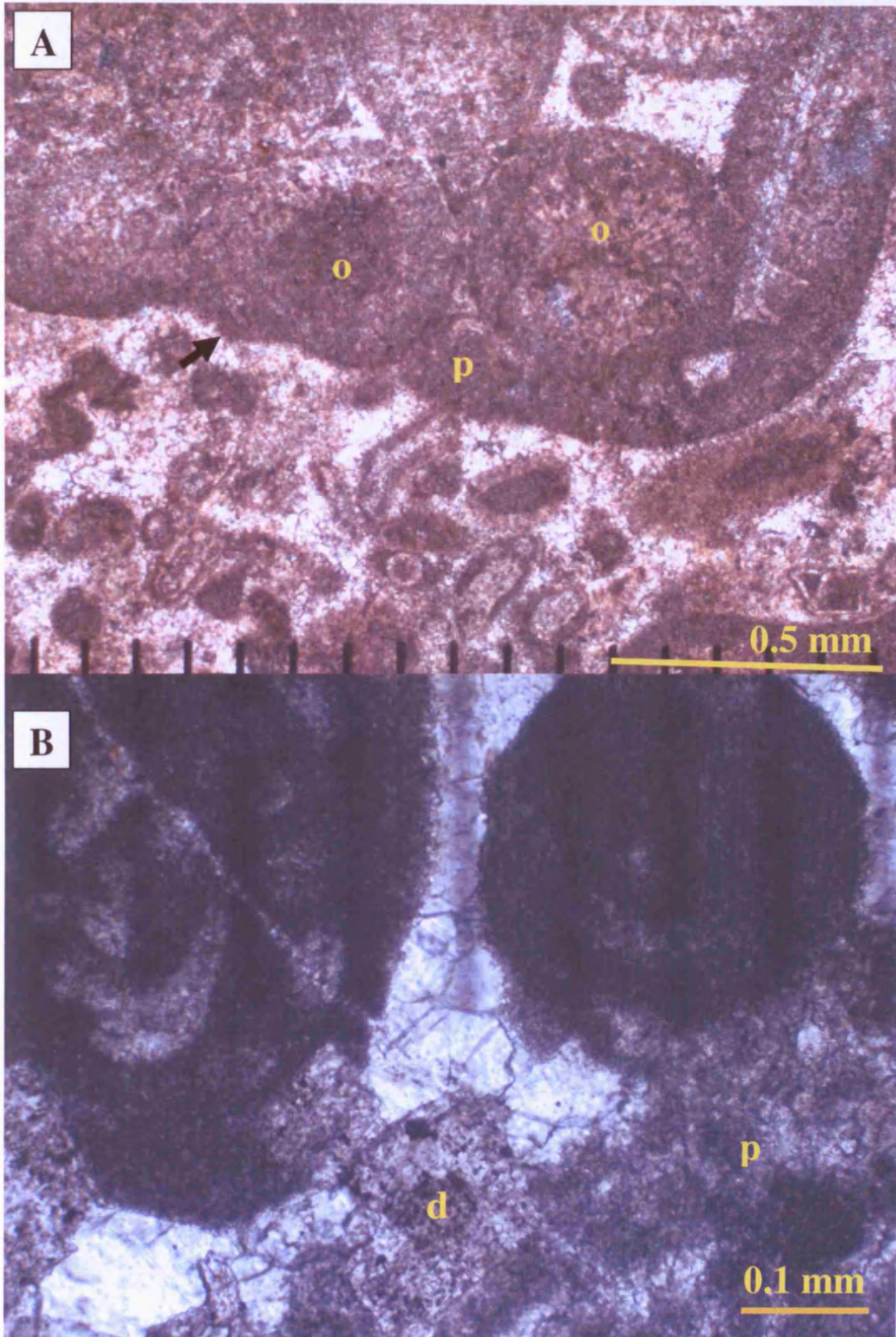


Figure 5.6: Photomicrographs of thin sections. A) High magnification stained section shows lithification of micritised ooids (o) in a hardground by peloidal cement (p). The erosional surface of the hardground is marked by a small arrow. Port Eynon Bay, TS# 32. B) High magnification of peloidal cement (p) and dolomite crystal (d) replacing the cement and penetrating into the grain and intraclasts. Langland Bay, TS# 28.

biological stabilisation (Dravis, 1979). Hardground localities are summarised by Dravis (1979) in the margins and crest areas of tidal bars, in the floor of channels between these bars, and in deep-water sandwaves close to the margins of the shelf.

5.5 Fibrous (Fringe) Cement

This diagenetic feature occurred locally in the pure oolitic lithofacies LB2 in the Langland Bay section (Fig. 5.7 A). The crystals of fibrous fringe non-ferroan calcite cement (size ranges between 100 to 200 μ m long) are parallel to each other and perpendicular to the ooid surface, in the form of radial texture around the grain, and usually capped by drusy cement (Fig. 5.7 B). This type of cement is common in modern marine settings especially hardgrounds (Tucker and Wright, 1990). The isopachous fibrous fringe cements are now calcite (non-ferroan) but originally may have been aragonite, or HMC. The absence of dissolution replacement effects suggests it was not aragonite. Therefore, further investigation for dolomite inclusion and magnesium content is needed to determine whether it is HMC or LMC.

5.6 Aragonite Dissolution

This feature rarely occurs in all three logged sections, however it had been found within lithofacies LD2 and LD3, where mollusc fragments show replacement of aragonite by non-ferroan, drusy calcite cements. This is often associated with constructive micrite envelopes, such as by sponges (Fig. 5.8).

Aragonite mineral is metastable, especially in meteoric environments that would form mouldic porosity after dissolution by water. This porosity may preserve or precipitate the marine calcite cement (LMC) as drusy mosaic fabric, instead, in the mould (Tucker and Wright, 1990).

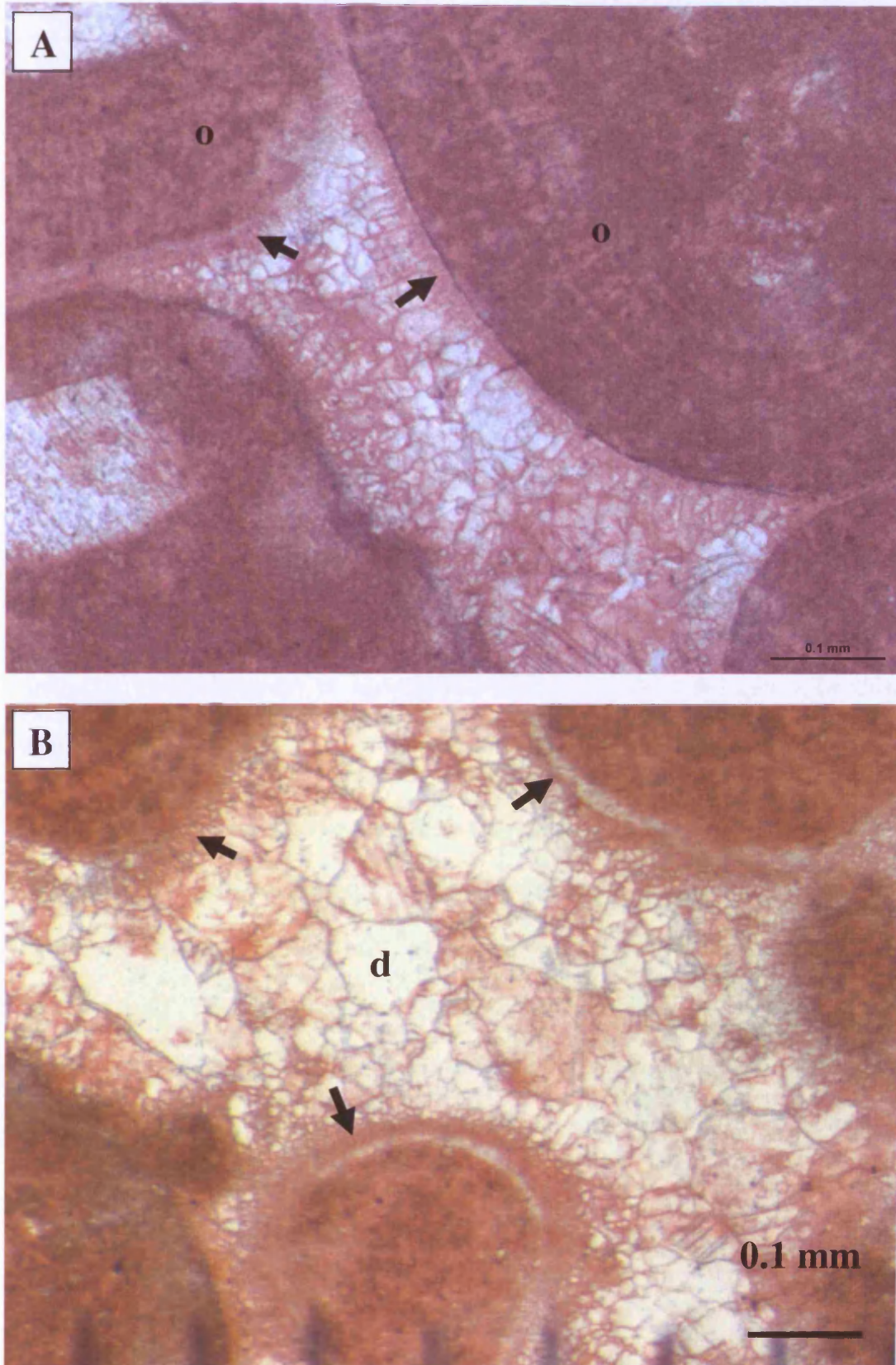


Figure 5.7: Photomicrograph of stained thin sections. A) Fibrous (fringe) non-ferroan calcite cement (arrowed) developed around the micritised ooids. B) Two type of non-ferroan calcite cement: fringe cement (arrowed), and drusy cement (d), where calcite crystals increase in size towards the centre of the pore space. Langland Bay, TS# 11.

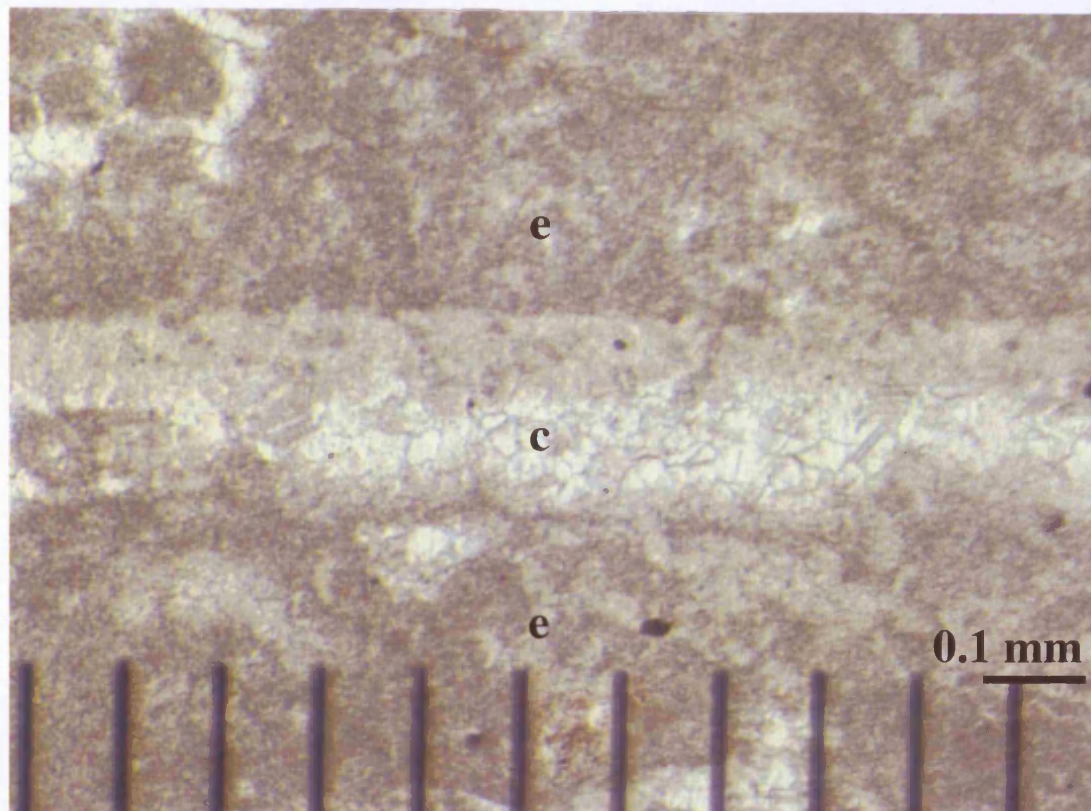


Figure 5.8: Photomicrograph of an unstained thin section. Bioclast fragment (mollusc) indicates the original aragonite mineral was dissolved and replaced by calcite crystals (c). Sponges encrustation created a constructive micrite envelope (e). Langland Bay, TS# 3.

5.7 Non-ferroan Calcite Cements (blocky and drusy)

Blocky non-ferroan calcite cement was found in all three sections within the oolitic grainstone lithofacies LC1 and LC2, as well as replacement within solitary coral in lithofacies LA2. The crystals average 0.05-0.1mm. Blocky or equant calcite spar shows a mosaic fabric with an irregular distribution pattern of relatively equal-size calcite crystals (Fig. 5.9). Based on Scholle and Ulmer-Scholle (2003), this type of cement is associated with a phreatic zone of meteoric water environments. Geochemical investigations would be needed to identify the origin of this cement type, whether formed from meteoric or deeper burial fluids, or even marine fluids.

Within the logged sections, drusy non-ferroan calcite cement has been found to be associated with three settings. First, it is widely distributed within the oolitic shoal complex (lithofacies LBs) (Fig. 5.10). Second, it is found locally in the

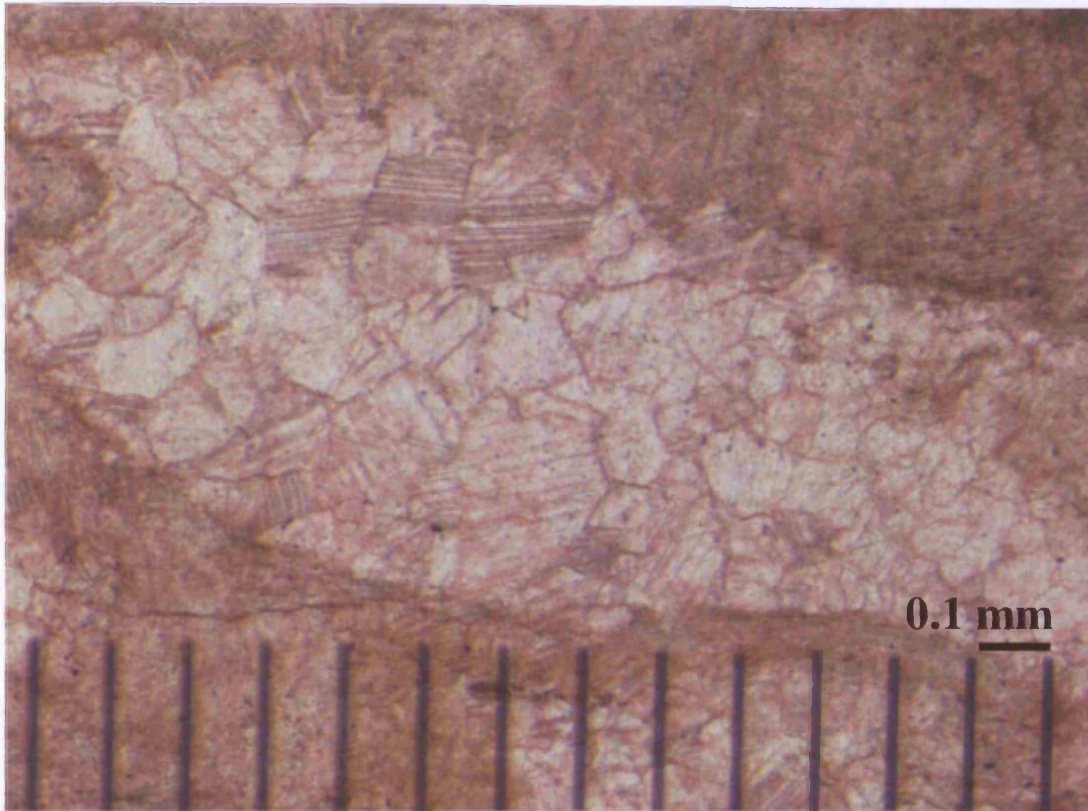


Figure 5.9: Photomicrograph of a stained thin section. A pore in a solitary coral was filled by blocky calcite cement. Three Cliffs Bay, TS# 23.

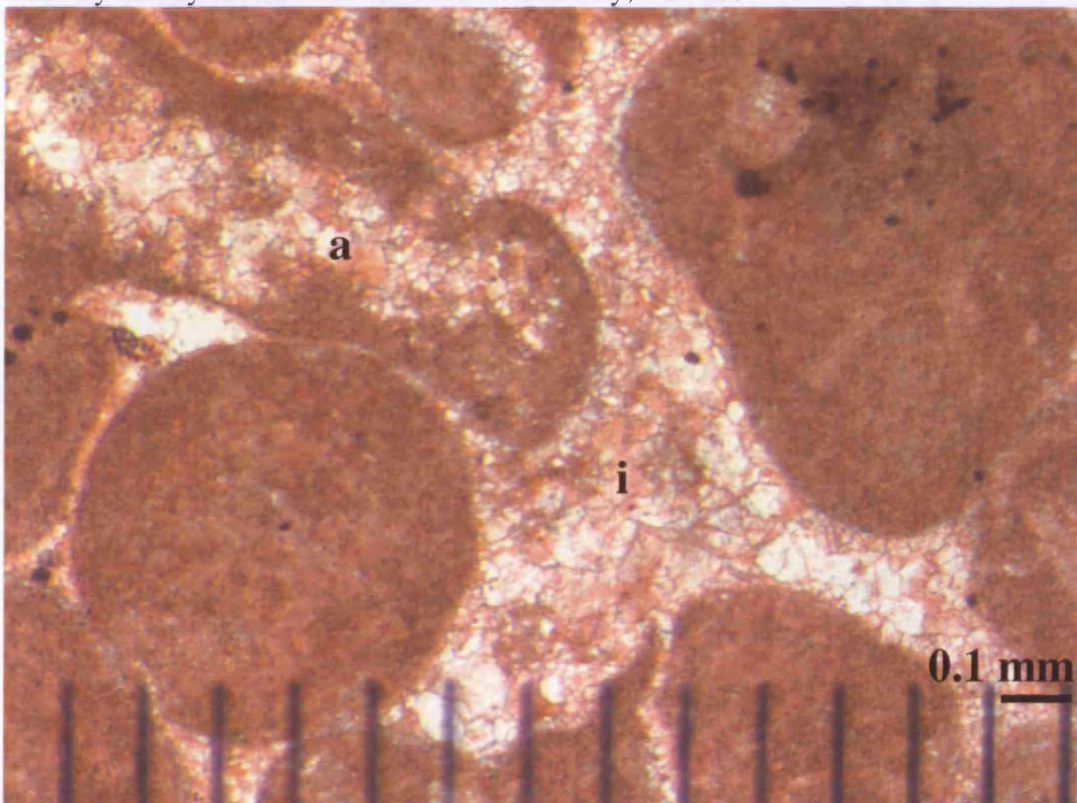


Figure 5.10. Photomicrograph of a stained thin section. Drusy calcite cement fills the intergranular pores between grains (i) and replaces the original aragonite after dissolution (a). Three Cliffs Bay, TS# 17.

Langland Bay section within the oolitic grainstones LC1 where it caps the fibrous (fringe) calcite cement (Fig. 5.7 B). Third, it is associated with a replacement for aragonite moulds within bioclasts fragments, especially molluscs (Fig. 5.10). Drusy calcite cement represents competitive growth where crystal size tends to increase toward the centre of the intergranular pore space (Tucker and Wright, 1990). Scholle and Ulmer-Scholle (2003) refer to it as burial indication, however it is very common in the pure ooids grainstones that represent a first generation cement of possibly meteoric origin.

5.8 Early Dolomitisation

Examples were found in all lithofacies of the three logged sections containing two forms of non-ferroan dolomite crystals. Dolomitisation is considered to be a minor diagenetic process in the HBO, as a replacement of the original limestone. On the diagenetic time scale, dolomitisation occurs at many different diagenetic stages (Adams and MacKenzie, 1998). The HBO is characterised by an early dolomite presence, and burial, post compaction dolomites. However, some dolomite crystals have been leached and replaced by calcite cementation. The early zoned dolomite pre-compaction is characterised by idiotopic mosaics of euhedral rhombs (Fig. 5.11), and late stage post-compaction dolomite with xenotopic mosaics of anhedral crystals (the latter is discussed in section 5.11). Most of the early zoned dolomite crystals are inclusion rich, and sometimes appear etched by the calcite cement. These rhombs were found almost in all lithofacies with very minor amount (up to 20%) with average size of about 0.2mm.

Figure 5.11 is a comparison between idiotopic crystals from HBO and from the Chadian Gully Oolite from near Cardiff described by Hird and Tucker (1988). Both examples are similar and Hird and Tucker differentiated the pre-compaction

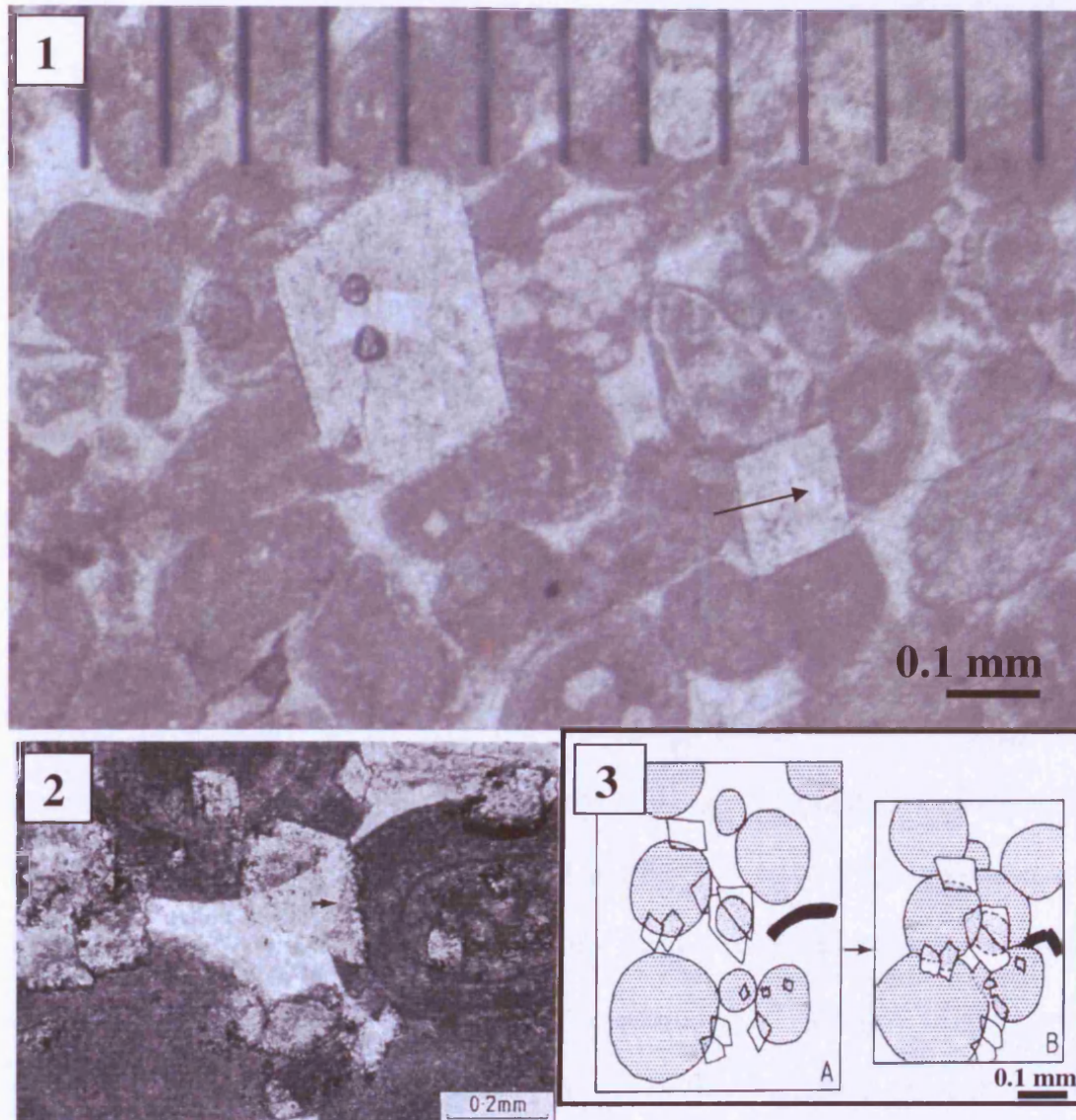


Figure 5.11: Photomicrographs of stained thin sections. 1) Idiomatic mosaic of euhedral dolomite rhombs. HBO, Three Cliffs Bay, TS# 20. 2) Dolomite rhombs in Gully Oolite. From Hird and Tucker (1988). Photos 1 and 2 explain the same feature of postdate compaction dolomite rhombs in oolitic facies. The rhomb on the right side of photo 1 and the centre rhomb in photo 2 show displaced outer margins of the grains (arrowed). 3) Diagram of pre-compaction (A) dolomite (early diagenesis) displays the effect of compaction on these rhombs and (B) post-compaction effects. (Dolomite crystals stippled and clear, ooids stippled, bioclast black) from Hird and Tucker (1988).

dolomite rhombs. This diagenetic effect is characterised by several stages. The first stage is determined where the dolomite rhombs overgrow the margins of two or more ooids and the intermediate pore space. The ooid margins are still preserved and observed through the dolomite rhombs. The second stage happens where the ooid grains are compacted together, and dissolution effects take place in the outside parts of the ooids margins, the preserved margins being displaced with further late compaction. Hird and Tucker (1988) interpreted the development of these dolomite rhombs in early diagenetic meteoric-marine, less active, water-mixing zones.

5.9 Syntaxial Cement

Syntaxial overgrowths, or syntaxial rim non-ferroan calcite cements (Adams and MacKenzie, 1998), are common in in all three sections studied especially in lithofacies LA1 and LA2, but are poorly developed (Fig. 5.12). They are associated with grainstones, which contain echinoderm fragments (in this example crinoid debris). However, it is not good indicator for determination of the three diagenetic stages (Scholle and Ulmer-Scholle, 2003). However, they can imply a long period of precipitation potentially through successive diagenetic settings (Adams and MacKenzie, 1998), and can develop near the surface under marine, meteoric or mixing-zone conditions (Tucker and Wright, 1990), and during deeper burial. In order to identify the right diagenetic setting for such a cement type, further investigation would be needed such as cathodoluminescence and geochemical analyses.

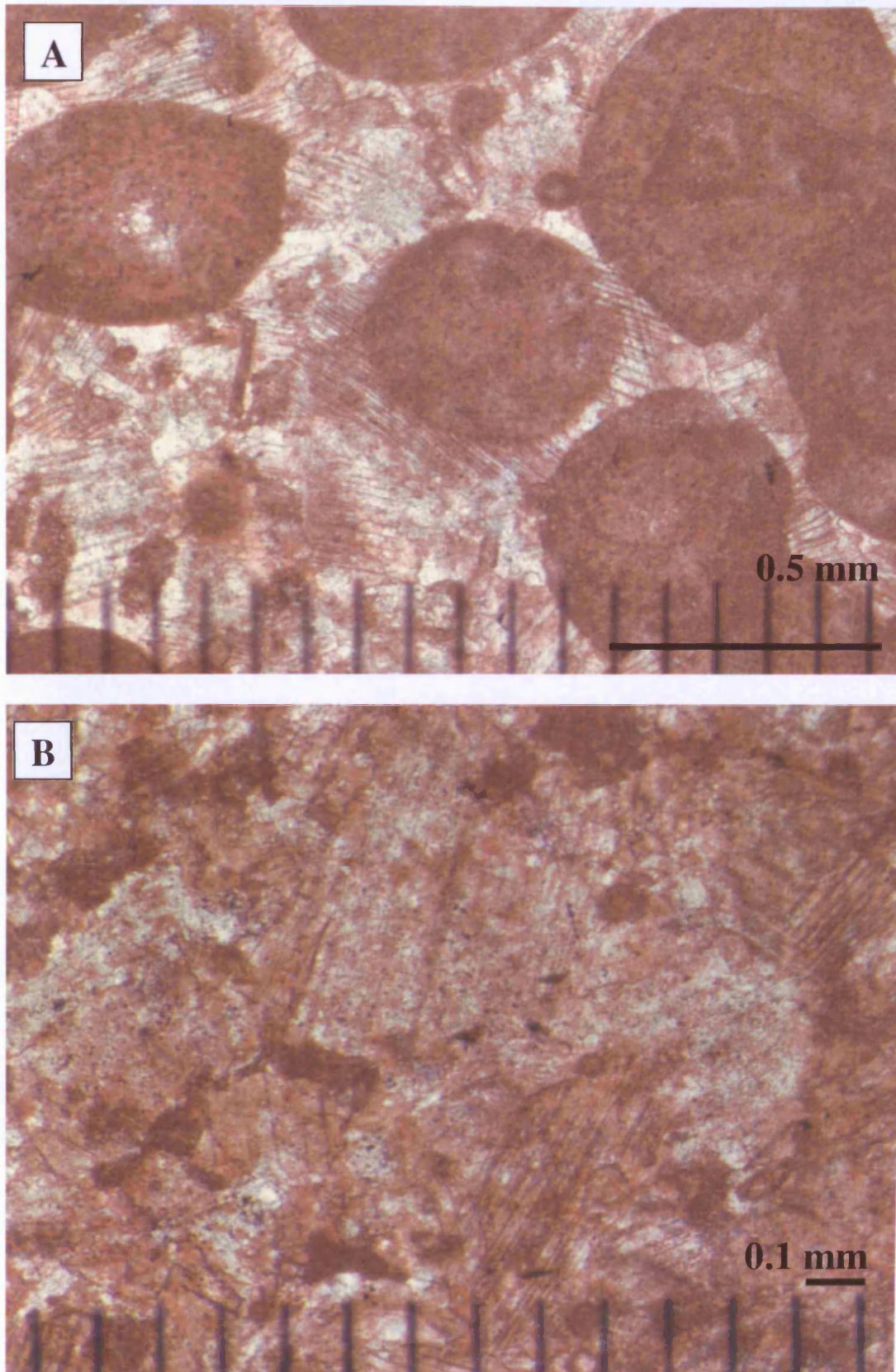


Figure 5.12: Photomicrograph of stained thin sections. A) Poorly developed echinoderm syntaxial overgrowth cement with cleavage planes in the oolitic lithofacies. Three Cliffs Bay, TS# 3. B) High magnification photo of the same cement type (A). Three Cliffs Bay, TS# 38.

5.10 Neomorphism/Recrystallisation

This is a process where fine texture can recrystallise into a coarser one, such as packstone recrystallised into grainstone texture. This is the result when the crystal size is enlarged (aggrading type neomorphism) without any change in the original mineralogy. This diagenetic feature is widely distributed in all three sections, especially where the dasycladacean palaeoberesellid fragments existed and resulted in recrystallised grains (Fig 5.13). Neomorphism is common within the oolitic shoal/barrier complex in lithofacies LB1, LB2, LC1, LC2, LC3 and also present in all the other lithofacies. This process allows the grains to be preserved as a brownish-yellow cement with irregular crystal shapes with average size 100-200 μ m (Figure 5.14) (Tucker and Wright, 1990). Neomorphism process takes place, for both aragonite and calcite, through dissolution and reprecipitation in the presence of water as a wet process.

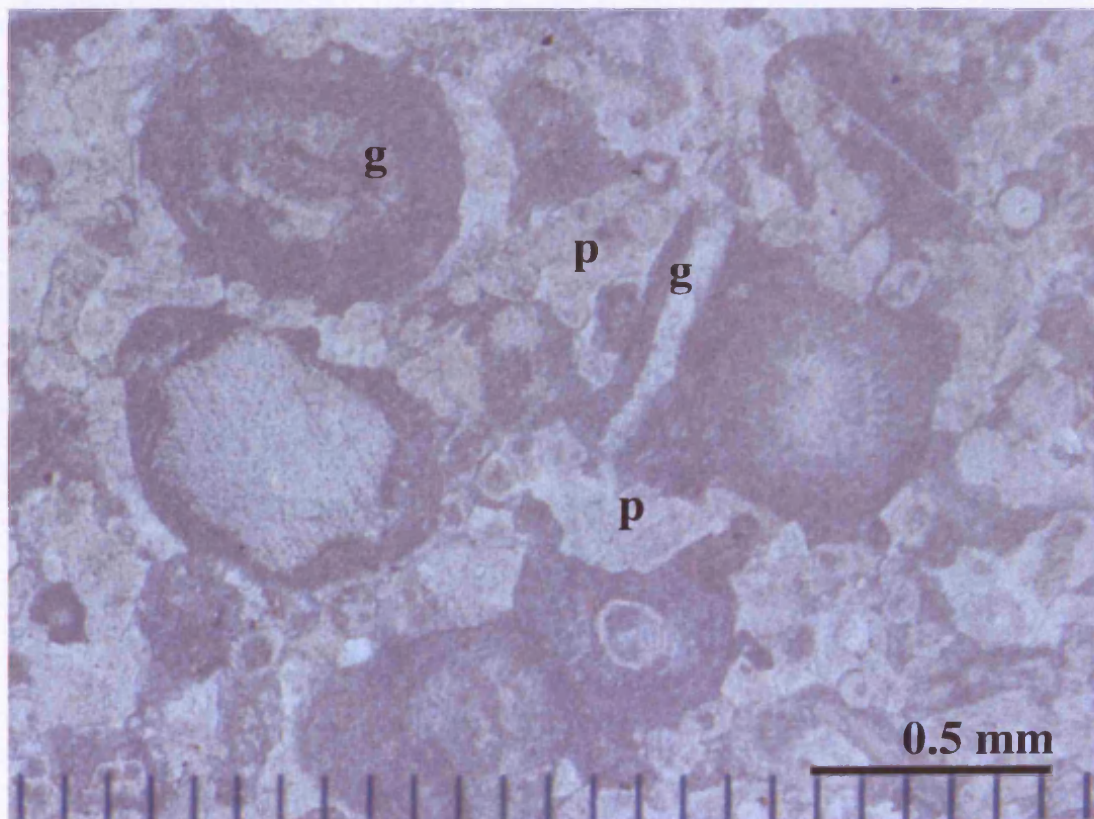


Figure 5.13: Photomicrograph of an unstained thin section. Recrystallised grains (g), possibly due to palaeoberesellid algae (p). Port Eynon Bay, TS# 56.

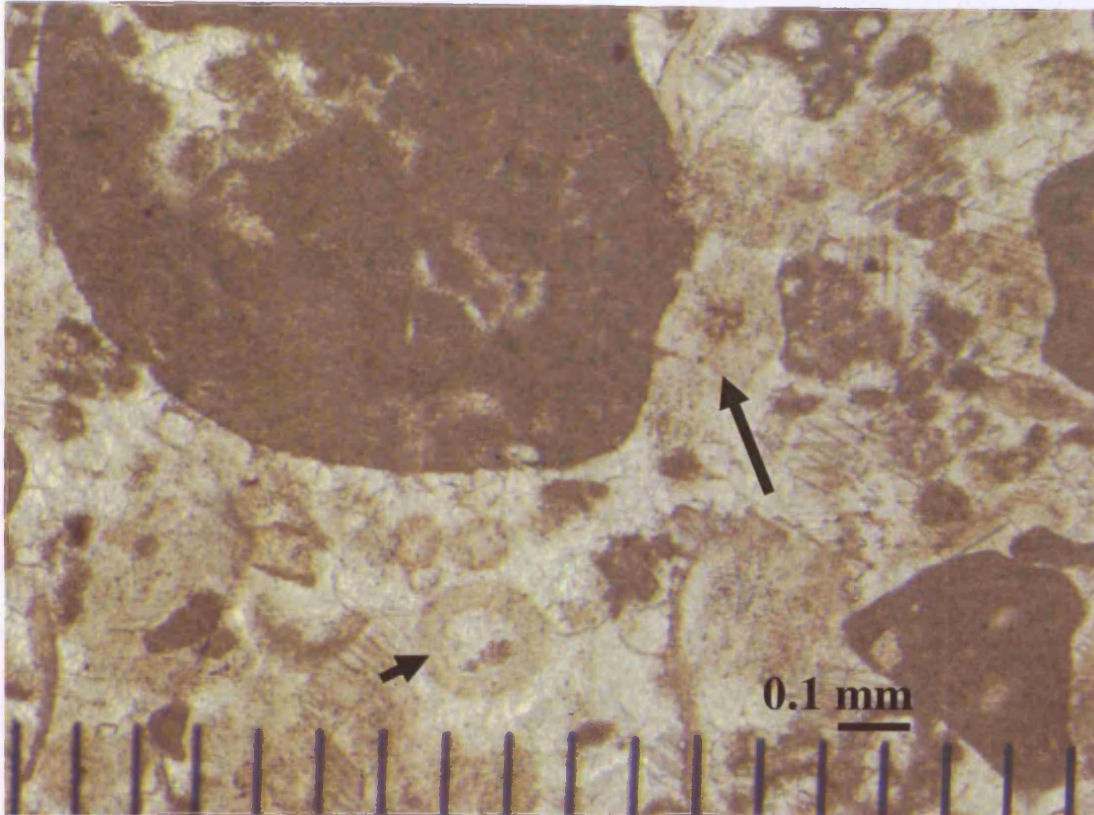


Figure 5.14: Photomicrograph of an unstained thin section. Neomorphic calcite shows recrystallised bioclasts such as transverse section of palaeoberesellid tube (arrow) and crinoid fragments (long arrow). Three Cliffs Bay, TS# 11.

5.11 Compaction / pressure solution

Compaction occurs in all lithofacies, but is common in LC1, LC2, LB1, LB2 and LB3; however, broken grains, fracture surfaces of the grains, detached fringe cement and collapsed micrite envelopes are not seen. Diagenetic compaction is categorised into two processes: mechanical and chemical. Their occurrence is controlled by an increase in the overburden stress on the sediments, and the outcome structures are controlled by the amount of carbonate mud and clay (Tucker and Wright, 1990). Mechanical compaction occurs just after the limestone is buried by other sediments and results in dewatering, rearrangement and closer packing of the grains, porosity loss and thickness reduction. This process takes place in stages, and it is not known at what depth it might start. One of the obstacles to this process occurring is early cementation (Tucker and Wright, 1990).

Chemical compaction and pressure solutions (common in all LCs lithofacies) occur by the same processes, that start at depths of several hundred meters. Budd (2001) has evaluated the diagenetic effects in the first 500m of burial depth on the carbonate of Florida. He concluded that the effect is greater on porosity and permeability of the carbonate grainstones. Cementation is less effective than the compaction (mechanical and chemical), however, pressure solution is the important factor in reducing permeability where it starts at 350m of shallow burial. They both cause grain dissolution, which can be an important source of CaCO_3 for burial cementation. Pressure dissolution occurs at grain contact sites and along sediment interfaces. Different structures are associated with this type of dissolution (Logan and Semeniuk, 1976; Wanless, 1979; Buxton and Sibley, 1981; Bathurst, 1987; Tucker and Wright, 1990), dissolution seams (Fig. 5.15), and stylolites (Fig. 5.16) are clearly seen in HBO.

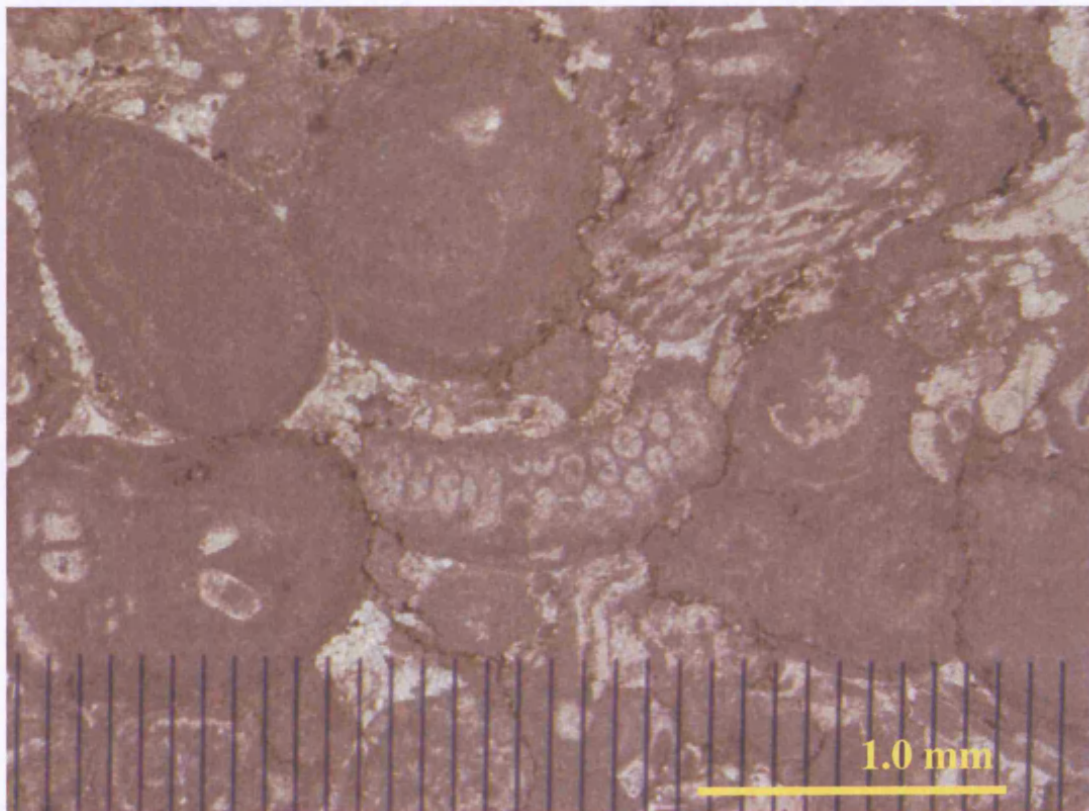


Figure 5.15: Photomicrograph of an unstained thin section. Dissolution seams are in black where the grains are in contact (skeletal and non-skeletal). Three Cliffs Bay, TS# 16.

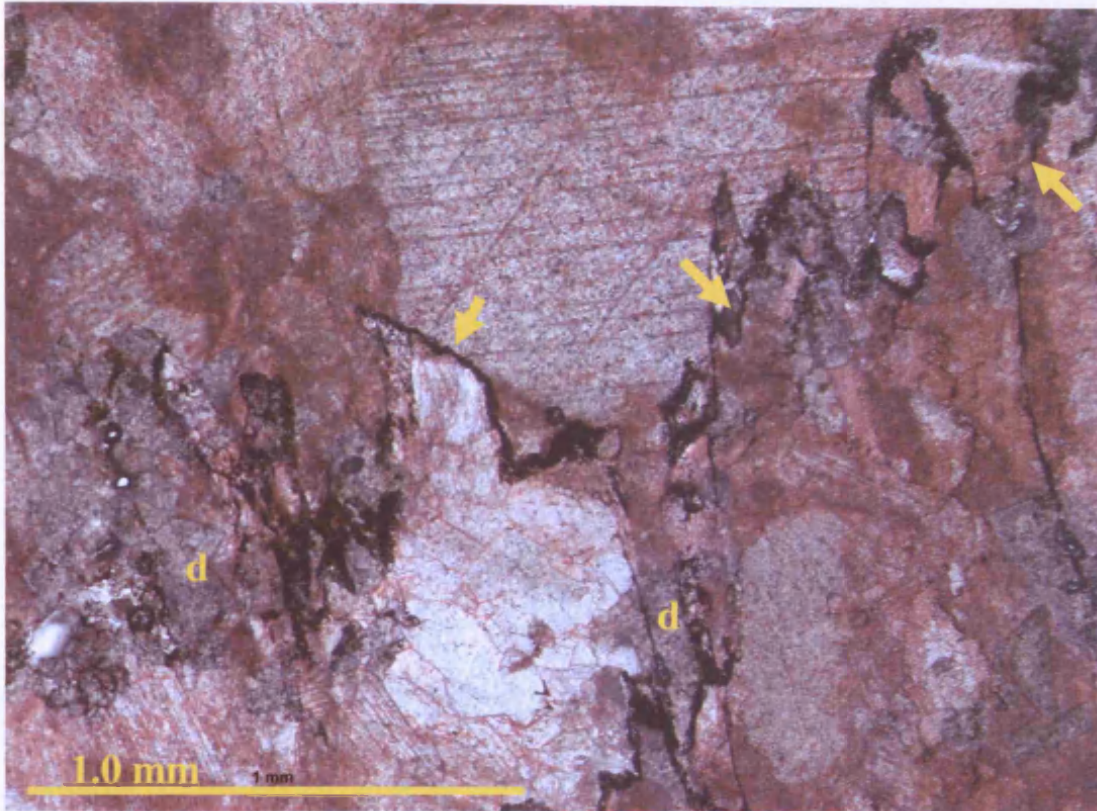


Figure 5.16: Photomicrograph of a stained thin section. Stylolite structure follows the dolomite (d) and is marked by black material (arrowed). Port Eynon Bay, TS# 42.

5.12 Late Stage Dolomitisation

This feature is found in all three sections as brown-weathering dykes that vary in width ranges between 1.5-3 metres. Dolomite crystals are characterized by very fine to fine (average crystal size 100-200 μ m) crystalline texture (xenotopic) with nonplanar (irregular) crystal boundaries (Fig. 5.17) (Sibley and Gregg, 1987). It also occurs rarely along stylolites (Fig. 5.16). Xenotopic dolomites form at temperature greater than 50 C (Gregg and Sibly, 1984). This type of dolomite is typical of burial (high temperature) diagenesis (Choquette and James, 1990). The dolomite has replaced partly and most likely all the original sediments. The mosaics crystals have not had apparent stain, indicating the replacement.

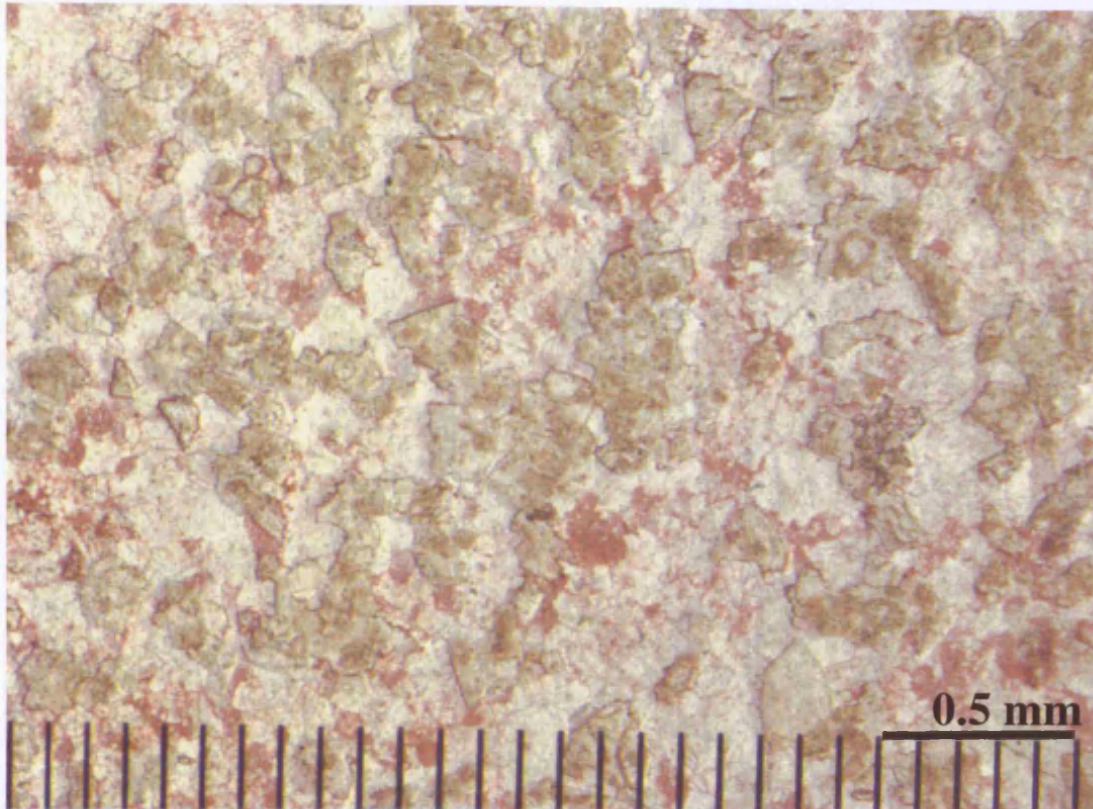


Figure 5.17: Photomicrograph of a stained thin section. A) Xenotopic mosaic of anhedral post-compaction dolomite which is inclusion rich. Three Cliffs Bay, TS# 42.

5.13 Dedolomitisation

It is rarely found in HBO, however, an example occurs within LD3 (Fig. 5.18). It has been recognised petrographically as the replacement of dolomite mineral by post-compaction ferroan calcite cement. This process occurs where the dolomite crystals dissolve and are replaced by calcite, and is commonly interpreted as having occurred in a meteoric water environment where dolomitised sediments are uplifted to the surface (Adams and MacKenzie, 1998).

5.14 Fractures with Non-ferroan and Ferroan Calcite

These fractures vary in their sizes, which can reach up to 1mm. wide. These fractures have been found almost in all HBO lithofacies. HBO is dominant with the two fracture systems, where the one with non-ferroan calcite is the older (Fig. 5.19). However, both represent post-compaction processes. Its importance is to know the post-sedimentary sequence of events in carbonate rocks (Flügel, 2004).

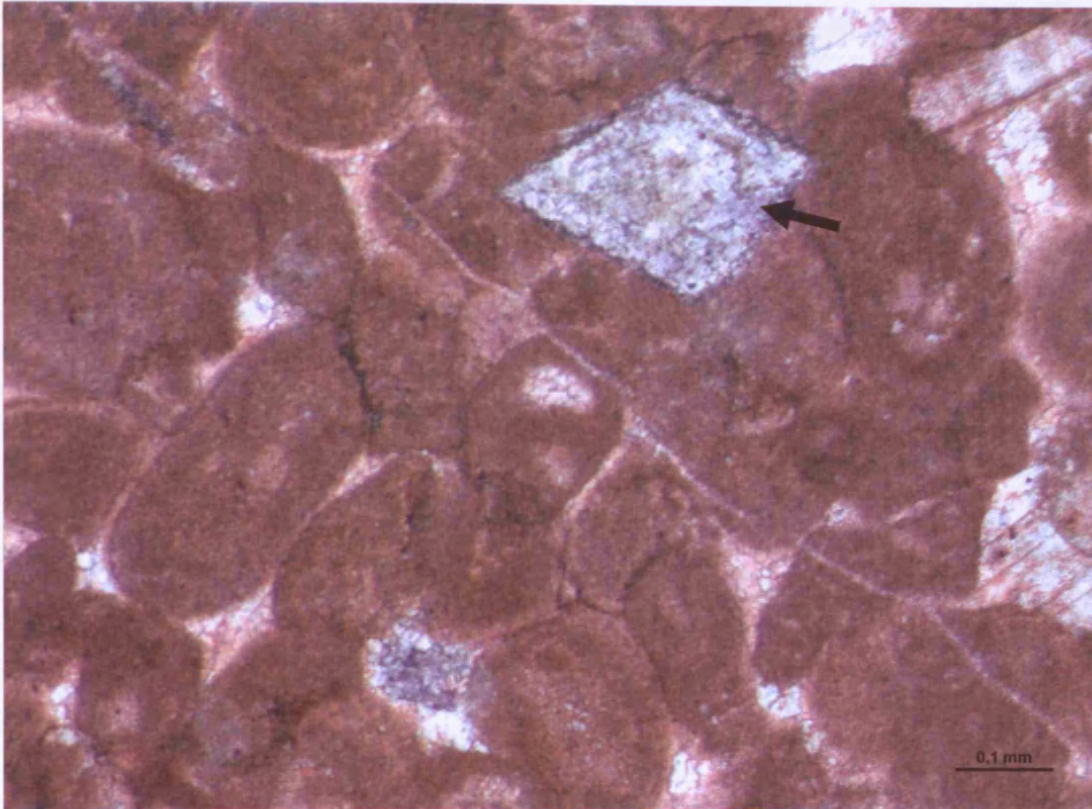


Figure 5.18: Photomicrograph of a stained thin section. Dolomite rhomb replaced by ferroan calcite cement (arrowed), within peloidal grainstone. Langland Bay, TS# 8.

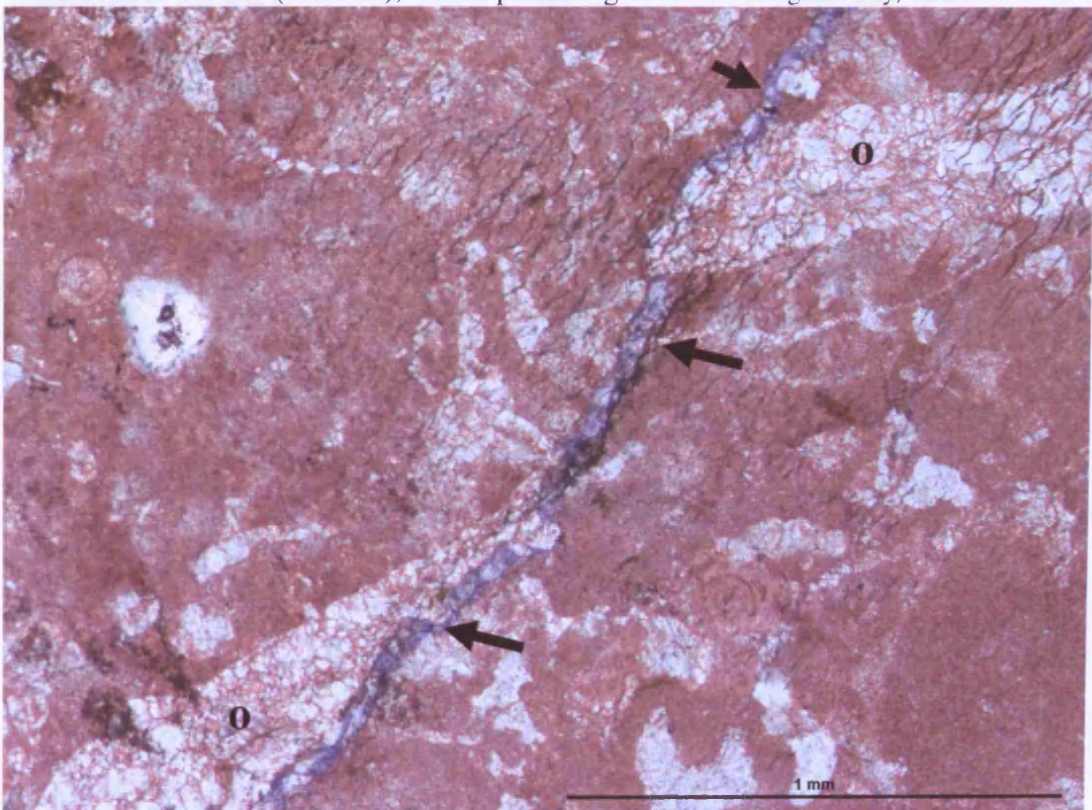


Figure 5.19: Photomicrograph of a stained thin section. Post-compaction fracture filled with non-ferroan calcite (o) cement cross-cut by younger fracture filled with ferroan calcite cement (arrowed). Langland Bay, TS# 21.

5.15 Comparison of the Logged HBO Sections with Gully Oolite of Gower

This section summarises the diagenetic features that are associated with the Chadian Gully Oolite of Gower based on Searl (1989), and the features present in HBO based on the logged sections. The Gully Oolite was widely influenced by phases of emergence, whereas the HBO does not show well-developed emergence features. The most common features of these two oolites during early diagenesis are microbially-bound sediments, localised isopachous fibrous fringing calcite cements, hardgrounds and intraclasts, and the presence of meniscus cement. However, the meniscus cement, in Gully Oolite, is associated with vadose type cement, whereas in HBO it is associated with a small number of fenestrae. Other features associated with ooids, such as the low degree of micritisation, are also present in HBO, especially at the top of the unit. This has been interpreted as an increase in the rate of sedimentation and/or high sand mobility. The preservation of radial fabric implies that the calcite is the original mineral.

In terms of compaction, both oolites have some similar features, such as pressure dissolution at interpenetrant grain boundaries which start at 600-900m burial (Dunnington, 1967). However, emergence played an important role in the compaction processes in Gully Oolite. Minor stylolites and microstylolites are also distinguished in HBO.

Two-generation calcite filled fractures are distinguishable in HBO by non-ferroan and ferroan calcite, which are also found in Gully Oolite. Fractures with non-ferroan calcite may relate to the Hercynian Orogeny and post-orogenic uplift, whereas ferroan calcite-filled fractures precipitated during the Mesozoic/Tertiary burial and uplift.

Less pervasive early dolomite rhombs identified within HBO are also present in Gully Oolite, and believed to be of mixing-zone origin. However, in Gully Oolite, there is a relationship between dolomitisation and emergence surfaces. Late stage post-compaction dolomite is also present in both oolites where they are inclusion rich. In Gully Oolite, late stage dolomite formed at the fault-line as brown-weathering dykes that vary in width. Similar features also exist in HBO where their average width ranges between 0.5-2 meters.

The above features are the major ones common to both oolitic units. However, the major differences between the two are the palaeoberesellid algal neomorphism in HBO and the ranges of emergence phases within Gully Oolite, which had not been seen in HBO, and the features associated with emergence such as vadose cementation and compaction, oomouldic fabrics, development of palaeosol and palaeokarsts in Gully Oolite. However, there is a prominent exposure surface capping the Holkerian over much of S. Wales, and the overlying Asbian exhibits numerous exposure surfaces (Cossey et al., 2004).

5.16 Conclusion

The general history of the major diagenetic processes of the HBO has been extracted from the studies of optical petrography. They are divided into three main stages which are eogenetic, mesogenetic and telogenetic. Eogenetic is the early diagenetic stage where its processes occur near surface on the sediments at the zone of influence. The early stage includes grain micritisation (peloids) and micrite envelopes, fenestral porosity, peloidal cements, fibrous (fringe) cement, aragonite dissolution, non-ferroan calcite cements (blocky and drusy) and early dolomitisation. Some of these processes affected all the logged sections depending on their palaeoenvironmental positions during the depositional time. Mesogenetic stage (or compaction stage) occur during

the time of burial which started at depth 350m (Budd, 2001), and includes syntaxial cement, neomorphism/recrystallisation and compaction/pressure solution. Post-compaction stage (telogenetic) occur during the tectonic uplift, and it includes the following processes; late-stage dolomitisation, dedolomitisation and fractures filled with non-ferroan and ferroan calcite. These processes are divided according to the classification of Choquette and Pray (1970).

Most of the diagenetic features of the HBO differ from the Gully Oolite, because the latter represents ranges of emergence phases and the features associated with emergence such as vadose cementation and compaction, oomouldic fabrics, development of palaeosol and palaeokarsts. Some diagenetic features in Gully Oolite are also present in HBO such as the early dolomitisation. It has been expected that the burial diagenesis of the HBO and the Gully Oolite to be similar but not the early diagenesis where the big difference is the subaerial exposures in the Gully Oolite and neomorphism in the HBO.

CHAPTER 6. CONCLUSION

6.1 Conclusion

The results of the present study address the aims and objectives stated in the first chapter, and can be summarised as follows:

- The Holkerian (Lower Carboniferous, Mississippian) Hunts Bay Oolite (HBO) was studied at three locations south of Gower, along a section 15km long, and up to 300m thick. These locations are: Langland Bay, Three Cliff Bay and Port Eynon Bay.
- The HBO has been divided petrographically into four main associations (A, B, C and D), and each association consists of up to three lithofacies. Association A consists of LA1 and LA2, the deepest deposits of the HBO, and dominated by crinoidal plates and bimodal grains of ooid, grapestone, aggregate grains and crinoidal plates, and represents open-marine offshore deposits. Association B comprises LB1 and LB2 that represent the main oolite factory in an active shoal setting, they vary both in their bioclast percentage content. Association C, which was deposited in back-shoal settings, is divided into LC1, LC2 and LC3, all are representative of aggregate accumulations where LC1 consists mainly of grapestone grains, LC2 is dominant with lumps and intraclasts of micritised aggregates and/or possible hardgrounds, and LC3 is dominant with incipient aggregates and grapestones. Associations B and C are the main sandbody constituents. Association D is the lagoonal part of the HBO and divided into LD1, LD2 and LD3, which include very fine to fine grained bioclasts and peloids, and are associated with sponges and ooids.

- The nature of the transition between the High Tor Limestone and the HBO is gradational, without any sharp boundaries; however, the top boundary, between the HBO and the Asbian Oxwich Head Limestone, is marked by a palaeokarst surface which was not found in this study.
- These associations accumulated in three shoaling-upward sequences: firstly offshore, via active shoal to back shoal settings; secondly, from offshore to the active shoal to back shoal settings; and the last sequence started with offshore, via an active shoal, punctuated with back-shoal deposits, to the lagoonal settings. All these sequences show a thickening trend from ESE-WNW, but represent shifting sandbodies. The main factor controlling these shallow-water sequences was believed to be sea-level oscillations.
- Ramsay's (1987) palaeocurrent readings have been used in this study to determine the palaeo-shoreline; however, these readings do not seem to be clear to describe the HBO palaeocurrent. Ramsay's (1987) and Scott's (1988) overall models of the HBO sandbody are also not applicable for the marine sand-belt model published by Ball (1967) and Handford (1988). The reasons are: first they lack differentiation between the main two parts of the marine sand belt, ramp and shield, and large bipolar cross-stratifications, which are several meters thick, were not found.
- In general, integrating all the features exhibited in the HBO, the deposystem does not seem to be analogous to any of the modern or ancient examples discussed in Chapter 2. The underlying reason could be the absence of major oolite shoals nearby as a source, instead a range of smaller sandbodies provided multiple sources.

- No glacio-eustatic cycles are identified. The present study shows three non-glacio-eustatic tectonically-controlled allocycles such that the HBO sea-level curve does not conform to the eustatic signal of the Holkerian.
- A paragenetic sequence has been derived and fifteen diagenetic events identified in the HBO. They are classified as syndepositional (Eogenetic), burial (Mesogenetic), or uplift (Telogenetic) diagenetic settings. The eogenetic stage includes grain micritisation (peloids) and micrite envelopes, fenestral porosity, peloidal cements, fibrous (fringe) cement, aragonite dissolution, non-ferroan calcite cements (blocky and dursy), and early dolomitisation. A Mesogenetic stage occurred during the time of burial, and includes syntaxial cement, neomorphism/recrystallisation, and compaction/pressure solution. A Telogenetic stage occurred during the tectonic uplift, and includes late-stage dolomitisation, dedolomitisation, and fractures filled with non-ferroan and ferroan calcite.
- Most of the diagenetic features of the HBO differ from the features of the Chadian Gully Oolite, especially in the early diagenesis phase, whereas some others are similar, especially the burial effects. This is because the Gully Oolite contains ranges of emergence phases, and the features associated with it, such as vadose cementation and cementation, oomouldic fabrics, development of palaeosols and palaeokarsts.

6.2 Further Research

- In the time available it was not possible to check all the HBO outcrops in the Gower or nearby. Any further studies might focus on extending the study, regionally, to better assess facies distribution.

- Cathodoluminescence and geochemical analysis (including C&O stable isotopes) should be carried out, especially on the early cements in the HBO to determine if any were formed from meteoric groundwater despite the lack of exposure features. The common occurrence of neomorphic textures associated with palaeoberesellids is an unusual feature and warrants further study.

REFERENCES

- Adams A. E. & Al-Zahrani M., 2000. Palaeoberesellids (Dasycladaceans) from the Upper Jurassic Arab-D Reservoir, Saudi Arabia. *Palaeontology*, **43**, p. 591-597.
- Adams, A. E. & Mackenzie, W. S., 1998. *A colour atlas of carbonate sediments and rocks under the microscope*. Manson, p.132.
- Adams, A. E., Horbury, A. & Ramsay, A., 1992. Significance of palaeoberesellids (Chlorophyta) in Dinantian sedimentation, UK. *Lethaia*, **25**, p. 375-382.
- Ahr, W., 1973. The carbonate ramp: an alternative to the shelf model. *Trans. Gulf Coast Assoc. Geol. Soc.*, **23**, p. 221-225.
- Aigner, T., 1985. Storm Depositional Systems: Dynamic Stratigraphy in Modern and Ancient Shallow-Marine Sequences, Springer-Verlag, Berlin.
- Aigner T. & Reineck H., 1982. Proximality trends in modern storm sands from the Helgoland Bight (North Sea) and their implications for basin analysis. *Senckenbergiana maritima*, **14**, p. 183-215.
- Bain R. & Kindler P., 1994. Irregular fenestrae in Bahamian eolianites: a rainstorm-induced origin. *Journal of Sedimentary Research-Section A-Sedimentary Petrology and Processes*, **64**, p. 140-146.
- Ball M., 1967. Carbonate sand bodies of Florida and the Bahamas. *Journal of Sedimentary Petrology*, **37**, p. 556-591.
- Barclay, W., 1989. Geology of the South Wales Coalfield, Part II, the Country around Abergavenny. *Memoir of the British Geological Survey. Sheet*, **232**.

Barclay, W., Taylor, K. & Thomas, L., 1988. Geology of the South Wales Coalfield, Part V. *The country around Merthyr Tydfil (3rd edn)*. HM Stationery Office: London. British Geological Survey (Memoir for England and Wales Sheet 231).

Bathurst, R.G.C., 1964. The replacement of aragonite by calcite in the molluscan shell wall. In: *Approaches to Palaeoecology* (Ed. By J. Imbrie and N.D. Newell), pp. 357-376. Wiley, New York.

Bathurst, R. G. C., 1966. Boring algae, micrite envelopes and lithification of molluscan biosparites. *Geological Journal*, **5**, p. 89-109.

Bathurst, R.G.C., 1987. Diagenetically enhanced bedding in argillaceous platform limestones: stratified cementation and selective compaction. *Sedimentology*, **34**, p. 749-78.

Batt L., Montañez I., Isaacson P., Pope M., Butts S. & Abplanalp J., 2007. Multi-carbonate component reconstruction of mid-carboniferous (Chesterian) seawater 13C. *Palaeogeography, Palaeoclimatology, Palaeoecology*, **256**, p. 298-318.

Bishop J., Montañez I., Gulbranson E. & Brenckle P., 2009. The onset of mid-Carboniferous glacio-eustasy: Sedimentologic and diagenetic constraints, Arrow Canyon, Nevada. *Palaeogeography, Palaeoclimatology, Palaeoecology*.

Brooks, M., Trayner, P., and Trimble, T., 1988. Mesozoic reactivation of Variscan thrusting in the Bristol Channel area, UK. *Journal of the Geological Society*, **145**, p. 439.

Bruckschen, P., & Veizer, J., 1997. Oxygen and carbon isotopic composition of Dinantian brachiopods: Paleoenvironmental implications for the Lower Carboniferous of western Europe. *Palaeogeogr. Palaeoclim. Palaeoecol*, **132**, p. 243– 264.

Budd D., 2001. Permeability loss with depth in the Cenozoic carbonate platform of west-central Florida. *American Association of Petroleum Geologists Bulletin*, **85**, p. 1253.

Burchette, T. P., Wright, V. P. & Faulkner T. J., 1990. Oolitic sandbody depositional models and geometries. Mississippian of southwest Britain: implications for petroleum exploration in carbonate ramp settings. *Sedimentary Geology*, **68**, p. 87-115

Burgess, P. M. & Gayer, R. A., 2000. Late Carboniferous tectonic subsidence in South Wales: implications for Variscan basin evolution and tectonic history in SW Britain. *Journal of the Geological Society*, **157**, p. 93-104.

Buxton, T. & Sibley, D., 1981. Pressure solution features in a shallow buried limestone. *Journal of Sedimentary Petrology*, **51**, p. 19-26.

Choquette, P. W. & James, N. P., 1990. Limestones the burial diagenetic environment. In *Diagenesis* (ed. McIlreath I. A. & Morrow D. W.), *Geoscience Canada, Reprint Series*, **4**, p. 75–111.

Choquette, P. W. & Pray, L. C., 1970. Geologic nomenclature and classification of porosity in sedimentary carbonates. *American Association of Petroleum Geologists Bulletin*, **54**, p. 207-50.

Cossey, P. J, Adams, A. E., Wright, V. P., Whiteley, M. J., Whyte, M. A. & Purnell, M. A., 2004. British Lower Carboniferous Stratigraphy. *Geological Conservation Review Series*, **29**, pp. 617.

Cros, P., 1979. Genèse d'oolithes et de grapestones, plate-forme des Bahamas (joulters Cays, Grand Banc)= Genesis of oolites and grapestones, the Bahama platform (joulters Cays and the Great Bank). *Bulletin des centres de recherches exploration-production Elf Aquitaine*,. *Boussens*, 1979, 3, p. 63-119.

Davydov V., Wardlaw B. & Gradstein F., 2004. The Carboniferous period. In: A geologic time scale (ed. Gradstein, F.M., Ogg, J.G. & Smith, A.G.). pp. 222-48. New York, Cambridge University Press.

Dehantschutter J. & Lees A., 1996. Waulsortian buildups of Waulsort, Belgium. *Geological Journal*, **31**, p.123-142.

Dickson, J. A. D., 1965. A modified staining technique for carbonates in thin section. *Nature*, **205**, p. 587.

Dickson, J. A. D., 1966. Carbonate identification and genesis as revealed by staining. *Journal of Sedimentary Petrology*, **36**, p. 491-505.

Dickson, J. A. D., 1985. Diagenesis of shallow-marine carbonates. *In Sedimentology: recent developments and applied aspects*, (ed. Brenchley, P. J. & Williams, B. P.), *Geological Society London Special Publications*, **18**, p. 173-89.

Dixon, E. & Vaughan, A., 1911. The Carboniferous Succession in Gower (Glamorganshire), with Notes on its Fauna & Conditions of Deposition. *Quarterly Journal of the Geological Society*, **67**, p. 477.

Dott Jr, R. & Bourgeois, J., 1982. Hummocky stratification: significance of its variable bedding sequences. *Bulletin of the Geological Society of America*, **93**, p. 663.

Dravis, J., 1979. Rapid and widespread generation of recent oolitic hardgrounds on a high energy Bahamian Platform, Eleuthera Bank, Bahamas. *Journal of Sedimentary Petrology*, **49**, p. 195-208.

Dunnington, H.V., 1967. Aspects of diagenesis and shape change in stylolitic limestone reservoirs. *Proceedings of the 7th World Petroleum Congress, Mexico*. **2**, p. 339-52.

Faber, P. & Riding, R., 1979. Uraloporella (microproblematicum) from the Middle Devonian of the Eifel (West Germany). *Neues Jb. Geol. Palaont. Mh.*, Stuttgart, **1979**, p. 139-146.

Fabricius, F., 1977. Origin of marine ooids and grapestones, *Contributions to Sedimentology*, Stuttgart, **7**, p. 113.

Fischer, A.G., 1964. The Lofer cyclothems of the Alpine Triassic. In: *Symposium on Cyclic Sedimentation* (ed. Merriam, D.F.), pp. 107-149. Kansas Geological Survey Bulletin, 169.

Flügel, E., 2004. *Microfacies of carbonate rocks: analysis, interpretation and application*. Springer, Berlin Heidelberg New York, 976 pp.

Folk, R. & Lynch, L. F., 2001. Organic matter, putative nannobacteria and the formation of ooids and hardgrounds. *Sedimentology*, **48**, p. 215-229.

Gallagher, S.J., 1996. The stratigraphy and cyclicity of the late Dinantian platform carbonates in parts of southern and western Ireland. In: *Recent Advances in Carboniferous Geology* (ed. Strogon, P., Somerville, I.D., & Jones, G.Ll). pp. 239-51. Geological Society Special Publication, **107**.

Gallagher, S. J., 1998. Controls on the distribution of calcareous Foraminifera in the Lower Carboniferous of Ireland. *Marine micropaleontology*, **34**, p. 187-211.

Gayer, R. A. & Jones, J., 1989. The Variscan foreland in South Wales. *Proceedings of the Ussher Society*, **7**, p. 177-79.

Gayer, R.A., Cole, J., Greiling, R.O., Hecht, C., & Jones, J., 1993. Comparative evolution of coal-bearing foreland basins along the Variscan northern margin in Europe. In: *The Rhenohercynian and Subvariscan Fold Belts*. (ed. Gayer, R.A., Greiling, R.O., & Vogel, A.), pp. 48-82. Vieweg Braunschweig.

- Gebelein, C., 1974. Guidebook for Modern Bahamian Platform Environments. *Geol. Soc. Am. Annu. Mtg. Fieldtrip Guide*, 93 pp.
- George, T. N., 1958. Lower Carboniferous palaeogeography of the British Isles. *Proceedings of the Yorkshire Geological Society*, **31**, p. 227-318.
- George, T. N., Johnson, G. A. L., Mitchell, M., Prentice, J. E., Ramsbottom, W. H. C., Sevastopulo, G.D. & Wilson, R. B., 1976. A correlation of the Dinantian rocks in the British Isles. *Geological Society London Special Publications*, No. 7.
- Gonzalez, R. & Eberli, G., 1997. Sediment transport and sedimentary structures in a carbonate tidal inlet; Lee Stocking Island, Exuma Islands, Bahamas. *Sedimentology*, **44**, p. 1015-1030.
- Grover, G. M., & Read, J. F., 1978. Fenestral and associated vadose diagenetic fabrics of tidal flat carbonates, Middle Ordovician New Market Limestone, southwestern Virginia. *Journal of Sedimentary Research*, **48**, p. 453-73.
- Handford, C., 1988. Review of carbonate sand-belt deposition of ooid grainstones and application to Mississippian reservoir, Damme Field, southwestern Kansas. *American Association of Petroleum Geologist Bull.*, **72**, p. 1184-1199.
- Hanley, J. & Steidtmann, J., 1973. Petrology of limestone lenses in the Casper Formation, southernmost Laramie Basin, Wyoming and Colorado. *Journal of Sedimentary Research*, **43**, p. 428.
- Haq, B. U. & Schutter, S. R., 2008. A chronology of Paleozoic sea-level changes. *Science*, **322**, p. 64-68.
- Harland, W.B., Cox, A.V., Llewellyn, P.G., Pickton, C.A.G., Smith, A.G., & Walters, R., 1982. *A Geologic Time Scale*. Cambridge University Press, New York.

- Harms, J., Choquette, P. & Brady, S. M., 1978. Carbonate Sand Waves, Isla Mujeres, Yucatan. *Geology and Hydrogeology of Northeastern Yucatan*, New Orleans Geological Society, p. 60-84.
- Harris, P.M., 1979. *Facies Anatomy and Diagenesis of a Bahamian Ooid Shoal*. *Sedimenta 7*, The Comparative Sedimentology Laboratory Miami, p. 163.
- Hillgartner, H., Dupraz, C. & Hug, W., 2001. Microbially induced cementation of carbonate sands: are micritic meniscus cements good indicators of vadose diagenesis?. *Sedimentology*, **48**, p.117-131.
- Hine, A., 1977. Lily Bank, Bahamas: history of an active oolite sand shoal. *Journal of Sedimentary Petrology*, **47**, p. 1554-1581.
- Hird, K. & Tucker, M. E., 1988. Contrasting diagenesis of two Carboniferous oolites from South Wales: a tale of climatic influence. *Sedimentology*, **35**, p. 587-602.
- Horbury, A.D. & Adams, A.E., 1996. Microfacies associations in Asbian carbonates: an example from the Urswick Limestone Formation of the southern Lake District, northern England. In: *Recent Advances in Carboniferous Geology* (ed. Strogon, P., Somerville, I.D., & Jones, G.L). pp. 221-37. Geological Society Special Publication, **107**.
- Isbell, J.L., Miller, M.F., Wolfe, K.L., & Lenaker, P.A., 2003. Timing of late Paleozoic glaciation in Gondwana: Was glaciation responsible for the development of Northern Hemisphere cyclothem?. In: *Extreme Depositional Environments: Mega End Members in Geologic Time*. (ed. Chan, M.A., & Archer, A.W.). Special paper of Geological Society of America, 370, p. 5-24
- Johnson, H. & Baldwin, C., 1996. Shallow clastic seas. In: *Sedimentary Environments: processes, facies and stratigraphy* (ed. Reading, H.G.). pp. 232-280.

Jones, P.J., 1995. Time Scales: 5. Carboniferous. Australian Geological Survey Organisation, Report 1995/34.

Kazmierczak, J. & Goldring, R., 1978. Subtidal flat-pebble conglomerate from the Upper Devonian of Poland; a multiprovenant high-energy product. *Geological Magazine*, **115**, p. 359 –66.

Keith, B. & Zuppman, C., 1993, Mississippian Oolites and Modern Analogs: American Association of Petroleum Geologists. *Studies in Geology*, **35**, 265pp.

Kellaway, G. & Welch, F., 1955. The Upper Old Red Sandstone and Lower Carboniferous rocks of Bristol and the Mendips compared with those of Chepstow and the Forest of Dean. *Bull. Geol. Surv. Gt. Brit*, **9**, p. 1-21.

Kelleher, G.T. & Smosna, R., 1993. Oolitic tidal-bar reservoirs in the Mississippian Greenbrier Group of West Virginia. In: Mississippian Oolite and Modern Analogs (ed. Keith, B.D., & Zuppman, C.W.). pp. 163-73. American Association of Petroleum Geologists, *Studies in Geology*, **35**.

Kelling, G., 1988. Silesian sedimentation and tectonics in the South Wales Basin: a brief review. In: *Sedimentation in a synorogenic Basin Complex; The Upper Carboniferous of Northwest Europe*. (ed. Besly, B., & Kelling, G.), pp. 38-42. Blackie, Glasgow and London.

Kobluk, D. R. & Risk, M. J., 1977. Micritization and carbonate-grain binding by endolithic algae. *American Association of Petroleum Geologist Bull.*, **61**, p. 1069-82.

Korde, K.B., 1950. On the morphology of the Dasycladaceae of the northern Urals. *Dokl. Akad. Nauk SSSR*. Moscow, **73**, 569-71. [In Russian; French transl. no. 304, Serv. Inf. geol., Bur. Rech. geol. Minieres, Paris].

Leeder, M.R. 1992. Dinantian. In: *Geology of England and Wales*. (ed. Duff, P.McL.D., & Smith, A.J.), pp. 207-38. The Geological Society, London.

Leeder, M.R. & McMahon, A.H., 1988. Upper Carboniferous (Silesian) basin subsidence in northern Britain. In: *Sedimentation in a Synorogenic Complex. The Carboniferous of Northwest Europe* (ed. Besly, B.M., & Kelling, G.) pp. 43-52. Blackie, Glasgow.

Lees, A., & Miller, J., 1985. Facies variation in Waulsortian buildups, Part 2; Mid Dinantian buildups from Europe and North America. *Geological Journal*, **20**, p. 159–180.

Lees, A., Hallet, V. & Hibo, D., 1985. Facies variation in Waulsortian build-ups. Part 1. A model from Belgium. *Geological Journal*, **20**, p. 133-58.

Lloyd, R., Perkins, R. & Kerr, S., 1987. Beach and shoreface ooid deposition on shallow interior banks, Turks and Caicos Islands, British west Indies. *Journal of Sedimentary Petrology*, **57**, 976–982.

Logan, B.W. & Semeniuk, V., 1976. Dynamic metamorphism; processes and products in Devonian carbonate rocks, Canning Basin, Western Australia. *Special Publication of Geological Society of Australia*, **16**, p. 1-138.

Lomando, A., 1999. Structural influences on facies trends of carbonate inner ramp systems, examples from the Kuwait–Saudi Arabian coast of the Arabian Gulf and Northern Yucatan, Mexico. *GeoArabia*, **4**, p. 339–60.

Mamet, B. & Roux, A., 1975. *Jansaella ridingi*, nouveau genre d'Algue? dans le Devonien de l'Alberta. *Canadian Journal of Earth Sciences*, Ottawa, **12**, p. 1480-4.

Menning, M., Weyer, D., Drozdowski, G., Van Amerom, H.W.J., & Wendt, I., 2000. A Carboniferous time scale 2000: Discussion and use of geological parameters as time indicators from Central and Western Europe. *Geologisches Jahrbuch*. **A156**, p. 3-44.

Mii, H., Grossman, E. & Yancey, T., 1999. Carboniferous isotope stratigraphies of North America: Implications for Carboniferous paleoceanography and Mississippian glaciation. *Bulletin of the Geological Society of America*, **111**, p. 960.

Mii, H., Grossman, E., Yancey, T., Chuvashov, B. & Egorov, A., 2001. Isotopic records of brachiopod shells from the Russian Platform—evidence for the onset of mid-Carboniferous glaciation. *Chemical Geology*, **175**, p. 133-147.

Newell, N., Purdy, E. & Imbrie, J., 1960. Bahamian oölitic sand. *The Journal of Geology*, **68**, p. 481-497.

Perry, C. T., 1998. Grain susceptibility to the effects of microboring: implications for the preservation of skeletal carbonates. *Sedimentology*, **45**, p. 39-51.

Purdy, E., 1963. Recent calcium carbonate facies of the Great Bahama Bank. 2. Sedimentary facies. *The Journal of Geology*, **71**, p. 472-497.

Ramsay, A. T. S., 1987. Depositional Environments of Dinantian Limestones in Gower, South Wales. In *European Dinantian Environments*, (ed. Miller, J., Adams, A. E. & Wright, V. P.), *Geological journal. Special issue*, **12**, p. 265-308.

Ramsay, A. T. S., 1991. Sedimentation and tectonics in the Dinantian limestones of South Wales. *International Association of Sedimentologists, Special Publications*, **12**, p. 485-511.

Ramsbottom, W. H. C., 1973. Transgressions and regressions in the Dinantian: a new synthesis of British Dinantian stratigraphy. *Proceedings of the Yorkshire Geological Society*, **39**, p. 567-607.

Ramsbottom, W. H. C., 1977. Major cycles of transgression and regression (mesothems) in the Namurian. *Proceedings of the Yorkshire Geological Society*, **41**, p. 261-91.

Ramsbottom, W. H. C., 1979. Rates of transgression and regression in NW Europe. *Journal of Geological Society*, London, **136**, p. 147-53.

Ramsbottom, W. H. C., 1981. Eustacy, sea level and local tectonism, with examples from the British Carboniferous. *Proceedings of the Yorkshire Geological Society*, **43**, p. 473-82.

Rankey, E., Riegl, B. & Steffen, K., 2006. Form, function and feedbacks in a tidally dominated ooid shoal, Bahamas. *Sedimentology*, **53**, p. 1191-1210.

Riding, R. & Jansa, L., 1974. Uraloporella Korde in the Devonian of Alberta. *Canadian Journal of Earth Sciences*, **11**, p. 1414-1426.

Riding, R. & Jansa, L., 1976. Devonian Occurrence of Uraloporella (? Foraminifer) in the Canning Basin, Western Australia. *Journal of Paleontology*, p. 805-807.

Ross, C. A. & Ross, J. R. P., 1988. Late Paleozoic transgressive-regressive deposition. In *Sea-Level Changes: An Integrated Approach*, (ed. Wilgus, C. K., Hastings, B. S., Kendall, C. G. St. C, Posamentier, H. W., Ross, C. A. & Van Wagoner, J. C.), *Society of Economic Palaeontologists and Mineralogists Special Publication*, **42**, p. 227-47.

Rowley, D.B., Raymond, A., Totman Parrish, J., Lottes, A.L., Scotese, C.R. & Ziegler, A.M., 1985. Carboniferous palaeogeographic, phytogeographic and palaeoclimatic reconstructions. *Inter. J. Coal, Geol.* **5**, p. 7-42.

Rygel, M. C., Fielding, C. R., Frank, T. D. & Birgenheier, L. P., 2008. The magnitude of late Paleozoic glacioeustatic fluctuations: a synthesis. *Journal of Sedimentary Research*, **78**, p. 500-11.

Scholle, P. A. & Ulmer-Scholle, D. S., 2003. A color guide to the petrography of carbonate rocks: grains, textures, porosity, diagenesis. *American Association of Petroleum Geologists Memoir* **77**, pp. 474.

Scotese, C. R., Bambach, R.K., Barton, C., Van der Voo, R., & Ziegler, A.M., 1979. Palaeozoic base maps. *Journal of Geology*, **87**, p. 217-77.

Scott, J., 1988. Sedimentology of the Holkerian rocks of South Wales. PhD. Thesis, University College of Wales, Aberystwyth, 358 pp. (unpublished).

Searl, A., 1989. Diagenesis of the Gully Oolite (Lower Carboniferous), South Wales. *Geological Journal*, **24**, p. 275-93.

Shinn, E.A., 1983. Birdseyes, fenestrae, shrinkage pores and loferites: a re-evaluation. *Journal of Sedimentary Petrology*, **53**, p. 619-629.

Sibley, D. F. & Gregg, J. M., 1987. Classification of dolomite rock textures. *Journal of Sedimentary Petrology*, **57**, p. 967-75.

Skompski, S., 1987. The dasycladacean nature of Late Paleozoic palaeoberesellid algae. *Acta Geologica Polonica*, **37**, p. 21-31.

Smith Jr, L. & Read, J., 2000. Rapid onset of late Paleozoic glaciation on Gondwana: Evidence from Upper Mississippian strata of the Midcontinent, United States. *Geology*, **28**, p. 279.

Sullivan, R., 1966. The stratigraphical effects of the mid-Dinantian movements in south west Wales. *Palaeogeography, Palaeoclimatology, Palaeoecology*, **2**, p. 213-244.

Tebbutt, G., Conley, C. & Boyd, D., 1965. Lithogenesis of a distinctive carbonate rock fabric. *Rocky Mountain Geology*, **4**, p. 1.

Tucker, M. E. & Wright, V. P., 1990. *Carbonate sedimentology*. Blackwell Scientific Publications, Oxford.

Vaughan, A., 1905. The Palaeontological Sequence in the Carboniferous Limestone of the Bristol Area. *Quarterly Journal of the Geological Society*, **61**, p. 181-307.

Veevers, J. & Powell, C., 1987. Late Paleozoic glacial episodes in Gondwanaland reflected in transgressive-regressive depositional sequences in Euramerica. *Bulletin of the Geological Society of America*, **98**, p. 475.

Wanless, H., 1979. Limestone response to stress: pressure solution and dolomitization. *Journal of Sedimentary Petrology*, **49**, p. 437-462.

Wanless, H. & Shepard, F., 1936. Sea level and climatic changes related to late Paleozoic cycles. *Geological Society of America Bulletin*, **47**, p.1177.

Wanless, H.R. & Tedesco, L.P., 1993. Comparison of oolitic sand bodies generated by tidal vs. wind-wave agitation. In: *Mississippian Oolites and Modern Analogs* (ed. Keith, B.D., & Zuppmann, C.W.), pp. 199-225. American Association of Petroleum Geologists, Studies in Geology, 35.

Wanless H. R., Tedesco L. P., & Tyrrell K. M., 1988. Production of subtidal tubular and surficial tempestites by Hurricane Kate, Caicos Platform, British West Indies. *Journal of Sedimentary Petrology*, **58**, p. 739-750.

Warnke, K., 1995. Calcification processes of siliceous sponges in Viséan Limestones (Counties Sligo and Leitrim, Northwestern Ireland). *Facies*, **33**, p. 215-227.

Wilson, D., 1990. *Geology of the South Wales coalfield*. Bernan Press (PA).

Wilson, R., 1967. Particle nomenclature in carbonate sediments. *Neues Jahrb. Geol. Paläont., Monatshefte*, **8**, p. 921-7.

Wilson, D., Davies, J.R., Fletcher, C.J.N. & Smith, M. 1990. Geology of the South Wales Coalfield, Part VI, the Country around Bridgend. *Memoir of the British Geological Survey*, p. 261-2.

Winland, H. & Matthews, R., 1974. Origin and significance of grapestone, Bahama Islands. *Journal of Sedimentary Petrology*, **44**, p. 921-927.

Wolf, K., 1965. Gradational sedimentary products of calcareous algae. *Sedimentology*, **5**, p. 1-37.

Wray, J., 1977. *Calcareous algae*. Elsevier Science & Technology.

Wright, V., 1981. Algal aragonite-encrusted pisoids from a Lower Carboniferous schizohaline lagoon. *Journal of Sedimentary Research*, **51**, p. 479.

Wright, V. P., 1982. The recognition and interpretation of paleokarsts: two examples from the Lower Carboniferous of South Wales. *Journal of Sedimentary Petrology*, **52**, p. 83-94.

Wright, V. P., 1986. Facies sequences on a carbonate ramp: the Carboniferous Limestone of South Wales. *Sedimentology*, **33**, p. 221-41.

Wright, V. P., 1987. The evolution of the early Carboniferous Limestone province in southwest Britain. *Geological Magazine*, **124**, p. 477-80.

Wright, V. P., 1990. Equatorial aridity and climatic oscillations during the early Carboniferous, southern Britain. *Journal of the Geological Society*, **147**, p. 359-63.

Wright, V. P., 2008. Carbonate Depositional Systems: Reservoir Sedimentation and Diagenesis. Course Notes, Geoscience Training Alliance (unpublished) Nautilus, Hermitage, UK.

Wright, V.P., & Burchette, T.P. 1996. Shallow-water carbonate environments. In: *Sedimentary Environments: Processes, Facies and Stratigraphy* (ed. Reading, H.G.), pp. 325-395. Blackwell Science Ltd, Oxford.

Wright, V. P., & Vanstone, S. D., 2001. Onset of Late Palaeozoic glacio-eustasy and the evolving climates of low latitude areas: a synthesis of current understanding. *Journal of the Geological Society*. **158**, p. 579-82.

Wright, V.P., & Burgess, P.M. 2005. The carbonate factory continuum, facies mosaics and microfacies: an appraisal of some of the key concepts underpinning carbonate sedimentology. *Facies*, **51**, p. 12–23.

APPENDICES

A-Procedure for the preparation of stained acetate peels and thin sections

Dickson's (1965, 1966) technique was used to produce the stained acetate peels and thin sections. This technique is summarised below:

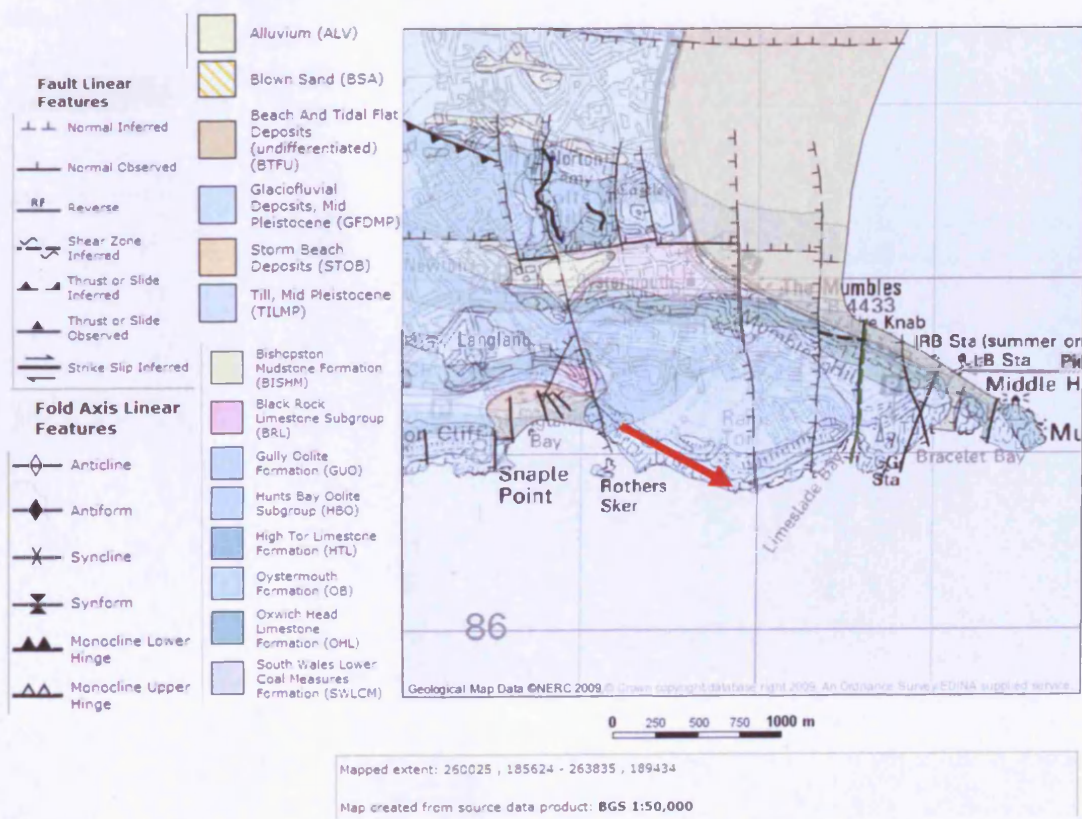
Three solutions were used in order to make the staining, these are: 1.5% hydrochloric acid (HCL), 0.2g Alizarin Red S (ARS) per 100ml 1.5% HCL and 2.0g of Potassium Ferricyanide (PF) mixed in a ratio of ARS: PF=3:2, and 0.2g ARS per 100ml HCL. These solutions were poured into three separate trays,. After that, each polished rock slab was submerged in the first solution for 15 seconds, then 45 seconds in the second one, and 15 seconds in the last one. Distilled water was used between each submerging process to gently rinse the slab in order to maintain the delicate stain coating. After the last rinse, the samples were placed on a level table, with the slabs facing upwards, to dry naturally, in about 45-60 minutes, at room temperature. Then, acetone solution was used to irrigate the slab face and an acetate sheet placed immediately over the slab surface. The next day, the acetate sheets were peeled off the slabs, trimmed with a pair of scissors, and numbered.

12 thin sections were half stained using the same process (at Cardiff University), placing each thin section, in each solution for the same time, as described above. They were rinsed with distilled water after each immersion.

B-Geological maps of the three studied localities (the HBO section is indicated by the red arrow where the base of the arrow lies on the older unit and the head of the arrow lies on the younger unit)

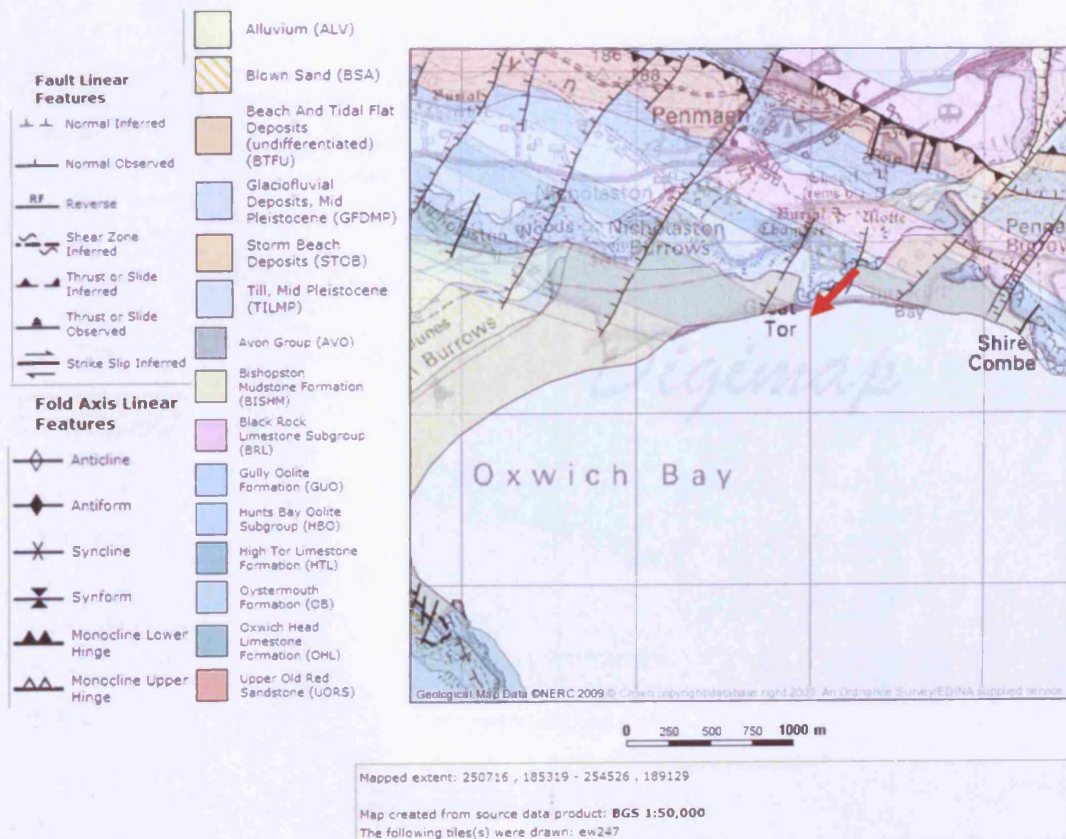
Langland Bay

- The Arundian-Holkerian boundary is covered with Quaternary sand.
- The Holkerian-Asbian boundary is not picked due to the steepness and the closeness of the cliff from the water.



Three Cliffs Bay

- The Arundian-Holkerian boundary is transitional.
- The Holkerian-Asbian boundary is not picked because the section pinched out to Quaternary sand.



Port Eynon Bay

- The Arundian-Holkerian boundary is transitional.
- The Holkerian-Asbian boundary is not picked because the section is covered with Quaternary sand.

